Matching Application Access Patterns to Storage Device Characteristics

JIRI SCHINDLER

May 2004

CMU-PDL-03-109

Dept. of Electrical and Computer Engineering
Carnegie Mellon University
5000 Forbes Ave.
Pittsburgh, PA 15213

Submitted in partial fulfillment of the requirements for the degree of Doctor of Philosophy.

Thesis committee

Prof. Gregory R. Ganger, Chair
Prof. Anastassia Ailamaki
Dr. John Howard, Sun Microsystems
Dr. Erik Riedel, Seagate Research

Keywords: storage systems performance, database systems, disk arrays, MEMS-based storage

To Katrina.

Abstract

Conventional computer systems have insufficient information about storage device performance characteristics. As a consequence, they utilize the available device resources inefficiently, which, in turn, results in poor application performance. This dissertation demonstrates that a few high-level, device-independent hints encapsulating unique storage device characteristics can achieve significant I/O performance gains without breaking the established abstraction of a storage device as a linear address space of fixed-size blocks. A piece of system software (here referred to as storage manager), which translates application requests into individual I/Os, can automatically match application access patterns to the provided characteristics. This results in more efficient utilization of storage devices and thus improved application performance.

This dissertation (i) identifies specific features of disk drives, disk arrays, and MEMS-based storage devices not exploited by conventional systems, (ii) quantifies the potential performance gains these features offer, and (iii) demonstrates on three different implementations (FFS file system, database storage manager, and disk array logical volume manager) the benefits to the applications using these storage managers. It describes two specific attributes: the ACCESS DELAY BOUNDARIES attribute delineates efficient accesses to storage devices and the PARALLELISM attribute exploits the parallelism inherent to a storage device. The two described performance attributes mesh well with existing storage manager data structures, requiring minimal changes to their code. Most importantly, they simplify the error-prone task of performance tuning.

Exposing performance characteristics has the biggest impact on systems with regular access patterns. For example in database systems, when decision support (DSS) and on-line transaction processing (OLTP) workloads run concurrently, DSS experiences a speed up of up to 3×, while OLTP exhibits a 7% speedup. With a single layout taking advantage of access parallelism, a database table can be scanned efficiently in both dimensions. Additionally, scan operations run in time proportional to the amount of query payload; unwanted portions of a table are not touched while scanning at full bandwidth.

Acknowledgements

The work presented here is a result of my collaboration with fellow graduate students John Linwood Griffin, Steve Schlosser, and Minglong Shao who contributed their talents, ideas, and many hours that went into developing prototypes, debugging, and result collection. Many thanks to John Bucy who developed disk model libraries that were used in the *Clotho* prototype.

I am indebted to many people for their support, encouragement, and friendship through my work on my dissertation. First and foremost, my advisor Greg Ganger has been tremendous in providing guidance and showing exceptional patience and dedication to my success. He has made himself always available and provided feedback on moment's notice on any and all aspects of my work. Anastassia Ailamaki, in addition to serving on my thesis committee, acted as my unofficial second advisor and mentor. Her help and extra push at the right time have been instrumental for my development. I am greatful to John Howard and Erik Riedel for agreeing to serve on my thesis committee and working it into their busy schedules. Their close monitoring of my progress and detailed comments have been invaluable.

I feel priviledged to have been part of a great research group: The Parallel Data Laboratory. My friends and research partners Steve Schlosser and John Linwood Griffin have been fabulous in both capacities. Without their help and encouragement I would not have been able to finish. I am also thankful to Craig Soules, Eno Thereska, Jay Wylie, Garth Goodson, John Strunk, Chris Lumb, Andy Klosterman, and David Petrou for their willingess to engage in discussions that shaped my ideas. I have enjoyed tremendously working with Minglong Shao who has tought me a lot about databases.

My special thanks to the member companies of the Parallel Data Lab Consortium for their generous contributions to my research. I am also indebted to the PDL and D-level staff. Karen Lindenfelser and Linda Whipkey have always kept my spirits high. Joan Digney has been instrumental in proof-reading my dissertation. Tim Talpas made sure that all the equipment in the machine room was always running. And finally, I am grateful for the D-level espresso machine that kept me going.

Contents

Figures

Tables

1 Introduction

1.1 Problem definition

The abstraction of storage devices into a linear space of fixed-size blocks plays an important role in the architecture of computer systems. It cleanly separates host system software from storage-device-specific control code, facilitating data access and retrieval. A new storage device can easily be plugged into an existing system, without requiring any modifications to the host software. Similarly, the storage device control code can transparently implement new algorithms for optimizing data access behind this abstraction. However, storage interface abstraction also hides important non-linearities in access times to different blocks, addressed by an integer called the *logical block number* (LBN). The difference in access times, ranging by more than an order of magnitude, stems from both the devices' physical characteristics and their architectural organizations. Thus, exercising efficient access patterns that yield shorter response times can bring about significant I/O performance improvements.

In order to work around the large non-linearities in access times, computer systems combine three different approaches. First, the host system software, which this dissertation refers to as the storage manager, and the storage device adhere to an unwritten contract, which states that (i) LBNs near each other can be accessed faster than those farther away and that (ii) accessing LBNs sequentially is generally much more efficient than accessing them in random order. Second, the storage manager (e.g., inside a file system or a database system) guesses device characteristics and adjusts access patterns to improve I/O performance. This guessing is based on assumptions about the underlying storage device technology and a set of manually-tunable parameters. Third, the storage device observes I/O access patterns and attempts to dynamically adapt its behavior to service requests more efficiently.

The simple unwritten contract mentioned above works well when access patterns are regular and static; the data layout can be linearized in the LBN address space to achieve efficient sequential access. However, the simple contract is not

sufficient for (i) mixed streams (i.e., regular but not sequential accesses), (ii) regular access patterns to non-linear structures (e.g., two dimensional data), or (iii) when access patterns change over time. Therefore, the latter two approaches described in the preceding paragraph are needed as well. However, they exhibit a common shortcoming; the storage interface used in today's systems does not allow the exchange of sufficient information. Even though both the storage manager and the storage device employ elaborate algorithms in attempting to maximize overall performance, they have only a crude notion of what the other is doing and make their decisions largely in isolation. In particular, the storage manager is unaware of the most efficient access patterns, and thus cannot exercise them. The storage device, in turn, tunes the execution of access patterns that are inherently far from optimal. In contrast, providing sufficient information could result in better I/O performance through more efficient use of storage device resources without guess work or duplication of effort at both sides of the storage interface.

Using storage managers that rely on built-in storage device models with manually tunable parameters poses another set of problems. These parameters often do not capture in enough detail underlying storage device mechanisms governing the I/O performance. They are also labor-intensive and prone to misconfiguration. Even whey they are set properly, they do not cope well with dynamic workload changes; they must be manually re-tuned by a system administrator each time a workload changes. Finally, the assumptions of the models describing storage device performance break the interface abstraction. As a consequence, when a new storage device is plugged into the system, the model may no longer be applicable.

In short, the absence of communication between the storage manager and the storage device leads to inefficient utilization of storage device resources and poor performance, especially for workloads that change dynamically.

1.2 Thesis statement

With sufficient information, a storage manager can exploit unique storage device characteristics to achieve better, more robust I/O performance. This information can be abstract from device specifics, device-independent, and yet expressive-enough to allow a storage manager to tune its access patterns to a given device.

1.3 Overview

This dissertation contends that storage device resources are not utilized to their full potential because too much information is hidden from storage manager. High-level storage interfaces abstracting a storage device as a linear address space of

fixed-size blocks do not convey sufficient information to allow storage managers make decisions leading to efficient use of the storage device.

With more expressive interfaces, storage managers and storage devices can exchange information and make more informed choices on both sides of the storage interface. For example, only the storage manager has detailed information about the application priorities of requests going to the storage device. On the other hand, only the storage device has exact information about its internal state. Combining this knowledge appropriately will allow a storage manager can take advantage of the device's unique strengths and avoid access patterns leading to inefficient execution at the storage device. This dissertation explores what information a storage device should expose to aid storage managers in making more informed decisions about access patterns that result in more efficient utilization of storage resources and improved application I/O performance.

1.3.1 Explicit performance hints

A storage device can expose its performance characteristics in a few, high-level *static* performance attributes. With detailed information about application, a storage manager uses these explicit hints to match the application access patterns to the characteristics of the storage device and generate requests that can be executed efficiently. However, the storage manager should not control how or when requests should be executed; such device-specific decisions depend on the state of the storage device and should be done below the storage interface, where appropriate information is available.

In addition to bridging the performance gap between the host and the storage device, static performance attributes simplify storage manager implementation. The storage manager need not implement models describing a device's performance or rely on possibly incorrect settings of the manually tunable parameters. Instead, with explicit hints, the storage manager can dynamically, and without human intervention, adjust application access patterns, simplifying the difficult and error-prone task of performance tuning.

This dissertation describes two examples of static performance attributes. The ACCESS DELAY BOUNDARIES attribute allows efficient execution of access patterns consisting of mid-sized I/Os (tens to hundreds of KB) for non-sequential accesses to mixed streams. The PARALLELISM attribute allows efficient accesses to multi-dimensional data structures laid out in the storage device's linear address space. Specifically, measurements described in this dissertation show it can facilitate efficient accesses to two-dimensional structures in both dimensions for a variety of access patterns with a single data layout.

If a storage device does not provide its performance characteristics directly, an intermediary, *separate* from the storage manager, can often discover these and encapsulate them into the performance hints to be passed to the storage manager. This intermediary, called a discovery tool, does not affect the critical path for I/O requests going to the storage device. This dissertation describes one such tool that works for modern disk drives.

1.3.2 Improving efficiency across a spectrum of access patterns

Application access patterns span a spectrum ranging from highly structured accesses to completely non-structured random ones. Because of their nature, random accesses can be made efficient only by qualitative changes in technology; no provision of more information between storage devices and applications can improve their efficiency. At the opposite end of the spectrum, complete control over access patterns (that do no change over time) allows an application to lay data out to take advantage of efficient sequential accesses.

The performance attributes proposed by this dissertation improve the efficiency of access patterns that fall between these two ends of the spectrum: regular access patterns that change over time due to dynamic workload changes. One example includes access patterns consisting of intermixed streams. While each stream in isolation could take advantage of efficient sequential access, a simultaneous access to multiple streams, whose number changes dynamically, results in non-sequential storage device accesses. Another example is a system with static (and possibly multi-dimensional) data structures where dynamic workload changes yield different access patterns. This behavior is typical for relational database systems, where different queries result in different accesses, while the data structures (relations) change very slowly relative to the changes in access patterns. The ACCESS DELAY BOUNDARIES and PARALLELISM attributes aid applications in data layout and construction of more efficient access patterns compared to traditional systems that, in the absence of sufficient information provided by storage devices, rely on guess work and duplicate effort on both sides of the storage interface.

1.3.3 Restoring interface abstractions

Providing explicit hints also restores storage interface abstractions. These hints replace assumptions about device's inner-workings built into current storage managers, yet they preserve the unwritten contract between the storage device and the storage manager. This dissertation does not argue that this contract is not useful. It shows that, by itself, it does not allow applications to take full advantage of the

performance available in today's storage devices, including single disk drives, disk arrays, and emerging technologies such as MEMS-based storage.

This approach does not prevent the storage device from further optimizing the execution of efficient access patterns based on explicit hints. The storage manager can, and should, relegate any device-specific decisions or optimizations (e.g., scheduling) to the storage device. Hidden away behind the storage interface, the storage device can make these decisions with more accurate and detailed information that would otherwise be difficult to expose to the storage manager. This clean separation allows code developers to write storage managers devoid of device-specific detail; yet the storage manager can still dynamically adapt its access patterns using the static hints provided by the storage device.

1.3.4 Minimal system changes

An alternative approach to the one proposed in this dissertation is to push information down to the storage device. While this approach may fulfill the same goals this dissertation sets forth, namely, more efficient use of storage resources, the mechanisms to achieve the goals may require extensive changes to the current storage interface. Specifically, the amount of application-specific state that must be conveyed to the storage device can be substantial. Thus, modifying the storage manager and application code for this purpose would likely involve larger amounts of new system design and software engineering.

The approach proposed and discussed in this dissertation, on the other hand, meshes well with the existing code and data structures of a variety of storage managers. It does not require a new system design and implementation to be developed from scratch. It makes minimal changes to the existing host software structures and requires no changes to the firmware of current storage devices. It contends that, together with knowledge of application state and its access patterns, the storage manager is the right place where a little bit of information provided in these explicit hints can bring significant performance wins. It shows that the data structures of the Shore database storage manager [Carey et al. 1994], Fast File System [McKusick et al. 1984], and Log-structured File System [Rosenblum and Ousterhout 1992] (all examples of storage managers), can easily accommodate and benefit from performance hints with only small changes to their source code.

The proposed mechanism for conveying performance hints to the storage manager follows the same minimalist approach. The performance characteristics are encapsulated into a well-defined (small) set of attributes. These attributes do not break established abstractions between the storage device and the storage manager; they simply annotate the current abstraction of a storage system, namely

the linear address space of fixed-size LBNs. The storage manager makes function calls with specific LBN values that return the values of the desired attribute.

1.4 Contributions

This dissertation makes four main contributions:

- It shows how static performance hints provided by a storage device can be used for dynamic adjustment of application access patterns, allowing them to utilize storage device resources more efficiently. It gives two specific examples of performance attributes that encapsulate performance characteristics of single disks, disk arrays, and MEMS-based storage.

- It describes the minimal changes to current storage manager structures necessary to take advantage of explicit performance hints and demonstrates them on two different storage manager implementations; a database storage manager, called Shore, and a block-based Fast File System, which is part of the BSD operating system.

- It quantifies performance improvements to different classes of applications using three different storage managers (e.g., FFS, Shore, and logical volume managers inside disk arrays). It measures the benefits to file system and database workloads on three different storage manager implementations. Finally, it analytically evaluates the benefits to a Log-structured File System and a multimedia streaming server.

- It demonstrates how this approach can be used in today's systems without modifications to current storage devices thanks to a specialized discovery tool. This tool, which sits between a storage manager and the storage device, can describe the performance characteristics of a specific device and transparently export them to the storage manager.

1.4.1 Analysis and evaluation

Today, disk drives are the most prevalent devices being used for on-line storage. This dissertation identifies performance characteristics of state-of-the-art disk drives. Building upon this evaluation, it explores the characteristics of disk arrays, which group several disks for better performance and reliability. It also explores the unique performance characteristics of an emerging storage technology, called MEMS-based storage. The performance impact of exposing device characteristics is evaluated both by analytical models and experimentation. This information can

provide up to 50% improvement in disk efficiency and a significant reduction in response time variance for accesses that utilize explicit information about disk characteristics. With proper data layouts, RAID configurations can leverage the per-disk improvements and deliver it to applications.

1.4.2 Improvements to system performance

Exposing performance characteristics has the biggest impact on systems with regular (but not necessarily sequential) access patterns. On the other hand, applications with random access patterns that cannot be tuned to achieve efficient accesses will experience only limited or no improvements. In particular random small I/O activity (e.g., online transactional processing), will see only limited, or no, performance improvements. Additionally, these limited improvements may only occur when random workloads occur concurrently with other workloads exhibiting more regular access patterns.

Fortunately, many systems and applications exhibit regular access patterns to large (relative to the individual I/O size) sets of related data. This regularity allows storage managers to dynamically adjust the sizes of individual I/Os that can be executed by storage devices more efficiently. The results described in this dissertation show a 20% reduction in run time for large file operations in block-based file systems. For log-structured file systems, a 44% lower write cost to segments is achieved. Multimedia servers achieve a 56% increase in the number of concurrent streams serviceable on a video server and up to 5× lower startup latency for streams newly admitted to the server.

A database storage manager using explicit performance attributes can achieve I/O efficiency nearly equivalent to sequential streaming, even in the presence of competing random I/O traffic. Exposing these attributes also simplifies manual configuration and restores the optimizer's assumptions about the relative costs of different access patterns expressed in query plans. The performance of stand-alone decision support workload (DSS) improves by 10% on average, with some queries seeing up to 1.5× speedup. More importantly, when running concurrently with an on-line transaction processing (OLTP) workload, DSS workload performance improves by up to 3×, while OLTP also exhibits a 7% speedup.

Utilizing the ACCESS DELAY BOUNDARIES and PARALLELISM attributes, a database storage manager can implement a single data layout for 2-D tables (relations) that yields efficient accesses in *both* dimensions. The access efficiencies are equal or very close (within 6%) to the efficiencies achieved with data layouts optimized for accesses in the respective dimension, but trading off efficiency in the other dimension. For example, scan operators operate with maximum efficiency, while

requesting only the data needed by the query. Unwanted portions of a table can be skipped while scanning at full speed, resulting in scan times proportional to the amount of data actually used by queries.

1.4.3 Automated characterization of disk performance

The discovery tool described in this dissertation, called DIXtrac, automatically characterizes the performance of modern disk drives. It can extract over 100 performance-critical parameters in 2–6 minutes without human intervention or special hardware support. While only a small fraction of these parameters is encapsulated as the set of performance attributes to be passed to the storage manager, this accurate characterization is useful for other applications requiring detailed knowledge of device parameters [Lumb et al. 2000; Wang et al. 1999; Yu et al. 2000]. In particular, the ACCESS DELAY BOUNDARIES performance attribute encapsulates the extracted disk track sizes and the PARALLELISM attribute additionally encapsulates the head-switch and/or one-cylinder seek time.

1.5 Organization

The reminder of the dissertation is organized as follows. Chapter 2 describes previous work related to exposing information about storage devices for application performance gains. Chapter 3 describes in detail the proposed approach of encapsulating storage device performance characteristics into a few high-level attributes annotating the device's LBN linear address space. It also discusses in detail the underlying storage device characteristics. Chapter 4 describes a discovery tool, which can determine the performance characteristics of modern disk drives using conventional SCSI interface. Chapter 5 describes a performance attribute called ACCESS DELAY BOUNDARIES, and evaluates how utilizing this attribute improves performance for file systems and database systems. Chapter 6 describes another performance attribute, called PARALLELISM, and shows how it improves performance for database query operators. Chapter 7 summarizes the contributions of this dissertation and suggests some avenues for future work.

2 Background and Related Work

2.1 Storage interface evolution

Virtually all of today's storage devices use an interface that presents them as a linear space of equally-sized blocks (e.g., SCSI or IDE [Schmidt 1995]) . Each block is uniquely addressed by an integer, called a *logical block number* (LBN), from 0 to LBN_{max} (which is the number of blocks minus one). This interface separates a storage device and its software from the host running applications; the clean separation between the two allows changes to occur on either side of the interface without affecting the other. For example, a new storage device can be simply connected to the host, without any modifications to the storage manager code.

The storage device abstraction offered by this interface also provides a simple programming model. Within this abstraction, a piece of system software, called the storage manager (SM for short), accepts requests for data from applications through a well-defined API. The SM then transforms these requests into individual I/O operations and issues them to the storage device on behalf of the host applications. Because the SM communicates with these applications, it can utilize the knowledge of all the applications' access patterns to generate non-competing I/O operations.

Before this storage interface existed, the storage manager was also responsible for controlling storage device specifics such as positioning of the read/write heads, data encoding, and handling of media errors. With such tight coupling between the storage device and the SM, plugging a new storage device into the host required software changes to the storage manager. It also had one important advantage. The storage manager could leverage its intimate knowledge of device's performance characteristics and application access patterns. This knowledge, combined with the ability to control the mechanics of the storage device, allowed the storage manager to fully utilize storage device resources by turning the application access patterns into efficient I/O operations.

In particular, many algorithms have been developed for efficient scheduling of read/write heads of rotating drums and disk drives, minimizing disk access latency

and/or variance in response time [Bitton and Gray 1988; Denning 1967; Daniel and Geist 1983; Fuller 1972; Geist and Daniel 1987]. These algorithms combine the knowledge of outstanding I/O requests, the ability to precisely control read/write head positioning, and detailed knowledge of device characteristics.

Current state-of-the art storage devices (i.e., disk drives and disk arrays) employ a variety of mechanisms for media defect management and for correcting transient read/write errors as well as algorithms for improving I/O performance such as prefetching, write-back caching, and data reorganization. Because these functions are tightly coupled to the electronics [Quantum Corporation 1999] or architecture [Hitz et al. 1994; Wilkes et al. 1996], it is difficult to cleanly expose them to the storage manager. Hence, today's device controllers include firmware algorithms for efficient request scheduling while hiding device details from the storage manager behind the storage device interface.

The high-level storage interface frees the storage manager from device-specific knowledge, allowing it to concentrate only on data allocation and the generation of I/Os according to application needs. The storage manager simply sends READ and WRITE commands to the device. Behind the storage interface, the device schedules outstanding requests and carries out the steps necessary to execute the commands. If an error occurs, the device tries to fix it locally. If not possible, it simply reports back to the storage manager that the command failed. The storage manager then decides how to handle the error according to the application's needs.

Unfortunately, the storage interface abstraction has a side effect: It hides the large non-linearities, which stem from both the device's physical characteristics and the firmware algorithms, forcing both the storage manager and the device to make decisions in isolation. Unlike before, scheduling decisions (now taking place inside the device firmware below the interface) are made without knowledge of application access patterns. The device sees a small part of the pattern, whereas the storage manager may know the entire pattern. On the other hand, the storage manager is not provided with enough knowledge to turn access patterns into efficient I/O operations. As a result, there exist complex approaches that attempt to bridge this information gap in order to achieve better performance.

The solutions for bring more information across storage interface fall into three categories. The first category relies on implicit contract between devices and storage managers. The second category either explicitly or implicitly breaks the existing interface abstraction by making assumptions about the device's architecture and inner-workings. Finally, the third category proposes different APIs that enable better matching of (specific) application access patterns to the underlying characteristics.

2.2 Implicit storage contract

The simplest, and perhaps most extensively used, hints about non-linear access times to logical blocks are captured in an unwritten contract between the storage manager and the storage device. This contract states that

(i) LBNs near each other can be accessed faster than those farther away, and

(ii) accessing LBNs sequentially is much more efficient than random access.

As instructed by this contract, the storage manager attempts to issue larger, more efficient I/O requests whenever possible. A prime example is the Log-structured File System [Rosenblum and Ousterhout 1992]. LFS accumulates small writes into contiguous segments of logical blocks and writes them in one large, more efficient access. Multimedia servers exploit sequentiality by allocating contiguous logical blocks to the same stream [Bolosky et al. 1996; Santos and Muntz 1997; Vin et al. 1995]. With sufficient buffer space, a video server can issue large sequential I/Os well ahead of the time the data is actually needed. Storage devices adhere to this contract by implementing algorithms that detect sequentiality and issue prefetch requests in an anticipation of a future I/O issued by the host [Quantum Corporation 1999; Worthington et al. 1995]. Similarly, they dynamically rearrange data on the media to improve access locality [Ruemmler and Wilkes 1991; Wilkes et al. 1996].

2.2.1 Request size limitations

System software designers would like to always use large requests to maximize efficiency. Unfortunately, in practice, resource limitations and imperfect information about future accesses make this difficult. Four system-level factors oppose the use of ever-larger requests: (1) responsiveness, (2) limited buffer space, (3) irregular access patterns, and (4) storage space management.

Responsiveness

Although larger requests increase efficiency, they do so at the expense of higher latency. This trade-off between efficiency and responsiveness is a recurring issue in computer system design with a cost that can be particularly steep for disk systems. A latency increase can manifest itself in several ways. At the local level, the non-preemptive nature of disk requests combined with the long access times of large requests (35–50 ms for 1 MB requests) can result in substantial I/O wait times for small, synchronous requests. This problem has been noted for both FFS and LFS [Carson and Setia 1992; Seltzer et al. 1995]. At the global level, grouping

substantial quantities of data into large disk writes usually requires heavy use of write-back caching.

Although application performance is usually decoupled from the eventual write-back, application changes are not persistent until the disk writes complete. Making matters worse, the amount of data that must be delayed and buffered to achieve large enough writes continues to grow. As another example, many video servers fetch video segments in carefully-scheduled rounds of disk requests. Using larger disk requests increases the time for each round, which increases the time required to start streaming a new video. Section 5.6 quantifies the start-up latency required for modern disks.

Buffer space

Although memory sizes continue to grow, they remain finite. Large disk requests stress memory resources in two ways. For reads, large disk requests are usually created by fetching more data farther in advance of the actual need for it; this prefetched data must be buffered until it is needed. For writes, large disk requests are usually created by holding more data in a write-back cache until enough contiguous data is dirty; this dirty data must be buffered until it is written to disk. The persistence problem discussed above can be addressed with non-volatile RAM, but the buffer space issue will remain. For video servers, ever-larger requests increase both buffer space requirements and stream initiation latency [Chang and Garcia-Molina 1996; 1997; Keeton and Katz 1993].

Irregular access patterns

Large disk requests are most easily generated when applications use regular access patterns and large files. Although sequential full-file access is relatively common [Baker et al. 1991; Ousterhout et al. 1985; Vogels 1999], most data objects are much smaller than the disk request sizes needed to achieve good disk efficiency. For example, most files are well below 32 KB in size in UNIX-like systems [Ganger and Kaashoek 1997; Sienknecht et al. 1994] and below 64 KB in Microsoft Windows systems [Douceur and Bolosky 1999; Vogels 1999]. Directories and file attribute structures are almost always much smaller. To achieve sufficiently large disk requests in such environments, access patterns across data objects must be predicted at layout time.

Although approaches to grouping small data objects have been explored [Gabber and Shriver 2000; Ganger and Kaashoek 1997; Ghemawat 1995; Rosenblum and Ousterhout 1992], all are based on imperfect heuristics, and thus they rarely group things perfectly. Even though disk efficiency is higher, incorrectly grouped

data objects result in wasted disk bandwidth and buffer memory, since some fetched objects will go unused. As the target request size grows, identifying sufficiently strong inter-relationships becomes more difficult.

Storage space management

Large disk requests are only possible when closely related data is collocated on the disk. Achieving this collocation requires that on-disk placement algorithms be able to find large regions of free space when needed. Also, when grouping multiple data objects, growth of individual data objects must be accommodated. All of these needs must be met with little or no information about future storage allocation and deallocation operations. Collectively, these facts create a complex storage management problem. Systems can address this problem with combinations of pre-allocation heuristics [Bovet and Cesati 2001; Giampaolo 1998], on-line reallocation actions [Lumb et al. 2000; Rosenblum and Ousterhout 1992; Smith and Seltzer 1996], and idle-time reorganization [Blackwell et al. 1995; Matthews et al. 1997]. There is no straightforward solution and the difficulty grows with the target disk request size, because more related data must be clustered.

2.2.2 Restricted expressiveness

The implicit contract does not fully exploit the performance potential of a storage device. For example, it does not convey to the storage manager when larger I/O sizes, which put more pressure on the host resources, do not yield any additional performance benefit. It also unduly increases the complexity of both the storage manager and the storage device firmware. For example, both implement prefetch algorithms that increase the efficiency of sequential accesses, unnecessarily duplicating identical functionality. Using more expressive methods that complement this contract without breaking the storage interface abstractions, can provide additional benefit. They also simplify the implementation of both systems, as demonstrated in this dissertation.

2.3 Exploiting device characteristics

A lot of research has focused on exploiting device-specific characteristics to achieve better application performance. These solutions, however, usually break the storage abstractions, because they require device-specific knowledge. As a result, when a new storage device is placed into the system, these solutions do not yield the expected benefit; the storage manager has to be reprogrammed to adapt to the specific features of the new device. Other approaches rely on detailed models with

configurable parameters that must be manually tuned to a specific device [IBM Corporation 2000; McKusick et al. 1984; Shriver et al. 1998].

2.3.1 Disk-specific knowledge

Much recent related work has promoted zone-based allocation and detailed disk-specific request generation for small requests. The Tiger video server [Bolosky et al. 1996] allocated primary copies of videos to the outer portions of each disk's LBN space in order to exploit the higher bandwidth of the outer zones. Secondary copies were allocated to the lower bandwidth zones. VanMeter [1997] suggested that there was general benefit in changing file systems to understand that different regions of the disk provide different bandwidths.

By utilizing even more detailed disk information, several researchers have shown substantial decreases in small request response times [Chao et al. 1992; English and Stepanov 1992; Huang and cker Chiueh 1999; Wang et al. 1999; Yu et al. 2000]. For small writes, these systems detect the position of the head and re-map data to the nearest free block in order to minimize the positioning costs [Huang and cker Chiueh 1999; Wang et al. 1999]. For small reads, the SR-Array [Yu et al. 2000] determines the head position when the read request is to be serviced and reads the closest of several replicas.

The Gamma database system [DeWitt et al. 1990] accessed data in track-sized I/Os by simply knowing the number of sectors per track. Unfortunately, simple mechanisms like this are no longer possible because of high-level device interfaces and built-in firmware functions. For example, zoned geometries and advanced defect management in current disks result in cylinders being composed of tracks with variable number of sectors (see Table 3.1). No single value for the number of sectors per track is correct across the device.

Using disk drive track size to set the RAID stripe unit size improves I/O performance. Chen and Patterson [1990] developed a method for determining proper stripe unit for a disk array and concluded that a stripe unit near track size is optimal. Similar to the database case, however, a single value is not sufficient for modern multi-zoned disks; it does not realize the full potential of modern disk drives. Using values that *exactly* match track size, on the other hand, can do so as illustrated in Section 5.7.6. At the file system level, aligning access to stripe unit boundaries and writing full stripes avoids expensive read-modify-write operations for RAID 4 and RAID 5 configurations [Chen et al. 1994; Hitz et al. 1994].

2.3.2 Storage models

Various storage managers have built more detailed models of the underlying storage devices [McKusick et al. 1984; VERITAS Software Company 2000], but these models may not reflect the functions inside the device. In general, the process of building storage models is ad-hoc, device-dependent, and often does not provide the right abstractions. Many SMs just ignore details because of the complexity involved in handling the various protocols and mechanisms. The SMs that do require and use detailed-information, i.e., current disk-head position to achieve the promised performance gains [Chao et al. 1992; Lumb et al. 2000; Wang et al. 1999; Yu et al. 2000], use very detailed models tailored to one specific disk type [Kotz et al. 1994].

The Fast File System allocation of data into cylinder groups [McKusick et al. 1984] is based on the notion that related data and metadata should be put in the same cylinder to minimize seeks. Similarly, the data allocation allowed block interleaving to accommodate disks that could not read two consecutive sectors. Even though these algorithms (and their tuning knobs) still exist inside the FFS and its derivatives, they cannot be properly set because of the high-level interface that does not expose the necessary information.

Built-in models (e.g.,inside database systems [IBM Corporation 1994]) can receive parameter values in two different ways. The SM can query the storage device, or alternatively, these parameters can be manually set by an administrator. Naturally, the former approach is more desirable. However, today's systems do not provide an effective way of conveying this information that is device-independent.

Device-provided parameters

The SCSI interface includes a variety of additional commands that query and/or control the device's internal organization and behavior [Schmidt 1995]. For disk drives, these commands include information about data layout, and cache organization. However, current commands are not getting the job done because they are vendor-specific, proprietary, and often too oriented to the particulars of a single storage device type.

Manually-tuned parameters

Similar to file systems, database systems include data allocation and access algorithms that use device parameters to influence their decisions. These parameters are manually set by a database administrator (DBA). For example, IBM DB2's `EXTENTSIZE` and `PREFETCHSIZE` parameters determine the maximal size of a single

I/O operation [IBM Corporation 2000], and the `DB2_STRIPED_CONTAINERS` parameter instructs the storage manager to align I/Os on stripe boundaries. Database storage managers complement DBA knob settings with methods that dynamically determine the I/O efficiency of differently-sized requests by issuing I/Os of different sizes and measuring their response time. Unfortunately, these methods are error-prone and often yield sub-optimal results. These mechanisms are also quite sensitive and prone to human errors. In particular, high-level generic parameters make it difficult for the storage manager to adapt to the device-specific characteristics and dynamic changes to workload. This results in inefficiency and performance degradation.

2.3.3 Extending storage interfaces

Many works demonstrated how extending storage interfaces with functions that expose information about device specifics can improve application performance. The following paragraphs discuss three specific aspects of this research that include the freedom to rearrange requests to improve aggregate performance and better utilization of resources by exposing some additional information about storage organization.

Masking access latency

Recent efforts have proposed mechanisms that exploit freedom to reorder storage accesses in order to mask access latency. Storage latency estimator descriptors estimate the latency for accessing the first byte of data and the expected bandwidth for subsequent transfer [VanMeter 1998]. Steere [1997] proposed a construct, called a set iterator, that exploits asynchrony and non-determinism in data accesses to reduce aggregate I/O latency. The River projects use efficient streaming from distributed heterogeneous nodes to maximize I/O performance for data-intensive applications [Arpaci-Dusseau et al. 1999; Mayr and Gray 2000].

Other research has exploited similar ideas at the file system level. Parallel file systems achieve higher I/O throughput from the underlying, inherently parallel, hardware [Freedman et al. 1996; Krieger and Stumm 1997]. As demonstrated by Kotz [1994], a parallel file system rearranging application requests into larger, more efficient I/Os to individual disks provides significant improvements to scientific workloads. Similarly, I/O request criticality annotations based on file system and application needs provide greater scheduling flexibility at the storage subsystem level, resulting in better application performance [Ganger 1995].

Exposing information about device organization

Arpaci-Dusseau and Arpaci-Dusseau [2001] recently termed a system building practice that exploits knowledge of the underlying subsystem structure gray-box approach. Using such approach, Burnett et al. [2002] built algorithms, which can determine the OS management policies for buffer caches. Their findings can be extended to the storage manager (e.g., a file system), allowing it to determine which I/Os are going to be serviced from cache and schedule I/O requests accordingly.

Wong and Wilkes [2002] proposed new storage interface operations which enable more intelligent buffer management. Using promote/demote operations, the host and the storage device can explicitly coordinate which data is cached where, avoiding double buffering and hence effectively increasing the cache footprint.

Denehy et al. [2002] extended the gray box approach to building an interface between storage devices and file systems. This interface exposes parallelism and failure-isolation information to a log-structured file system, which can make dynamic decisions about data placement and balance load between individual disks of the exposed RAID group. Their approach is similar to the one presented here; the storage device provides hints to a file system storage manager, called I-LFS, which then adjusts its behavior to improve performance and reliability.

Object-based storage interface

The object-based storage interface, advocated by the NASD project [Gibson et al. 1998] and drafted as an ANSI interface specification [National Committee for Information Technology Standards 2002], proposes to use variable size objects, instead of fixed size blocks, as the interface between hosts and storage devices. These higher level semantics pass hints to the storage device. Combined with the ability to assign various attributes to different objects, these hints can be used within the storage device to allow, for example, object collocation and other performance-related operations behind the object-based storage interface. However, there must still exist some kind of a storage manager within the storage device to be able to allocate and manage the individual blocks of the storage media and map them into an object exported by the storage interface. Although the storage manager is now found on the opposite side of the physical interface, the work explored in this dissertation is suited to this object model as well.

Applications providing hints to storage managers

Patterson et al. [1995] proposed a mechanism, called informed prefetching and caching, whereby applications provide hints about intended access patterns to a

storage manager, called TIP. Based on these hints, which are inserted by the application programmer, the storage manager makes a decision which blocks it should prefetch, cache for reuse, or discard. TIP uses cost-benefit analysis to allocate buffers when they have the biggest impact on application performance. Brown et al. [2001] devised a method for using compiler-generated hints about out-of-core application access patterns. The hints, which are similar to those manually generated for TIP, inform an operating system buffer manager which data are likely to be accessed in the future and which are likely no longer needed. With such information, the manager can discard data no longer needed and prefetch data ahead of the time they are actually accessed.

While this dissertation takes the approach of exposing information from the lower layers up, the two approaches are complimentary. The performance attributes advocated in this dissertation allow a storage manager (e.g., TIP or the virtual memory manager) to efficiently execute prefetching requests and compute more accurate estimates for the costs of different access patterns.

2.4 Device performance characterization

Worthington et al. [1995] have described methods for retrieving various parameters from SCSI disk drives for several disk drives. The combination of interrogative and empirical extraction techniques can determine information about disk geometry, data layout, mechanical overheads, cache behavior, and command processing overheads. The accuracy of these techniques has been evaluated by a highly-configurable disk simulator called DiskSim [Bucy and Ganger 2003]. This event-driven simulator offers over 100 parameters characterizing the disk drive module, though some are dependent on others or meaningful only in certain cases.

Talagala et al. [2000] extracted approximate values for disk geometries, mechanical overheads and layout parameters using micro-benchmarks consisting of only read and write requests, by timing the requests with progressively increasing request strides. Their approach is independent of the disk's interface and thus works for potentially any disk. The emphasis being on extracting approximate values quickly, their algorithms achieve lower accuracy of the extracted information than the combination of interrogative and empirical extraction for SCSI disks.

2.5 Accesses to multidimensional data structures

Mapping multi-dimensional data structures (e.g., large non-sparse matrices or database tables) into a linear LBN space without providing additional information to applications generally makes efficient access possible only along one

dimension. However two important classes of systems, namely relational database systems and data-intensive out-of-core scientific computation applications, often access data along multiple dimensions. Thus, they can benefit from methods that can allow efficient accesses along multiple dimensions without the need to reorganize data every time their access patterns change.

2.5.1 Database systems

Relational database management systems (DBMS) facilitate efficient access to two-dimensional structured data in response to application's or user's requests (a.k.a. queries). A component of a relational DBMS, usually called the storage manager, is responsible for the layout of two-dimensional tables (relations) and facilitation of efficient accesses to these tables. Access patterns are governed by the type of query and depend on data layout within and across relations. Ultimately, they are determined by a query optimizer whose goal is to minimize the overall query execution cost.

At a high level, database access patterns can be divided into two broad categories: random accesses or regular accesses (either in row- or column-major) to a portion of data in a table. The former access pattern is a result of point queries. Whenever possible, point queries use an index structure to determine the address where the data is stored. Walking through the index and fetching the desired data typically results in random accesses. The latter access type is called scan and it is a basic building block for the SELECT, PROJECT, and JOIN relational operators when indexes cannot be used. Thus, the main responsibility of a database storage manager is to ensure efficient execution of these operations for a variety of workloads executing different queries against the two-dimensional relations.

Data organization

Today's DBMSs leverage the efficiency of sequential accesses, stated in the unwritten contract, for laying out 2D relational tables. They predict the common order of access by a workload and choose a layout optimized for that order, knowing that accesses along the other major axis will be inefficient.

In particular, online transaction processing (OLTP) workloads, which make updates to full records, favor efficient row-order access. On the other hand, decision support system (DSS) workloads often scan a subset of table columns and get better performance using an organization with efficient column-order access [Ramamurthy et al. 2002]. Without explicit support from the storage device, however, a DBMS system cannot efficiently support both workloads with one data organization.

The different storage models (a.k.a. page layouts) employed by current DBMSs trade the performance of row-major and column-major order accesses. The page layout prevalent in commercial DBMSs, called the N-ary storage model (NSM), stores a fixed number of full records (all n attributes) in a single page (typically 8 KB). This page layout is optimized for OLTP workloads with row-major access and random I/Os. This layout is also efficient for scans of entire tables; the DBMS can sequentially scan one page after another. However, when only a subset of attributes is desired (e.g., the column-major access prevalent in DSS workloads), the DBMS must fetch full pages with *all* attributes, effectively reading the entire table even though only a fraction of the data is needed.

To alleviate the inefficiency of column-major access with NSM, a decomposition storage model [Copeland and Khoshafian 1985] (DSM) vertically partitions a table into individual columns. Each DSM page thus contains a *single* attribute for a fixed number of records. However, fetching full records requires n accesses to single-attribute pages and $n - 1$ joins on the record ID to reconstruct the entire record.

The stark difference between row-major and column-major efficiencies for the two layouts described above is so detrimental to database performance that Ramamurthy et al. [2002] proposed maintaining two copies of each table to avoid it. This solution requires twice the capacity and must propagate updates to each copy to maintain consistency. The PARALLELISM attribute proposed in this dissertation eliminates this need for two replicas while allowing efficient access in both orders.

Exploiting device characteristics

Memory latency has been recognized as an increasingly important performance bottleneck for some compute- and memory-intensive database applications [Ailamaki et al. 1999; Boncz et al. 1999]. To address the problem, recent research proposed two approaches to improving the utilization of processor caches: (i) employing data layouts utilizing cache characteristics and (ii) incorporating the cost of different memory access patterns into query optimization costs.

The first approach uses a new data page layout [Ailamaki et al. 2001] and indexing structures [Chen et al. 2002; Rao and Ross 1999] tailored to cache characteristics. The cache-sensitive data layout, called PAX, partitions data into clusters of the same attribute and aligns them on cache line boundaries. This organization minimizes the number of cache misses and leverages prefetching (fetching whole cache line) when sequentially scanning (in memory) through a subset of table columns (attributes). The second approach factors processor cache access parameters into the optimization process by incorporating data access pattern and cache characteristics into the query operator cost functions [Manegold et al. 2002].

The previously proposed techniques optimize cache and memory accesses. This dissertation extends that work by bridging the performance gap between non-volatile memory (storage devices) and main memory. For example, similar to in-page data partitioning, the storage manager can allocate data on ACCESS DELAY BOUNDARIES and prefetch them in extents corresponding to the number of LBNs between two consecutive boundaries. The PARALLELISM attribute gives database storage managers the flexibility to request just the data needed by the query. With a single data layout, it can request data both in row- and column-major orders while utilizing the available access parallelism to achieve maximal aggregate bandwidth afforded by the particular access pattern.

2.5.2 Scientific computation applications

Scientific applications access large sets of data to perform calculations. To provide the required bandwidth, application runtime environments spread data across many disks to leverage access parallelism and speed up execution time.

Since I/O operations are the dominant factor in execution time, parallel algorithms strive to minimize the amount of data transfered between main memory and non-volatile storage. The parallel disk model (PDM) [Vitter and Shriver 1994] has become the de facto standard for analyzing algorithm performance. It expresses algorithm execution time in terms of four parameters: N is the number of items in the problem instance, M is the number of items that can fit into main memory, B is the number of items per disk block, and D is the number of disks. This model, however, does not account for different access efficiencies of sequential and random I/O [Vengroff and Vitter 1995].

Execution environments for parallel applications include interfaces for parallel I/O, memory management, and communication with remote processors. Parallel I/O can be realized by parallel filesystems [Corbett and Feitelson 1994; Krieger and Stumm 1997] or direct block access [Kotz et al. 1994; Vengroff 1994]. Regardless of the specific mechanism, these components collectively provide the functions of a storage manager – data layout across parallel-accessible storage devices and I/O execution.

Data organization

Many out-of-core parallel algorithms do I/O in memory loads; that is, they repeatedly load some subset of the data into memory, process it, and write it out. Each transfer is a large, but not necessarily contiguous, set of data [Kotz et al. 1994]. The memory load operations include scanning and sorting [Vengroff and Vitter 1995] and bit-permute/complement permutations [Cormen 1993] of one-

dimensional data (a.k.a. streams). The streams are striped across all the available storage devices to achieve access parallelism.

Another type of parallel algorithms accesses two-dimensional data structures to perform linear algebra operations on large matrices such as LU factorization and matrix multiply. These operations form the basis for many scientific applications; their kernels are used as benchmarks for parallel computers running scientific out-of-core applications [Bailey et al. 1993]. The majority of these operations access one element in row-major and the other in column-major. Depending on the type of operation, the two elements can be two different matrices (matrix multiply), the same matrix (LU factorization), or a matrix and a vector (solving a linear system $Az = x$). With current storage device abstractions, the data organization has shortcomings similar to relational databases — one of the matrix dimensions is chosen as the primary access order (typically row-major) [Vengroff and Vitter 1995], to take advantage of the unwritten contract's efficient sequential access. Naturally, access along the other order is less efficient.

A third type of scientific applications performs range queries through multi-dimensional space. To perform these searches efficiently, application execution environments use indexing structures (e.g., K-D-B-tree, R*-tree, and B-tree). When applications execute point and range queries in multi-dimensional space, the execution environment uses these index structures for data access [Arge et al. 2002].

The three types of scientific computing applications exhibit access patterns that are very similar to the common access patterns exercised by database systems. The access patterns of the first application type are analogous to regular, but not necessarily purely sequential, accesses to relational tables with the SELECT, PROJECT, and JOIN operators. The second type of applications accesses two-dimensional structures in row- or column-order. Finally, the third type of applications exercises access patterns that are analogous to random accesses of OLTP workloads through index structures.

Exploiting device characteristics

It is apparent from the preceding paragraphs that execution of scientific applications is indeed similar to query execution in relational DBMS. Both use optimization techniques for minimizing I/O costs and exercise similar access patterns. Just like for database systems, exposing performance attributes to the storage managers of scientific applications can improve their execution.

The ACCESS DELAY BOUNDARIES attribute can yield more efficient execution of the first two types of scientific applications; a storage manager can match I/O size (i.e., the block size, B, of the parallel disk model) to the number of LBNs

between two consecutive boundaries. The PARALLELISM attribute is instrumental for the second type of applications in determining the mapping of two-dimensional matrices. It can ensure efficient access in both dimensions as well as help the first type of applications exploit the level of parallelism inherent to the storage device. Not only can the PDM D parameter be automatically matched to the p value of the PARALLELISM attribute, but the explicit LBN mappings provided by the storage device will allow application execution environments' storage managers to properly map data structures to ensure parallel access. Since the accesses of the third type of scientific applications are mostly random, the overall benefit of exposing performance attributes will have only a limited effect; this is analogous to OLTP workloads in database systems.

This dissertation focuses on evaluating the benefits of exposing performance attributes to database systems. However, we believe that the results reported here are equally applicable to scientific computation applications given their similarity to database systems and the similarity of access patterns they exercise.

3 Explicit Performance Characteristics

A carefully designed storage interface can provide device-specific performance characteristics and encapsulate them in device neutral attributes. These attributes annotate the linear address space of fixed-size blocks, identified by a logical block number (LBN), which is a storage device abstraction provided by current interfaces such as SCSI or IDE [Schmidt et al. 1995]. With these annotations, a piece of host software, called the storage manager (SM), can match application access patterns to these explicitly stated characteristics, take advantage of the device's unique strengths, and avoid accesses that are inefficient.

This chapter describes the storage interface model and the mechanisms for conveying performance attributes. It also describes performance characteristics of devices for secondary storage. It describes the characteristics of disk drives (the most prevalent on-line storage device in today's systems), disk arrays, and MEMS-based storage devices (MEMStore) [Carley et al. 2000] that are still being researched. These devices are expected to complement or even replace disk drives as on-line storage in the future [Schlosser et al. 2000; Uysal et al. 2003]. Finally, it discusses how these characteristics influence different access patterns.

3.1 Storage model

The storage model, depicted in Figure 3.1, builds upon established computer systems architecture, which consists of, among others, two components relevant to this dissertation: a host and a storage device. The host (e.g., a web server) is a separate component that includes memory and a general purpose CPU capable of running various applications. The storage device includes the media for non-volatile storage and any additional hardware required for control and access to this media. These controllers may include ASICs, memory, and even CPUs.

A high-level storage interface cleanly separates the host functions from those of the storage device. It abstracts device-specifics away from the host, allowing it to work transparently with any storage device. This dissertation extends this interface to provide performance information to the applications running on the host,

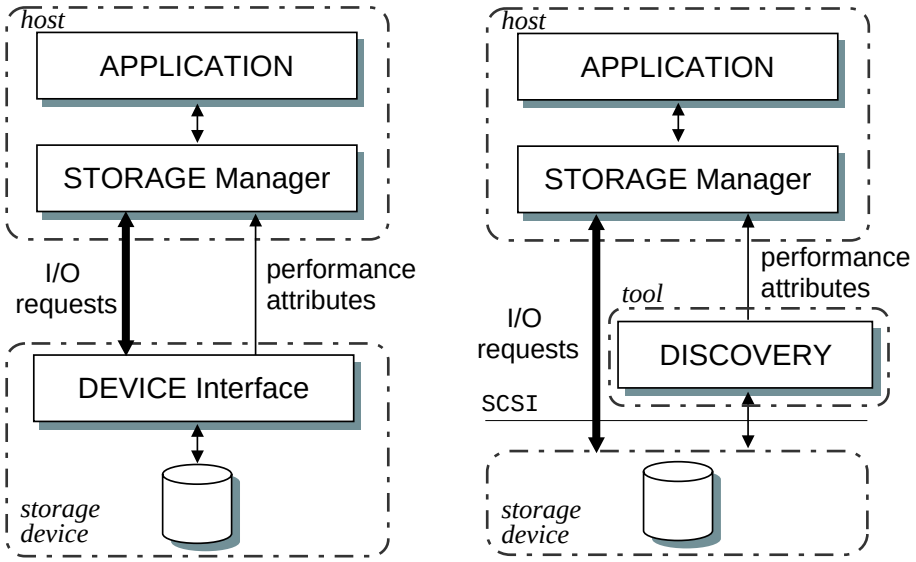

(a) **Storage model.** (b) **Discovery tool.**

Fig. 3.1: **Two approaches to conveying storage device performance attributes.** Figure (a) illustrates a host and a storage device that communicate via the extended interface that conveys the necessary performance attributes. The device interface is physically a part of the storage device. Figure (b) shows an alternate apporach where the storage device speaks through a conventional SCSI. A device-specific discovery tool extracts performance chatacteristics and exports them to the SM. Note that the same SM works with either approach.

while requiring minimal changes to the host software and maintaining the established interface abstractions. With these explicit hits, encapsulated in performance attributes, hosts can adjust their access patterns and thus utilize device-unique features to transparently improve application performance. These attributes are expressed in a device-neutral way and are provided by the device; applications do not require manual tuning. Thus, they also simplify the task of storage administration.

3.1.1 Storage manager

At the most basic level, a storage manager is a piece of software running on the host that translates API calls, originating from the host application, to I/O requests that are issued to the storage device. The SM uses a set of policies and mechanisms that harmonize application needs with efficient I/O accesses. The SM fulfills three different roles for applications: (i) data allocation, (ii) data access, and (iii) buffer management. The application simply requests data in the format prescribed by the API; it is not concerned with where the data is and how it is retrieved.

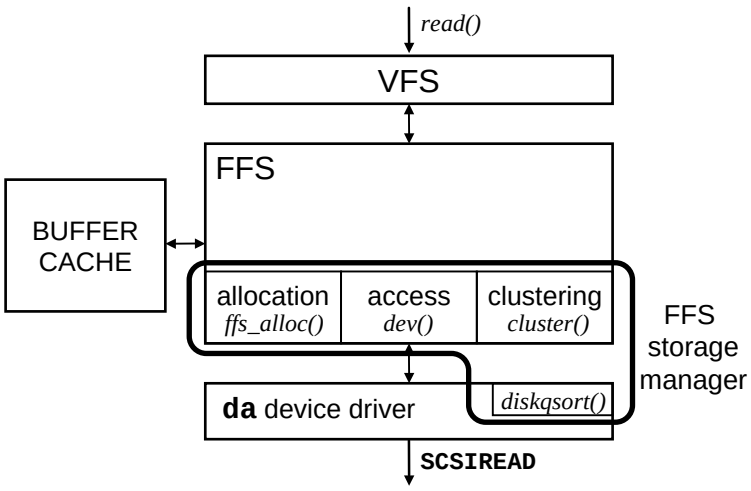

Fig. 3.2: **Mapping of application *read()* calls to storage device** READ **requests by a FFS storage manager.** The application system call enters the virtual file system. The call then enters the FFS and is handled appropriately either from the buffer cache or from the storage itself. The device is accessed by a device driver that includes a request scheduler (implemented by the *diskqsort()* function). Note that the storage manager includes various functions that are spread out in different parts of the kernel.

There are many different, and often specialized, SMs. For example, they can be built into a file system, which itself is a part of an OS, or be a part of specialized applications (e.g., databases) that bypass the OS file system and talk directly to storage devices. They can even be a part of a storage subsystem; for example many high-end storage arrays include an SM that maps logical volumes to back-end storage devices. In this case, the storage manager is physically collocated with the storage device where it manages the underlying storage devices, but not the array itself.

Architecturally, the SM and the application are separate, as depicted in Figure 3.1. In practice, the storage manager can be entangled with the application code. For example, the functions of BSD's Fast File System (FFS) that constitute the storage manager, as depicted in Figure 3.2, communicate directly with the functions for file management (e.g., access control, naming etc.). In this case, the API between the storage manager and the FFS "application" are individual file system blocks. It is the responsibility of the storage manager to assign individual LBNs to the file system blocks and to collocate file system blocks of the same file. The FFS application merely requests the appropriate file system blocks of a given file.

Data allocation

Data allocation performed by an SM utilizes knowledge of application needs. It receives hints, either explicitly or implicitly, that disclose application's intents. Using the FFS as an example, the file system tells a storage manager that it needs to allocate new blocks for this file when new data is appended to a particular file. With this information, the SM can make an intelligent decision and allocate new blocks next to the already-allocated ones. This enables the efficient execution of a sequential access pattern to the file, thanks to the implicit storage contract described in Section 2.2. More generally, a storage manager uses *static* information, both from the application and the storage device, to make a decision in anticipation of likely application behavior (e.g., sequential access).

Data access

While allocation decisions are based on static information, data access is a result of the application's dynamic state. Using the FFS example, when several applications want to simultaneously read several files, the resulting accesses are a mix of the sequential file accesses originally anticipated by the applications. The I/Os seen by the storage device, however, are not sequential and hence much less efficient. Thus, the storage manager makes a dynamic decision that balances the needs of all applications without undue performance penalty. Providing static information about performance characteristics to the storage manager can help it make these decisions about *dynamic* behavior. With explicit performance attributes, the storage device can hint at proper I/O sizes that will be turned into efficient accesses by the device's internal mechanisms.

3.1.2 Storage devices

A storage device is any device that can hold data for at least a limited amount of time, such as a disk drive, tape, high-performance storage array, or even a cache appliance [Network Appliance, Inc. 2002; Tacit Networks 2002]. It communicates with the storage manager via a well-defined storage interface. This device interface encapsulates the specifics of the device's underlying mechanisms into device-independent performance attributes of the storage interface as shown in Figure 3.1.

A storage device, however, need not support the proposed storage interface. An existing device that communicates via traditional storage protocols (e.g., SCSI or IDE) can sit behind a specialized performance characteristics discovery tool. This tool then substitutes the functionality of the device interface, which would normally export a device's performance attributes (see Figure 3.1(b)).

The architecture that includes the discovery tool has two advantages. First, it allows device performance characteristics, not normally communicated via their interfaces, to be exploited. Second, it does not require any changes to the host SM. When a new device is added to the system, it is plugged in together with a new discovery tool. Transparent to the storage manager, the tool knows how to extract the device's performance characteristics. The downside of this approach is that the discovery tool may not work with the storage device.

Ideally, a discovery tool would be supplied by the storage device manufacturers and implemented, for example, within a device driver. This way, the tool can also exploit proprietary interfaces to communicate with the storage device. Although labor intensive, it is also possible to build a discovery tool for a device that support just standard READ and WRITE commands. Such a tool can assemble test vectors of individually timed READ and WRITE commands [Worthington et al. 1995] to determine device characteristics.

These test vector requests can be either interjected into the stream of requests coming from the storage manager or the discovery can be made off-line as a one-time cost during device initialization. The advantage of the former approach is that the discovery tool can dynamically tune the performance attributes at a cost of interfering with the normal stream of requests. The latter approach does not slow down the device, but depending on the type of the device, its characteristics may change over time due to device's internal optimizations or grown media defects.

Chapter 4 describes a discovery tool that can accurately extract detailed disk drive performance characteristics. While it is specific to a particular type of storage device (it uses assumptions about the innards of the particular device), it fulfills its role; the device-specifics do not propagate to the storage manager. This ensures that the same storage manager can utilize the new device's performance characteristics without any modifications to the SM code. More importantly, it allows us to experimentally evaluate the architecture described in this dissertation.

3.1.3 Division of labor

Both components in the storage model make decisions that are governed by what information is readily available at the component and what additional information, if any, will be provided by the other component. The storage manager controls how application access patterns are turned into individual requests to the storage device. It can make better informed decisions than the storage device itself because it has more context about application activities. To aid the SM in deciding what access patterns its storage requests should use, the device provides static hints to the SM.

Dynamic decisions that depend on the current state of the storage device (e.g., current position of the read/write heads, or the content of prefetch buffers) should be made below the interface. A storage manager should relegate these device-specific decisions (e.g., I/O request scheduling) to the storage device where they can be made more efficiently. Instead, the SM is only concerned with generating I/Os that can be executed efficiently. How these I/Os are executed, however, is decided by the device.

The FFS storage manager example in Figure 3.2 includes a C-LOOK scheduling algorithm (a variant of a SCAN algorithm [Denning 1967], which is implemented as a part of the *diskqsort()* routine). The FFS scheduler makes its decisions on a crude notion of relative distances in the LBN space. Instead, the scheduling should be pushed down to the device, where it can be made more efficiently with more detailed information (for instance, by using a SPTF scheduler [Seltzer et al. 1990; Worthington et al. 1994], which is built into modern disk drive firmware [Quantum Corporation 1999]).

3.1.4 LBN address space annotations

A storage device exports static performance attributes that annotate the linear address space of fixed-size blocks, identified by a logical block number (LBN). This annotation creates relations among the individual LBNs of the storage interface. Given an attribute with particular semantics and a single LBN, other LBNs satisfying the relation described by the attribute are returned.

This dissertation describes in detail two examples of these attributes and evaluates the benefits these attributes have for a variety of applications and workloads.

– ACCESS DELAY BOUNDARIES

  This attribute denotes preferred storage request access patterns (i.e., the sets of contiguous LBNs that yield most efficient accesses). This attribute encapsulates *traxtent* (an extent of LBNs mapped onto one disk drive track) [Schindler et al. 2002] or a stripe unit in RAID configurations. This attribute captures the following notions: (i) requests that are exactly aligned on the reported boundaries and span all the blocks of a single unit are most efficient, and (ii) requests smaller than the preferred groupings, should be aligned on the boundary. If they are not aligned, they should not cross it.

– PARALLELISM

  Given an LBN, this attribute describes which other LBNs can be accessed in parallel. The level of parallelism depends on the striping and RAID groups and the number of spindles. For example, a logical volume of a storage array

that has n mirrored replicas can access up to n different LBNs in parallel. Similarly, a MEMStore can access a collection of LBNs in parallel thanks to the many read/write tips that move in unison.

Denehy et al. [2002] describe other attributes, not pertaining to performance, that annotate a device's LBN address space. These attributes describe different fault isolation domains that occur due to different RAID levels and mappings of LBNs of a single logical volume to disks with different performance characteristics. They can be exposed in much the same way as the performance attributes described in this dissertation.

3.1.5 Storage interface

The following functions allow storage managers to take advantage of the performance attributes described above and use them during data allocation and access. Each function is described in more detail in the subsequent chapters devoted to the respective attributes. Appendix B lists the C definition of all storage inteface functions.

get_parallelism(*LBN****)*** returns the number of blocks, p, that can be accessed by the storage device in parallel with the provided LBN.

get_equivalent(*LBN****)*** returns a set of disjoint LBNs, called an equivalence class, E_{LBN}, that can be potentially accessed together. A set of p equivalence class members can be accessed in parallel.

get_ensemble(*LBN****)*** returns the exact access delay boundaries, LBN_{min} and LBN_{max}, where $LBN_{min} \leq LBN \leq LBN_{max}$.

batch() marks a batch of READ and WRITE commands that are to access the media in parallel.

Conceptually, the storage device interface provides the functions that are called by the storage manager. In practice, going from the storage manager to the storage device across a bus or network with every function call is too expensive. Thus, these functions should be implemented within the storage device driver and run locally at the host. During system initialization, the storage device can provide the necessary parameters to the device driver. The device driver then uses these parameters to figure out any associations among the LBNs and return them to the storage manager.

Alternatively, these functions could be implemented with commands already defined in the SCSI protocol. The *get_parallelism()* function can be implemented

by INQUIRY SCSI command. The *batch()* function corresponds to linking individual SCSI commands with the Link bit set. SCSI linking ensures that no other commands are executed in the middle of the submitted linked batch. The *get_ensemble()* function maps to the READ CAPACITY SCSI command with the PMI bit set. According to the specification, this command returns the last LBN before a substantial delay in data transfer. The *get_equivalent()* function can use the MODE SENSE SCSI command to return a list of LBNs in a new mode page. However, because of the performance penalties described above, the SCSI interface should not implement these functions. Instead, the SCSI Mode Pages should only provide the information necessary for local execution of these functions.

3.1.6 Making storage contract more explicit

Exposing performance characteristics by annotating the LBN address space fits well with current system designs. It builds upon, rather than replaces, the implicit storage contract. Providing more explicit performance hints allows storage managers to make better, more informed decisions. Because of this contract, storage managers administer devices in fixed blocks that make allocation policies and space management easier. Extent-based file systems are one example [McVoy and Kleiman 1991; VERITAS Software Company 2000]. Other storage managers group individual LBNs into larger blocks (e.g., file system blocks or database pages) to be used by the API above a storage manager.

Developing mechanisms that minimize the changes required to take advantage of the performance benefits described in the subsequent chapters is one of the goals of this research. As a consequence of this decision, these mechanisms are still based on best-effort performance. These static annotations, by themselves, do not provide any performance guarantees suitable for quality-of-service applications. However, they aid in building such applications, as demonstrated in Section 5.6.

The more explicit contract between a storage manager and storage devices promoted in this dissertation does not limit the storage device. It is free to apply dynamic optimizations behind the storage interface as long as the contract stays in place. For example, it can dynamically remap logical blocks to different areas of storage device to better accomodate the needs of the application.

3.2 Disk drive characteristics

Disk drives are the most prevalent storage device in today's computer systems. Desktops use single disk drives while high-end storage systems aggregate several. Grouping disk drives into a single logical volume enhances performance and failure protection [Patterson et al. 1988]. A logical volume is thus an abstraction of a

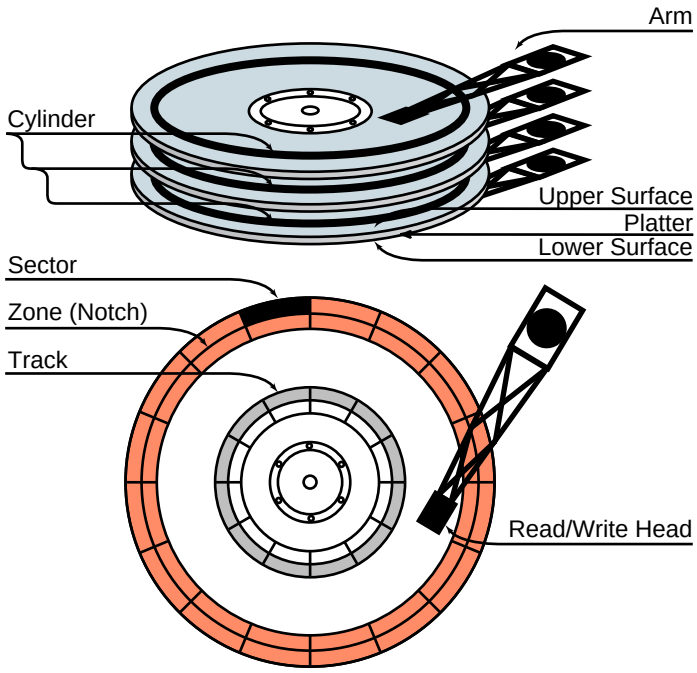

Fig. 3.3: **The mechanical components of a modern disk drive.**

storage device with a linear address space whose LBNs are mapped to the LBNs of the individual disks comprising the logical volume. This section describes the components of disk drives with an impact on I/O performance.

3.2.1 Physical organization

As depicted in Figure 3.3, a disk drive consists of a set of round platters that rotate on a spindle. Each platter is coated with magnetic media on both sides and each surface is accessed by a separate read/write head. The head is attached to an arm and the set of arms holding all read/write heads pivots the radius of the platter to access all media as the platter spins around. All heads share a channel responsible for transforming the magnetic signal into bit values. Thus only one head can be engaged at any time, accessing data on only one surface.

The magnetic media is formatted into concentric circles called tracks. A single track is divided into individual 512-byte sectors, each uniquely addressable. The set of tracks on all surfaces with the same circumference is called a cylinder. Since the inner tracks have smaller circumference than the outer ones, they contain fewer sectors. A set of cylinders consisting of tracks with the same number of sectors per track is called a zone. Disk platters of a typical 2003 disk drive are approximately 2.5 in. in diameter and include 8 to 15 zones. The ratio of sectors per track of the

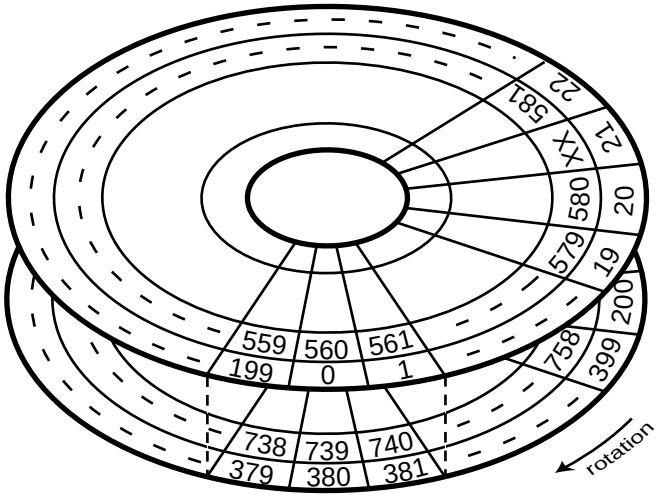

Fig. 3.4: **Typical mapping of LBNs onto physical sectors.** For clarity, this disk maps LBNs only onto a single surface of a platter. Normal disks map those on both surfaces before moving to the next platter.

outermost and innermost zone is slightly less than two (typically 1.6–1.8). More details on current disk characteristics are given by Anderson et al. [2003].

To access data on the disk, the set of arms pivots to seek to a cylinder with a particular radial distance from the center of the platter. Once the set of arms is positioned and the correct head engaged, the head waits for the requested data to rotate around. This is commonly referred to as rotational latency. When the desired set of sectors arrives underneath the head, the disk starts media transfer. If the set of contiguous LBNs of a single I/O request spans two tracks, the disk head must move the the adjacent cylinder or another head must be engaged to read the second track of the same cylinder. Since the individual tracks comprising a cylinder are not perfectly aligned, the head needs to be repositioned above the correct track. Collectively, this is called head switch.

The disk can start bus transfer of the data as soon as the data starts streaming from the media. Alternatively, the disk can buffer the data and transfer them all at once. The latter approach has the advantage that the interconnect between the disk and the host is not blocked for extended periods of time; bus transfer is usually faster than media transfer.

3.2.2 Logical block mappings

Disk drives map the LBNs of the linear space abstraction to physical sectors. The LBNs are assigned sequentially on each track with the subsequent LBN

being assigned to the nearest track that is either part of the same, or immediately adjacent, cylinder. This mapping is optimized for the unwritten contract, where as many sectors as possible are read before repositioning the read/write heads to a new location.

Figure 3.4 illustrates the mapping of LBNs onto disk media. The depicted disk drive has 200 sectors per track, two media surfaces, and a track skew of 20 sectors. Logical blocks are assigned to the outer track of the first surface, the outer track of the second surface, the second track of the first surface, and so on. The track skew accounts for the head switch delay to maximize streaming bandwidth. Figure 3.4 also shows a defect between the sectors with LBNs 580 and 581, depicted as XX, which has been handled by slipping. Therefore, the first LBN on the following track is 599 instead of 600.

3.2.3 Mechanical characteristics

Head switch

A head switch occurs when a single request accesses a sequence of LBNs whose on-disk locations span two tracks. The head is switched when the drive turns on the electronics for the appropriate read/write head and adjusts the head's position to account for inter-surface alignment imperfections. The latter step requires the disk to read servo information to determine the head's location and then to shift the head towards the center of the second track. In the example of Figure 3.4, head switches occur between LBNs 199 and 200, 399 and 400, and 598 and 599.

Compared to other disk characteristics, head switch time has improved little in the past decade. While disk rotation speeds have improved by 3× (from 5400 to 15000 RPM) and average seek times by 2.5×, head switch times have decreased by only 20–40% (see Table 3.1). At 0.6–1.1 ms, a head switch now takes about 1/5–1/4 of a revolution for a current 15,000 RPM disk while a decade ago it was less than 1/10. This trend has increased the significance of head switches in terms of read/write latencies. This situation is expected to worsen; rapid decreases in inter-track spacing require increasingly precise head positioning.

Naturally, not all requests span track boundaries. The probability of a head switch, P_{hs}, depends on workload and disk characteristics. For a request of S sectors and a track size of N sectors, $P_{hs} = (S-1)/N$, assuming that the requested locations are uncorrelated with track boundaries. For example, with 64 KB random evenly distributed requests ($S = 128$) and an average track size of 192 KB ($N = 384$), a head switch occurs for every third access, on average.

A storage manager using a disk drive that encapsulates explicit boundaries into the ACCESS DELAY BOUNDARIES attribute can use this information to enforce

Disk	Year	RPM	Head Switch	Avg. Seek	Sectors per Track	Number of Tracks	Capacity
HP C2247	1992	5400	1 ms	10 ms	96–56	25649	1 GB
Quantum Viking	1997	7200	1 ms	8.0 ms	216–126	49152	4.5 GB
IBM Ultrastar 18 ES	1998	7200	1.1 ms	7.6 ms	390–247	57090	9 GB
IBM Ultrastar 18LZX	1999	10000	0.8 ms	5.9 ms	382–195	116340	18 GB
Quantum Atlas 10K	1999	10000	0.8 ms	5.0 ms	334–224	60126	9 GB
Fujitsu MAG3091	1999	10025	0.7 ms	5.2 ms	420–273	49125	9 GB
Quantum Atlas 10K II	2000	10000	0.6 ms	4.7 ms	528–353	52014	9 GB
Seagate Cheetah X15	2000	15000	0.8 ms	3.9 ms	386–286	103750	18 GB
Seagate Cheetah 36ES	2001	10028	0.6 ms	5.2 ms	738–574	105208	36 GB
Maxtor Atlas 10K III	2002	10000	0.6 ms	4.5 ms	686–396	124088	36 GB
Fujitsu MAN3367MP	2002	10025	0.6 ms	4.5 ms	738–450	118776	36 GB

Table 3.1: **Representative SCSI disk characteristics.** Note the small change in head switch time relative to other characteristics. Although there exist versions of the Seagate Fujitsu, and Maxtor drives with higher capacities, the lower capacity drives are typically installed in disk arrays to maximize the number of available spindles.

track-aligned access. This improves the response time of most requests by the 0.6–1.1 ms head switch time. For a conventional system that is not aware of track boundaries, almost every request will involve a head switch as S approaches N.

Seek

Since a seek involves moving the set of arms from one radial location (i.e., cylinder) to another, seek time is expressed as a function of cylinder distance rather than as a function of distance in the LBN space. Figure 3.5 shows seek profiles for representative disks from Table 3.1. For small distances (i.e., several cylinders) and medium distances, the seek time profile follows a curve that can be approximated by $\sqrt{d}$, where d equals cylinder distance [Ruemmler and Wilkes 1993]. For sufficiently large d, the seek time is a linear function of cylinder distance. Finally, the average seek time listed in Table 3.1 corresponds to d being equal to 1/3 of the full-strobe seek distance; the average seek value of every possible distance from every possible location on the disk.

Thanks to a steady increase in linear bit densities in today's disk, more LBNs fit within a track (e.g., 686 for a 2002 Maxtor Atlas 10K III disk vs. 96 for a 1992 HP C2247) and due to improvements in servo technology, a seek of a few cylinders, for some disks up to five, is now equivalent to a head switch. With these two trends combined, an increasingly larger number of LBNs can be serviced with a fixed positioning cost.

Rotational speed

Another factor that contributes to the total positioning cost is rotational latency. Even though rotational speed improvements have kept up with improvements in seek times, accessing two randomly chosen locations within a few cylinders (i.e., a few thousand LBNs away) will produce, on average, a rotational latency of half a revolution. Compared to a short-distance sub-millisecond seek, this 2–3 ms delay becomes increasingly more important. With properly chosen access patterns able to exploit firmware features that minimize the impact of rotational latency, as discussed in the next section, the access cost penalty can be minimized to that of a seek.

3.2.4 Firmware features

Zero-latency access and scheduling are two prominent disk firmware features that improve I/O performance by reducing the time disk head is not transferring data. With all else being equal, overall request service time is reduced and thus the

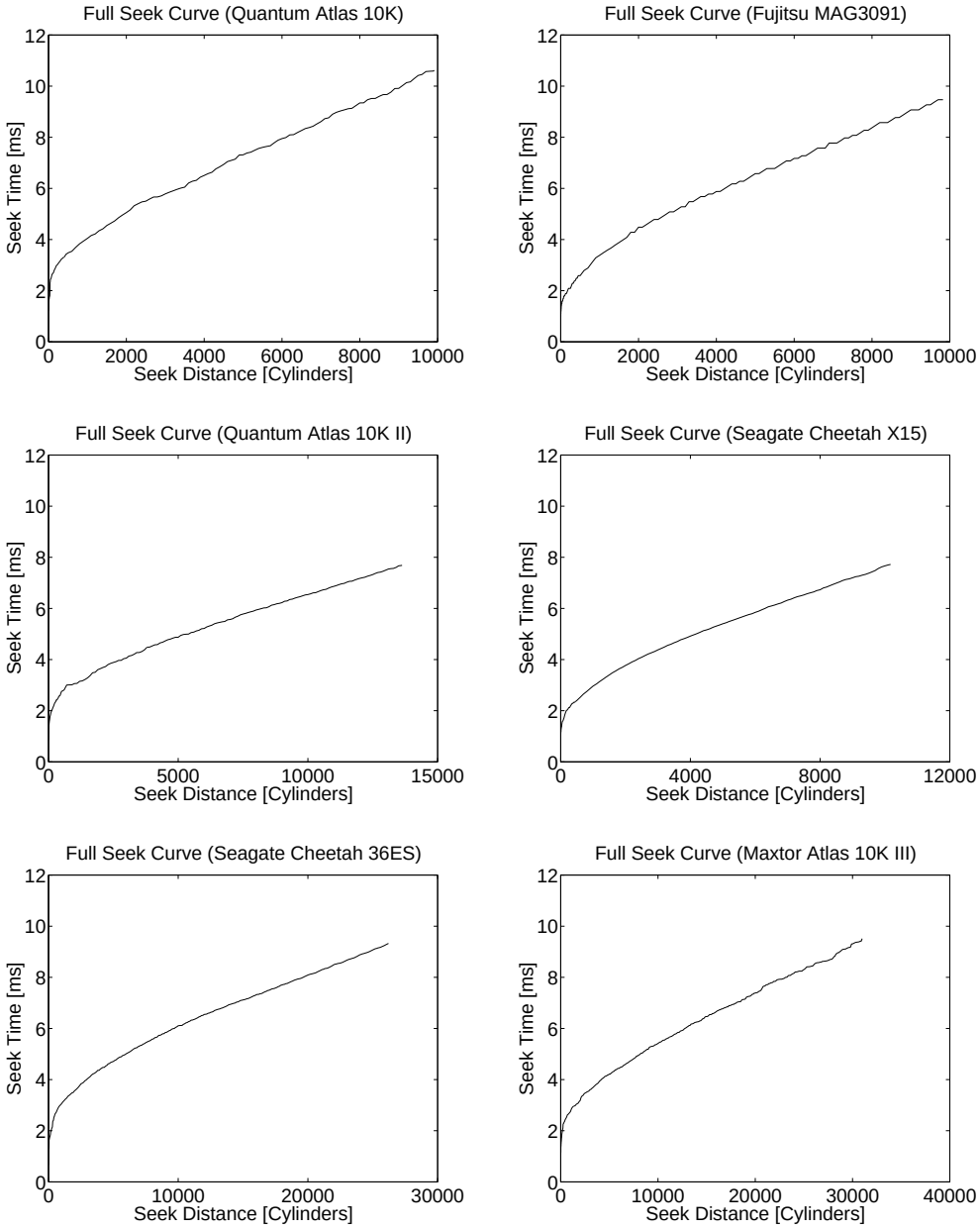

Fig. 3.5: **Representative seek profiles.**

efficiency of disk accesses increases. We define disk efficiency as the ratio between the time spent in useful data transfer (i.e., media read or write) to total request service time.

Zero-latency access

Zero-latency access, also known as immediate access or access-on-arrival, improves request response time by accessing disk sectors as they arrive underneath the disk head. When disk wants to read S contiguous sectors, the simplest approach is to position the head (through a combination of seek and rotational latency) to the first sector and read the S sectors in ascending LBN order. With zero-latency access support, disk firmware can read the S sectors from the media into its buffers in any order. In the best case, in which exactly one track is read, the head can start reading data as soon as the seek is completed; no rotational latency is involved because all sectors on the track are needed. The S sectors are read into an intermediate buffer, assembled in ascending LBN order, and sent to the host. The same concept applies to writes, except that data must be moved from host memory to the disk's buffers before it can be written onto the media.

As an example of zero-latency access on the disk from Figure 3.4, consider a read request for LBNs 200–399. First, the head is moved to the track containing these blocks. Suppose that, after the seek, the disk head is positioned above the sector containing LBN 380. A zero-latency disk can immediately read LBNs 380–399. It then reads the sectors with LBNs 200–379. This way, the entire track can be read in one rotation even though the head arrived in the "middle" of the track.

The expected rotational latency for a zero-latency disk decreases as the request size increases, as shown in Figure 3.6. Therefore, a request to the zero-latency access disk for all N sectors on a track requires only one revolution after the seek. An ordinary disk, on the other hand, has an expected rotational latency of $(N-1)/(2 \cdot N)$, or approximately 1/2 revolution, regardless of the request size and thus a request requires anywhere from one to two (average of 1.5) revolutions. Appendix A derives a formula for computing expected rotational latency as a function of request size.

Scheduling

High-end disk drives [Quantum Corporation 1999] include algorithms for request scheduling. These algorithms are variants of the SPTF (Shortest Positioning Time First) algorithm [Seltzer et al. 1990; Jacobson and Wilkes 1991; Worthington et al. 1994] and strive to increase disk efficiency by minimizing overall positioning time (i.e., the sum of seek and rotational latency). Given the current disk head position

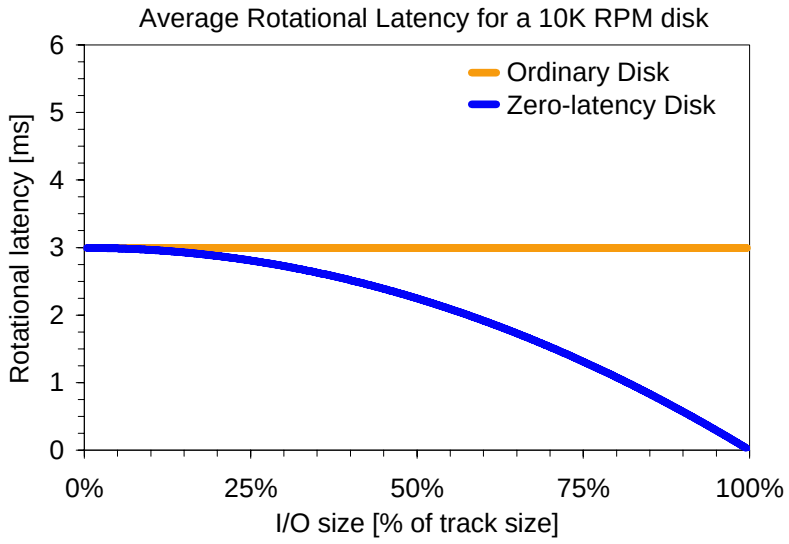

Fig. 3.6: **Average rotational latency for ordinary and zero-latency disks as a function of track-aligned request size.** The request size is expressed as a percentage of the track size.

and a queue of pending requests, the SPTF algorithm chooses its next request from the queue based on which request can be serviced with the smallest positioning time. Minimizing the disk head positioning time results in smaller request response times and hence improved efficiency.

As SPTF-based scheduling algorithms require detailed information about current disk head position, the natural place for their implementation is inside the firmware behind the storage device interface. Even though several research projects implemented SPTF-like algorithms outside of disk firmware [Huang and cker Chi-ueh 1999; Lumb et al. 2002; Yu et al. 2000], doing so required either detailed disk models calibrated to specific disks or significant efforts that did not yield the efficiency afforded by algorithms built into the firmware. Hence, for best-effort workloads, a storage manager should use scheduling as a transparent feature of a modern disk drive that sits below the storage interface rather than implementing it itself.

As described by previous studies [Jacobson and Wilkes 1991; Worthington et al. 1994], the efficiency of disk accesses improves with increased queue depth of pending requests. However, the complicated spatio-temporal relationships between the LBNs of the storage interface are quite difficult to capture in a high level attribute annotating the device LBN address space. Hence, a storage manager should exploit this feature by adding a rule that larger queue depths improve efficiency to the unwritten contract. In today's systems, this fact is overlooked.

Device capacity	3.46 GB
Average random seek	0.56 ms
Streaming bandwidth	38 MB/s

Table 3.2: **Basic MEMS-based storage device parameters.** MEMStores will have a capacity of a few GB, sub-millisecond random seek times, and streaming bandwidth on par with disk drives.

3.3 MEMS-based storage devices

Microelectromechanical systems (MEMS) are mechanical structures on the order of 10–1000 μm in size fabricated on the surface of silicon wafers [Maluf 2000; Wise 1998]. These microstructures are created using photolithographic processes similar to those used to manufacture other semiconductor devices (e.g., processors and memory) [Fedder et al. 1996]. MEMS structures can be made to slide, bend, and deflect in response to electrostatic or electromagnetic forces from nearby actuators or from external forces in the environment. A MEMS-based storage device uses MEMS for either positioning of recording elements (e.g., magnetic read/write heads) or the magnetic media sled.

MEMStores are the goal of efforts at several research centers, including IBM Zurich Research Laboratory [Vettiger et al. 2000] and Carnegie Mellon University (CMU). While actual devices do not yet exist, Table 3.2 shows their predicted high-level characteristics. This section briefly describes relevant physical characteristics including their interesting form of internal parallelism. This description is based on the CMU MEMStore design [Griffin et al. 2000a; Schlosser et al. 2000].

3.3.1 Physical characteristics

Most MEMStore designs, such as that illustrated in Figure 3.7, consist of a media sled and an array of several thousand probe tips. Actuators position the spring-mounted media sled in the X-Y plane, and the stationary probe tips access data as the sled is moved in the Y dimension. Each read/write tip accesses its own small portion of the media, which naturally divides the media into square regions and reduces the range of motion required by the media sled. For example, in the device shown in Figure 3.7, there are 100 read/write tips and, thus, 100 squares.

Data are stored in linear columns along the Y dimension. As with disks, a MEMStore must position the probe tips before media transfer can begin. This positioning is done by moving the sled in the X direction, to reach the right column, and in the Y direction, to reach the correct starting offset within the column. The X and Y seeks occur in parallel, and so the total seek time is the maximum of the two independent seek times. Once the media sled is positioned, read/write tips access data as the sled moves at a constant rate in the Y direction.

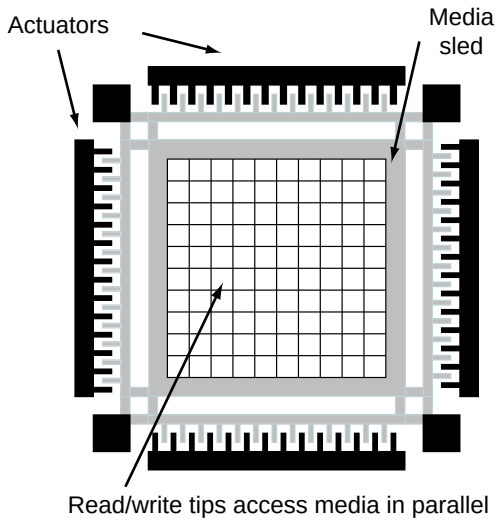

Fig. 3.7: **High-level view of a MEMStore.** The major components of a MEMStore are the sled containing the recording media, MEMS actuators to position the media, and the read/write tips that access the media. This picture emphasizes the media organization, which consists of a two-dimensional array of *squares*, each of which is accessed by a single read/write tip (not shown). As the media is positioned, each tip accesses the same position within its square, thus providing parallel access to data.

As in disks, data are stored in multi-byte sectors, such as 512 bytes, to reduce the overhead of extensive error correction coding (ECC). These sectors generally map one-to-one with the LBNs exposed via the device interface. Unlike disks, a MEMStore stripes each sector across many tips for two reasons: performance and fault tolerance. A single tip's transfer rate is quite low, and transferring an entire sector with a single tip would require 10× more time than a random seek. In addition, some of the 1000s of probe tips will be defective, and encoding each sector across tips allows the ECC to cope with tip failures. Data are striped across multiple tips for these reasons and grouped together into 512 byte LBNs.

Once striping is assumed, it is useful to consider that the number of active tips has been reduced by the striping factor (the number of tips over which a single LBN has been striped), and that each tip accesses a single, complete 512 byte LBN. In this way, there is a virtual geometry which is imposed on the physical media, one which exposes full 512 byte LBNs. The example shown in Figure 3.7 has, in reality, 6400 read/write tips with each LBN striped over 64 tips. But once striping is assumed, the virtual device shown in the figure has only 100 read/write tips, each accessing a single (striped) LBN at a time.

Given the implicit storage contract described in Section 2.2, MEMStores assign LBNs to physical locations in accordance with the general expectations of host

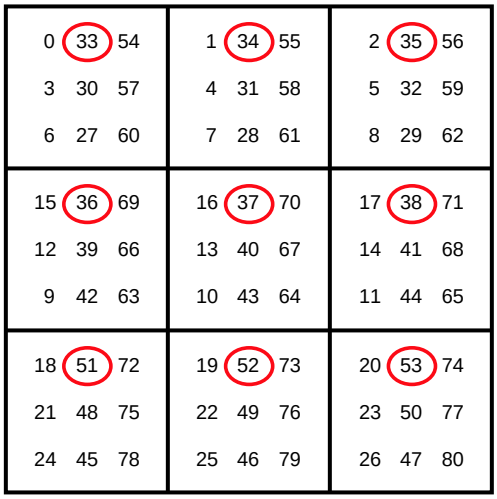

Fig. 3.8: **Data layout with** *LBN* **mappings.** The *LBN*s marked with ovals are at the same location within each square and can potentially be accessed in parallel. Depending on other constraints, only a subset of those *LBN*s can be accessed at once.

software: that sequential *LBN*s can be streamed with maximum efficiency and that similar *LBN*s involve shorter positioning delays than very different ones. As with disk drives, the focus is on the former, with the latter following naturally.

Figure 3.8 shows how *LBN* numbers are assigned in a simple device. Starting in the first square, ascending *LBN* numbers are assigned across as many squares as can be accessed in parallel to exploit tip parallelism. In this example, three *LBN*s can be accessed in parallel, so the first three *LBN*s are assigned to the first three squares. The next *LBN*s are numbered downward to provide physical sequentiality. Once the bottom of the squares is reached, numbering continues in the next set of squares, but in the upward direction until the top of the squares is reached. This *reversal* in the *LBN* numbering allows the sled to simply change direction to continue reading sequential data, maintaining the expectation that sequential access will be fast.

It is useful to complete the analogy to disk storage, as illustrated in Figure 3.9. A MEMStore cylinder consists of all *LBN*s that can be accessed without repositioning the sled in the X dimension. Because of power constraints, only a subset of the read/write tips can be active at any one time, so reading an entire cylinder will require multiple Y dimension passes. Each of these passes is referred to as a track, and each cylinder can be viewed as a set of tracks. In Figures 3.8 and 3.9, each cylinder has three tracks. As in disks, sequential *LBN*s are first assigned to tracks within a cylinder and then across cylinders to maximize bandwidth for

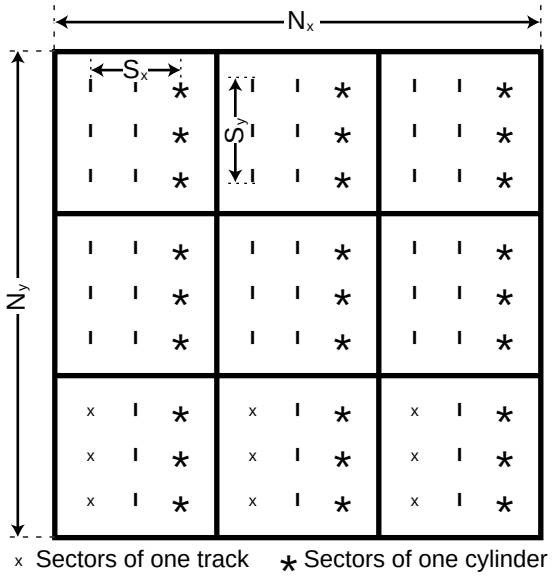

Fig. 3.9: **MEMStore data layout.** This picture illustrates the organization of LBNs into tracks and cylinders and the geometric parameters of the MEMStore. Cylinders are the groups of all LBNs which are at the same offset in the X dimension. In this picture, all of the LBNs of a sample cylinder are marked as stars. Because the number of LBNs that can be accessed at once is limited by the power budget of the device, a cylinder is accessed sequentially in tracks. The LBNs of a sample track are marked as squares in this picture. Three tracks comprise a single cylinder, since it takes three passes to access an entire cylinder. The parameters N_x and N_y are the number of squares in the X and Y directions, and S_x and S_y are the number of LBNs in a single square in each direction.

sequential streaming and to allow LBN locality to translate to physical locality.

3.3.2 Parallelism in MEMS-based storage

Although a MEMStore includes thousands of read/write tips, it is not possible to do thousands of entirely independent reads and writes. There are significant limitations on what locations can be accessed in parallel. Thus, MEMStores can treat tip parallelism as a means to increase sequential bandwidth or to access a small set of LBNs in parallel. The size of the set and the locations of these LBNs are constrained by physical characteristics.

When a seek occurs, the media is positioned to a specific offset relative to the entire read/write tip array. As a result, at any point in time, all of the tips access the same locations within their squares. An example of this is shown in Figure 3.8 in which LBNs at the same location within each square are identified with ovals. Hence, they can potentially be accessed in parallel.

It is important to note that the number of parallel-accessible LBNs is very small relative to the total number of LBNs in a MEMStore. In the 3.46 GB device described in Table 3.2, only 100 LBNs are potentially accessible in parallel at any point out of a total of 6,750,000 total LBNs in the device. Limitations arise from two factors: the power consumption of the read/write tips, and components shared among read/write tips. It is estimated that each read/write tip will consume 1–3 mW when active and that continuously positioning the media sled would consume 100 mW [Schlosser et al. 2000]. Assuming a total power budget of 1 W, only between 300 and 900 read/write tips can be utilized in parallel which, for realistic devices, translates to 5–10% of the total number of tips. This gives the true number of LBNs that can *actually* be accessed in parallel. In our example device, perhaps only 10 of 100 LBNs can actually be accessed in parallel.

In most MEMStore designs, several read/write tips will share physical components, such as read/write channel electronics, track-following servos, and power buses. Such component sharing makes it possible to fit more tips, which in turn increases volumetric density and reduces seek distances. It also constrains which subsets of tips can be active together.

Figure 3.8 shows a simple example illustrating how LBNs are parallel-accessible. If one third of the read/write tips can be active in parallel, a system could choose up to 3 LBNs out of 9 (shown with ovals) to access together. The three LBNs chosen could be sequential (e.g., 33, 34, and 35), or could be disjoint (e.g., 33, 38, and 52). In each case, all of those LBNs would be transferred to or from the media in parallel. The pictures showing tracks within contiguous rows of squares are just for visual simplicity. The tips over which any sector is striped would be spread widely across the device to distribute the resulting heat load and to create independence of tip failures. Likewise, the squares of sequentially numbered LBNs would be physically spread.

Table 3.3 lists parameters describing the virtual geometry of a device with example values taken from the device shown in Figures 3.8 and 3.9. The number of parallel-accessible LBNs p, is set by the power budget of the device, as described in Section 3.3.1. The total number of squares, N, is defined by the virtual geometry of the device. Since sequential LBNs are laid out over as many parallel tips as possible to optimize for sequential access, the number of squares in the X dimension, N_x, is equal to the level of parallelism, p. The number of squares in the Y dimension is the total number of squares, N, divided by p. The sectors per square in either direction, S_x and S_y, is determined by the bit density of each square. These parameters, along with N_x and N_y, determine the number of sectors per track, S_T, and the number of sectors per cylinder, S_C. The number of parallel-accessible LBNs is simply equal to the total number of squares, N, as

Name	Symbol		Example
p	Level of parallelism		3
N	Number of squares		9
S_x	Sectors per square in X		3
S_y	Sectors per square in Y		3
N_x	Number of squares in X	p	3
N_y	Number of squares in Y	N/p	3
S_T	Sectors per track	$S_y \times N_x$	9
S_C	Sectors per cylinder	$S_T \times N_y$	27

Table 3.3: **MEMS-based storage device parameters.** These are the parameters required to determine equivalence classes of LBNs that can be potentially accessed in parallel. The first five parameters are determined by the physical capabilities of the device and the last four are derived from them. The values in the rightmost column are for the simple device shown in Figures 3.8 and 3.9.

there is an equivalent LBN in each square. A two-step algorithm that uses the MEMStore parameters can calculate all the LBNs that can be accessed in parallel, as described in Section 6.1.4.

3.3.3 Firmware features

Although physical MEMS-based storage devices do not yet exist, they are expected to use the storage interface abstraction of fixed-size blocks [Schlosser et al. 2000; Schlosser et al. 2003].

Scheduling

Griffin et al. [2000b] showed that sled-position-sensitive scheduling algorithms (e.g., SPTF) outperform basic algorithms such as LOOK or FCFS that do not require detailed device information. Hence, MEMStores, when implemented, are likely to include scheduling algorithms built into their firmware just like disk drives. The storage manager atop a MEMStore can thus exploit scheduling in much the same way it would with disk drives as described in Section 3.2.4.

3.4 Disk arrays

Since disk drives are the basic building blocks of RAID groups, their media access characteristics are the same. However, two unique features distinguish RAID groups from single disks: data striping and parallel access.

3.4.1 Physical organization

To achieve higher concurrency of data accesses and to improve data reliability, high-end storage systems group together several disk drives to form a single logical storage device, also called a logical volume. The various RAID levels [Patterson et al. 1988] trade off reliability, capacity, and performance by striping the logical volume's LBNs across individual disks in different patterns [Chen et al. 1994; Menon and Mattson 1992; Hou et al. 1993]. At the most basic level, the RAID controller firmware algorithms control striping and initiate data repair after a disk failure. More advanced controllers can automatically spread out load among the individual disks or switch to a different RAID level to adapt to changes in workloads [Wilkes et al. 1996]. They also implement advanced algorithms for caching and prefetching of data to mask access latencies.

A RAID controller performs the functions described in the previous paragraphs atop individual disk drives. It exports a logical volume as a linear address space of LBNs, which, for current storage interfaces, provides no additional information to the application-specific storage managers (e.g., inside a filesystem or a relational database system) about the available parallelism. This disk array-unique feature, however, is important for parallel access to two-dimensional data structures such as relational database systems as well as the algorithms (e.g., sort or join) that operate on these two-dimensional structures [Graefe 1993; Mehta and DeWitt 1995; 1997]. Exposing this information via a well-defined interface, as proposed in this dissertation, can provide significant performance benefits to these algorithms.

A RAID controller can be thought of as a specialized storage manager; it exploits the characteristics of its underlying devices i.e., individual disks. However, it sits behind the device interface, as depicted in Figure 3.1, encapsulating disk characteristics and other disk-array-unique features into performance attributes, which are then exposed to the application-specific storage manager.

3.4.2 Data striping

Striping is the process of mapping the logical blocks that form the exported logical volume to the LBNs of the individual disks comprising the RAID group. While there are many different ways to do this [Patterson et al. 1988], in general, the striping process takes a fixed number of blocks, called a stripe unit, and maps it into LBNs of one disk drive. The next logical stripe unit (e.g., the collection of the same number of consecutive LBNs that are immediately adjacent in the logical volume's address space) is then mapped to the next disk drive. This process is repeated with stripe units being mapped to the disks in a round-robin fashion. Thus, stripe units that are not consecutive in the logical volume's address space

are mapped to consecutive locations of the individual disk's LBN address space.

In addition to protecting against data loss (e.g., with parity stripe or a mirrored copy of the data), the stripe units can provide the aggregate bandwidth from all disks in the RAID group. With appropriately sized I/Os that are correctly aligned on stripe unit boundaries, each disk can perform sequential access. The RAID controller then assembles the returned data to a single stream.

Choosing the appropriate stripe unit size has direct impact on the performance for a given workload [Patterson et al. 1988; Chen and Patterson 1990; Chen et al. 1994; Ganger et al. 1994]. In the absence of other information, stripe units approximating the disk track size provide good overall performance [Chen and Patterson 1990]. However, the inability to express these track boundaries, combined with the zoned-geometries of modern disk drives, results in a loss of potential performance at the RAID controller level and subsequently at the application level [Schindler et al. 2003]. Matching stripe units to a disk's track size, and exporting this exact size to the application's storage manager, can recover the lost performance, as demonstrated in this dissertation.

3.4.3 Parallel access

Striping also provides parallel access to data. With stripe units mapped to different disk drives and I/Os sized to match stripe unit size and boundaries, the disk drives in the RAID group can access data in parallel. RAID 1 and RAID 5 configurations (the two most often used in disk arrays) can achieve n reads in parallel, where n is the number of disks in the RAID group. While the proper access parallelism is known at the RAID controller level, this information is not propagated to the application-specific storage managers where it is needed to determine appropriate access patterns for workloads with parallel accesses.

4 Discovery of Disk Drive Characteristics

Today's storage devices do not support the architecture proposed in this dissertation wherein storage devices expose performance attributes to storage managers. However, by building specialized tools, it is possible to evaluate the benefits of this type of architecture with current of-the-shelf storage devices. These tools can discover a device's performance characteristics, encapsulate them, and expose them to the storage manager. With assumptions about the inner-workings of the device, they can do so by using basic READ and WRITE commands. The device-specific algorithms are confined to the discovery tool, which sits between the storage device and the storage manager, neither of which needs to be changed. It appears to the storage manager as if the performance attributes were exported directly from the storage device.

This chapter describes a discovery tool called DIXtrac (DIsk eXtractor), which can quickly and automatically characterize disk drives that understand the Small Computer System Interface (SCSI) protocol [Schmidt et al. 1995]. Without human intervention, DIXtrac can discover accurate values for over 100 performance-critical disk parameters.

In the context of this dissertation, however, only a small fraction of the parameters are encapsulated into the ACCESS DELAY BOUNDARIES and PARALLELISM attributes that realize the performance improvements reported in Chapter 5 and 6. In particular, the ACCESS DELAY BOUNDARIES performance attribute encapsulates the extracted disk track sizes and the PARALLELISM attribute additionally encapsulates the head-switch and/or one-cylinder seek time. The vast majority of the parameters extracted by DIXtrac are used for detailed disk models (e.g., in disk subsystem simulators [Bucy and Ganger 2003] and implementations of rotationally sensitive schedulers outside disk firmware using SPTF [Lumb et al. 2000; Yu et al. 2000] or freeblock scheduling [Lumb et al. 2000]) but need not be exposed to strorage managers.

DIXtrac determines most disk characteristics by measuring the per-request service times for specific test vectors of READ and WRITE commands. Other characteristics are determined by interrogative extraction, which uses the wealth of

SCSI command options. Most of these techniques were first proposed in previous work [Worthington et al. 1995] and they have been improved and enhanced for DIXtrac in several ways. First and foremost, the entire parameter extraction process has been automated, which required a variety of changes. By automating this process, DIXtrac greatly simplifies the process of collecting disk drive characteristics and works seamlessly as a discovery tool in the alternative storage model architecture described in Section 3.1 and depicted in Figure 3.1(b). Second, DIXtrac includes an expert system for interactively discovering a disk's layout and geometry. Third, DIXtrac's extraction techniques account for (some) advances in current disk drives.

4.1 Characterizing disk drives with DIXtrac

To completely characterize a disk drive, one must describe the disk's geometry and layout, mechanical timings, cache parameters and behavior, and all command processing overheads. Thus, the characterization of a disk consists of a list of performance-critical parameters and their values. Naturally, such a characterization makes implicit assumptions about the general functionality of a disk. For example, DIXtrac assumes that data are stored in fixed-size sectors laid out in concentric circles on rotating media.

To reliably determine most parameters, one needs a detailed disk map that identifies the physical location of each logical block number (LBN) exposed by the disk interface. Constructing this disk map requires some mechanism for determining the physical locations of specific LBNs. Using this disk map, appropriate test vectors consisting of READ and WRITE commands can be sent to the disk to extract various parameters. For many parameters, such as mechanical delays, test vectors must circumvent the cache. If the structure and behavior of the cache is known, the actual test vector can be preceded with requests that set the cache such that the test vector requests will access the media. While it is possible to devise such test vectors, it is more convenient if the cache can be turned off.

Therefore, to accurately characterize a disk drive, there exists a set of requirements that the disk interface must meet. First, it must be possible to determine the disk's geometry either experimentally or from manufacturer's data. Second, it must be possible to read and write specific LBNs (or specific physical locations). Also, while it is not strictly necessary, it is very useful to be able to temporarily turn off the cache. With these few capabilities, DIXtrac can determine the 100+ performance-critical parameters expected by a detailed event-driven disk simulator such as DiskSim [Bucy and Ganger 2003].

DIXtrac currently works for SCSI disks, which fulfill the three listed require-

ments. First, the Translate option of the SEND DIAGNOSTIC and RECEIVE DIAGNOSTIC commands translates a given LBN to its physical address on the disk, given as a <*cylinder,head,sector*> tuple. SCSI also provides the READ DEFECT LIST command, which gives the physical locations of all defective sectors. With these two commands, DIXtrac can create a complete, concise, and accurate disk map. Second, the SCSI READ and WRITE commands take a starting LBN and a number of consecutive blocks to be read or written, respectively. Third, the cache can usually be enabled and disabled by changing the Cache Mode Page with the SCSI MODE SELECT command. The validation results in Section 4.4 show that these are sufficient for DIXtrac.

4.2 Characterization algorithms

DIXtrac's disk characterization process can be divided into five logical steps. First, complete layout information is extracted and a disk map is created. The information in the disk map is necessary for the remaining steps, which involve issuing sequences of commands to specific physical disk locations. Second, mechanical parameters such as seek times, rotational speed, head switch overheads, and write settling times are extracted. Third, cache management policies are determined. Fourth, command processing and block transfer overheads are measured; these overheads rely on information from the three prior steps. Fifth, request scheduling policies are determined. The remainder of this section details the algorithms used for each of these steps.

4.2.1 Layout extraction

In addition to differences in physical storage configurations, the algorithms used for mapping the logical block numbers (LBNs) exposed by the SCSI interface to physical sectors of magnetic media vary from disk model to disk model. A common approach places LBNs sequentially around the topmost and outermost track, then around the next track of the same cylinder, and so on until the outermost cylinder is full. The process repeats on the second outermost cylinder and so on until the locations of all LBNs have been specified. This basic approach is made more complex by the many different schemes for spare space reservation and the mapping changes (e.g., reallocation) that compensate for defective media regions. The firmware of some disks may reserve part of the storage space for its own use.

DIXtrac's approach to disk geometry and LBN layout extraction experimentally characterizes a given disk by comparing observations to known layout characteristics. To do this, it requires two things of the disk interface: an explicit mechanism for discovering which physical locations are defective, and an explicit

mechanism for translating a given LBN to its physical cylinder, surface and sector (relative to other sectors on the same track).

DIXtrac accomplishes layout extraction in several steps, which progressively build on knowledge gained in earlier steps.

1. It uses the READ CAPACITY command to determine the highest LBN, and determine the basic physical geometry characteristics such as number of cylinders and surfaces by mapping random and targeted LBNs to physical locations using the SEND/RECEIVE DIAGNOSTIC command.
2. It uses the READ DEFECT LIST command to obtain a list of all media defect locations.
3. It determines where spare sectors are located on each track and cylinder, and detect any other space reserved by the firmware. This is done by an expert-system-like process of combining the results of several queries, including whether or not (a) each track in a cylinder has the same number of LBN-holding sectors; (b) one cylinder within a set has fewer sectors than can be explained by the defect list; and (c) the last cylinder in a zone has too few sectors.
4. It determines zone boundaries and the number of sectors per track in each zone by counting the sectors on a defect-free, spare-free track in each zone.
5. It identifies the remapping mechanism used for each defective sector by back-translating the LBNs returned in step 2[1].

Steps 3–5 all exploit the regularity of disk geometry and layout characteristics to efficiently zero-in on the parameter values, rather than translating every LBN. DIXtrac identifies the spare space reservation scheme by determining the answers to a number of questions, including: Does each track in a cylinder have the same number of sectors? Does one cylinder within a set have fewer sectors than can be explained by defects? Does the last cylinder of a zone have too few sectors? By combining these answers, DIXtrac decides which known scheme the disk uses; so far, we have observed nine different approaches: spare tracks per zone, spare sectors per track, spare sectors per cylinder, spare sectors per group of cylinders, spare sectors per zone, spare sectors at the end of the disk, combinations of spare sectors per cylinder (or group of cylinders), and spare cylinders per zone or smaller

[1]Remapping approaches used in modern disks include slipping, wherein the LBN-to-physical location map is modified to simply skip the defective sector, and remapping, wherein the LBN that would be located at the given sector is instead located elsewhere but other mappings are unchanged. Most disks will convert to slipping whenever they are formatted via the SCSI FORMAT command.

group of cylinders. The zone information is determined by simply counting the sectors on tracks as appropriate. The remapping scheme used for each defect is determined by back-translating the LBN that should be mapped to it (if any) and then determining to where it has been moved.

DIXtrac uses built-in expertise to discover a disk's algorithms for mapping data on the disk in order to make the characterization efficient in terms of both space and time. An alternate approach would be to simply translate each LBN and maintain a complete array of these mappings. However, this is much more expensive, generally requiring over 1000× the time and 300× the result space. The price paid for this efficiency is that DIXtrac successfully characterizes only those geometries and LBN layouts that are within its knowledge base.

In order to avoid one extra rotation when accessing consecutive blocks across a track or cylinder boundary, disks implement track and cylinder skew. The skew must be sufficiently large to give enough time for the head switch or seek. With the cache disabled, the track and cylinder skew for each zone can be determined by issuing two WRITE commands to two consecutive blocks located on two different tracks or cylinders. The response time of the second request is measured and the value of track or cylinder skew is obtained as

$$\text{Skew} = \frac{T_{Write_2} * \text{sectors per track}}{T_{one\ revolution}}$$

Detecting track boundaries

Knowing exact track boundaries is important for determining efficient I/O sizes in order to avoid unnecessary head switches and rotational latencies. DIXtrac implements two different methods: a general one applicable to any disk interface supporting a READ command and a specialized one for SCSI disks, which uses the algorithm described above.

The general extraction algorithm locates track boundaries by identifying discontinuities in access efficiency. Recall that the disk efficiency for requests aligned on track boundaries increases linearly with the number of sectors being transferred until a track boundary is crossed. Starting with sector 0 of the disk ($s = 0$), the algorithm issues successive requests of increasing size, each starting at sector s (i.e., read 1 sector starting at s, read 2 sectors starting at s, etc.). The extractor avoids rotational latency variance by synchronizing with the rotation speed, issuing each request at (nearly) the same offset in the rotational period; rotational latency could also be addressed by averaging many observations, but at a substantial cost in extraction time. Eventually, an S-sector read returns in more time than a linear model suggests (i.e., $S = N + 1$), which identifies sector $s + N$ as the

start of a new track. The algorithm then repeats with $s = s + S - 1$.

The method described above is clearly suboptimal; the actual implementation uses a binary search algorithm to discover when $S = N + 1$. In addition, once N is determined for a track, the common case of each subsequent track being the same size is quickly verified. This verification checks for a discontinuity between $s+N-1$ and $s+N$. If one exists, it sets $s = s+N-1$ and moves on. Otherwise, it sets $S = 1$ and uses the base method; this occurs mainly on the first track of each zone and on tracks containing defects. With these enhancements, the algorithm extracts the track boundaries of a 9 GB disk in four hours. Talagala et al. [2000] describe a much quicker algorithm that extracts approximate geometry information; however, for our purposes, the exact track boundaries must be identified.

One difficulty with using read requests to detect track boundaries is the caching performed by disk firmware. To obviate the effects of firmware caching, the algorithm interleaves 100 parallel extraction operations to widespread disk locations, such that the cache is flushed each time it returns to block s. An alternative approach would be to use write requests; however, this is undesirable because of the destructive nature of writes and because some disks employ write-back caching.

4.2.2 Disk mechanics parameters

Similar to previous work [Worthington et al. 1995], DIXtrac's central technique for extracting disk mechanics parameters is to measure the minimum time between two request completions, called the $MTBRC$. $MTBRC(X, Y)$ denotes the minimum time between the completions of requests of type X and Y. Finding the minimum time is an iterative process in which the inter-request distance is varied until the minimal time is observed, effectively eliminating rotational latency for request Y. An $MTBRC$ value is a sum of several discrete service time components, and the individual components can be isolated via algebraic manipulations as described below.

Time stamps are taken at the initiation and completion of each request, and $MTBRC$ is computed as the difference of the two completion times as depicted in Figure 4.1. Finding the minimum time is an iterative process in which the inter-request distance is varied until the minimal time is observed. The inter-request distance is the rotational distance between the physical starting locations of request X and Y.

Since $MTBRC$ includes overheads, e.g., thermal re-calibration or interrupt delivery to the host computer, it is not sufficient to measure $MTBRC$ only once, but rather to conduct a series of measurements for each request pair. The computation of $MTBRC$ proceeds as follows: Take several sets of measurements with

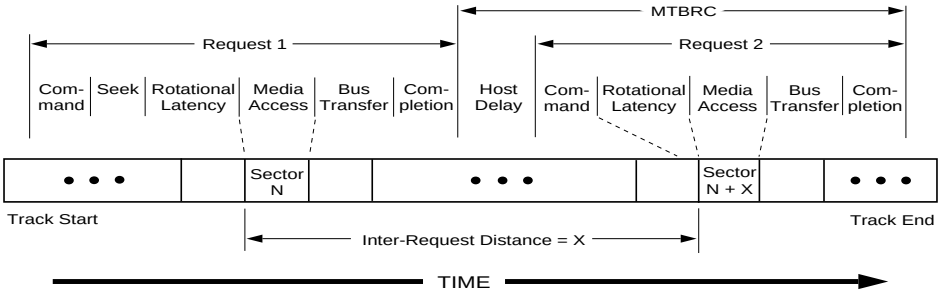

Fig. 4.1: **Computing MTBRC.** The depicted time-line shows the service time components for $MTBRC_1$(1-sector-read, 1-sector-read on the same track) request pair. The accessed track is shown as a straight line. Timestamps are taken at the start and completion of each request. The inter-request distance is the difference between the starting locations of the two requests. Figure reproduced with the permission of authors [Worthington et al. 1995].

each set containing at least 10 measurements. Discard from each set any values that differ by more that 10% from the median of the set. Find a mean value from the remaining values. The number of sets and the number of values in each set can vary and depends on the type of measurement.

Head switch time

To access sectors on a different surface, a disk must switch on the appropriate read/write head. The time for head switch includes changing the data path and re-tracking (i.e., adjusting the position of the head to account for inter-surface variations). The head switch time can be computed from two $MTBRC$s:

$$\begin{aligned}&\text{MTBRC}_1 = \\ &\quad \text{Host Delay}_1 + \text{Command} + \text{Media Xfer} + \text{Bus Xfer} + \text{Compl} \\ &\text{MTBRC}_2 = \\ &\quad \text{Host Delay}_2 + \text{Command} + \text{Head Switch} + \text{Media Xfer} + \text{Bus Xfer} + \text{Compl}\end{aligned}$$

to get

$$\text{Head Switch} \quad = \quad (\text{MTBRC}_2 - \text{Host Delay}_2) - (\text{MTBRC}_1 - \text{Host Delay}_1)$$

This algorithm measures the *effective* head switch (i.e., the time not overlapped with command processing or data transfer). While it may not be physically exact, it is appropriate for disk models and schedulers [Worthington et al. 1995].

Seek time

To extract seek times, DIXtrac uses the SEEK command that, given a logical block number, positions the arm over the track with that block. Extracted seek time for distance d consists of measuring 5 sets of 10 inward and 10 outward seeks from a randomly chosen cylinder. Seek times are measured for seeks of every distance between 1 and 10 cylinders, every 2nd distance up to 20 cylinders, every 5th distance up to 50 cylinders, every 10th distance up to 100 cylinders, every 25th distance up to 500 cylinders, and every 100th seek distance beyond 500 cylinders. Seek times can also be extracted using $MTBRC$s, though using the SEEK command is much faster. For disks that do not implement SEEK (although all of the disks tested here did), DIXtrac measures $MTBRC$(1-sector write, 1-sector read) and $MTBRC$(1-sector write, 1-sector read incurring k-cylinder seek). The difference between these two values represents the seek time for k cylinders.

Write settle time

Before starting to write data to the media after a seek or head switch, most disks allow extra time for finer position verification to ensure that the write head is very close to the center of the track. The write settle time can be computed from head switch and a pair of $MTBRC$s: $MTBRC_1$(one-sector-write, one-sector-write on the same track) and $MTBRC_2$(one-sector-write, one-sector-write on a different track of the same cylinder). The two $MTBRC$ values are the sum of head switch and write settle. Therefore, the head switch is subtracted from the measured time to obtain *effective* write settle time. As with head switch overhead, the value indicates settling time not overlapped with any other activity. If the extracted value is negative, it indicates that write settling completely overlaps with some other activity (e.g., command processing, bus transfer of data, etc.).

Rotational speed

DIXtrac measures rotation speed via $MTBRC$(1-sector-write, same-sector-write). In addition, the nominal specification value can generally be obtained from the Geometry Mode Page using the MODE SENSE command.

4.2.3 Cache parameters

SCSI disk drive controllers typically contain 512 KB to 8 MB of RAM. This memory is used for various purposes such as: working memory for firmware, a speed-matching buffer, a prefetch buffer, a read cache, or a write cache. The prefetch buffer and read/write cache space is typically divided into a set of circular buffers,

called segments. Unlike segments of processor caches, they have variable lengths and start points. The cache management policies regarding prefetch, write-back, etc. vary widely among disk models. More recent disks provide algorithms that dynamically partition the cache into different number of segments that are of variable size. While DIXtrac can recognize such a policy, its current algorithms cannot determine the exact behavior of these dynamic algorithms.

The extraction of each cache parameter follows the same approach: construct a hypothesis and then validate or disprove it. Testing most hypotheses consists of three steps. First, the cache is polluted by issuing several random requests of variable length, each from a different cylinder. The number of random requests should be larger than the number of segments in the cache. This pollution of the cache tries to minimize the effects of adaptive algorithms and ensures that the first request in the hypothesis test will propagate to the media. Second, a series of cache setup requests are issued to put the cache into a desired state. Finally, the hypothesis is tested by issuing one or more requests and determining whether or not they hit in the cache. In its cache characterization algorithms, DIXtrac assumes that a READ or WRITE cache hit takes, at most, 1/4 of the full revolution time.

This value has been empirically determined to provide fairly robust hit/miss categorizations, though it is not perfect (e.g., it is possible to service a miss in less than 1/4 of a revolution). Thus, the extraction algorithms are designed to explicitly or statistically avoid the short media access times that cause miscategorization.

Basic parameters

DIXtrac starts cache characterization by extracting four basic parameters. Given the results of these basic tests, the other cache parameters can be effectively extracted. The four basic hypotheses are:

Cache discards block after transferring it to the host. A READ is issued for one block followed immediately by READ of the same block. If the second READ command takes more than 1/4 of a revolution to complete, then it is a miss and the cache does not keep the block in cache after transferring it to the host.

Disk prefetches data to the buffer after reading one block. A READ is issued to block n immediately followed by a READ to block $n+1$. If the second READ command completion time is more than 1/4 of a revolution, then it is a cache miss and the disk does not prefetch data after the read. This test assumes that the bus transfer and host processing time will cause enough

delay to incur a "miss" and a subsequent one rotation delay on reading block $n + 1$ if the disk were to access the media.

WRITEs are cached. A READ is issued to block n immediately followed by a WRITE to the same block. If the WRITE completion time is more than 1/4 of a revolution, then the disk does not cache WRITEs.

READs hit on data placed in cache by WRITEs. A WRITE is issued to block n followed by a READ of the same block. If the READ completion time is more that 1/4 of a revolution, then the READ is a cache miss and READ hits are not possible on written data stored in cache.

Cache segments

Number of read segments. The number of segments is set to some hypothesized number N (e.g. $N = 64$). First, the cache is polluted as described above. Second, N READs are issued to the first logical block LBN_k of N distinct cylinders, where $1 \leq k \leq N$. Third, the contents of the cache is probed. If the disk retains the READ value in the cache after transferring it to the host, N READs are issued to LBN_k; otherwise, if the disk prefetches blocks after a READ, N READs are issued to $LBN_k + 1$. If any of the READs take longer than 1/4 of a revolution, it is assumed that a cache miss occurred. The value of N is decremented and the algorithm repeated. If all READs were cache hits, the cache used at least N segments. In that case, N should be incremented and the algorithm repeated.

Using a binary search, the correct value of N is found. DIXtrac also determines if the disk cache uses an adaptive algorithm for allocating the number of segments by keeping track of the upper boundaries during the binary search. If an upper boundary for which there has been both a miss and a hit is encountered, then the cache uses an adaptive algorithm and the reported value may be incorrect.

DIXtrac's algorithm for determining the number of segments assumes that a new segment is allocated for READs of sectors from distinct cylinders. It also assumes that every disk's cache either retains the READ block in cache or uses prefetching. Both assumptions have held true for all tested disks.

Number of write segments. DIXtrac counts write segments with the same basic algorithm as for read segments, simply replacing the READ commands with WRITEs. Some disks allow sharing of the same segment for READs and WRITEs. In this case, the number of write segments denotes how many segments out of the total number (which is the number of read segments) can be also used for caching WRITEs. For disks where READs and WRITEs do not share segments, simply adding the two numbers gives the total number of segments.

Size of a segment. An initial value is chosen for the segment size S (e.g., the number of sectors per track in a zone). If the cache retains cached values after a transfer to the host, N READs of S blocks are issued each starting at LBN_k, where N is the previously determined number of read segments. Then, the cache is probed by issuing N one-block READs at LBN_k. If there were no misses, S is incremented and the algorithm repeated.

If the cache discards the cached value after a READ, one-block READs are issued to LBN_k, after waiting sufficiently long for each prefetch to finish (e.g., several revolutions). This will help determine if there are hits on $LBN_k + 1$. As before, binary search is used to find the segment size S and to detect possible adaptive behavior. This algorithm assumes that prefetching can fill the entire segment. If it is not the case, the segment size may be underestimated.

Prefetching

Number of prefetched sectors. A one-block READ is issued at LBN_1 which is the logical beginning of the cylinder. After a sufficiently long period of time (i.e., 4 revolutions), the cache is probed by issuing a one-block READ to $LBN_1 + P$ where P is the hypothesized prefetch size. By selecting appropriate LBN_1 values, DIXtrac can determine the maximum prefetch size and whether the disk prefetches past track and cylinder boundaries.

Track prefetching algorithm. Some disks implement an algorithm that automatically prefetches all of track $n + 1$ only after READ requests fetch data from track $n-1$ and n on the same cylinder. This algorithm minimizes the response time for the READ blocks from $n+1$st track which is a part of a sequential access pattern. To test for this behavior, DIXtrac pollutes cache then issues entire-track READs track $n - 1$ and n. After waiting at least one revolution, a it issues a one-block READ to a block on track $n + 1$. If there was a cache hit and the previous prefetch size indicated 0, then the disk implements this track-based prefetch algorithm.

Zero-latency access

To minimize the media access time, some disks can access sectors as they pass under the head rather than in strictly ascending order. This is known as zero-latency read/write or read/write-on-arrival. To test for read-on-arrival, a one-block READ is issued at the beginning of the track followed by an entire-track READ starting at the same block. If the completion time is approximately two revolutions, the disk does not implement read-on-arrival, because it takes one revolution to position to the original block and another revolution to read the data. If the time is much less, the disk implements read-on-arrival.

Degrees of freedom provided by the Cache Mode Page

The SCSI standard defines a Cache Mode Page that allows one to set the various cache parameters described above. However, since the Cache Mode Page is optional, typically only a subset of the parameters is changeable. To determine what parameters are changeable and to what degree, DIXtrac runs several versions of the cache parameter extractions. This information is also valuable for systems that want to aggressively control disk cache behavior [Shriver et al. 1999]. The first version observes the disk's default cache behavior. Other versions explore the effects of changing different Cache Mode Page fields, such as the minimal/maximal prefetch sizes, the number/size of cache segments, the Force-Sequential-Write bit, and the Discontinuity bit. For each, DIXtrac determines and reports whether changing the fields has the specified effect on disk cache behavior.

The next version of tests sets the appropriate bits in the mode pages and examines the possibly changed behavior. For example, the Discontinuity bit that is defined as "continue prefetching past a boundary" can control the amount of prefetched data. Together with setting minimal and maximal prefetch sizes, DIXtrac can determine if the cache allows prefetching past boundaries and if the behavior differs from the default one. Similarly, DIXtrac disables the Force-Sequential-Write bit and determines if the disk implements write-on-arrival under this setting.

Finally, if possible, DIXtrac sets the number and size of segments on the Cache Mode Page to different values and determines if the cache characteristics change. If implemented, modifying those parameters can reveal the relationship between the number and the size of the segments.

4.2.4 Command processing overheads

DIXtrac's refined and automated $MTBRC$-based scheme extracts eight command processing overheads:

MTBRC_1(1-sector write, 1-sector read on other cylinder) =
Host Delay + **Read Miss After Write** + seek + Media Xfer + Bus Xfer

MTBRC_2(1-sector write, 1-sector write on other cylinder) =
Host Delay + **Write Miss After Write** + seek + Media Xfer + Bus Xfer

MTBRC_3(1-sector read, 1-sector write on other cylinder) =
Host Delay + **Write Miss After Read** + seek + Bus Xfer + Media Xfer

MTBRC_4(1-sector read, 1-sector read miss on other cylinder) =
Host Delay + **Read Miss After Read** + seek + Media Xfer + Bus Xfer

$$\text{Time}_5(\text{1-sector read hit after a 1-sector read}) = \text{Host Delay} + \textbf{Read Hit After Read} + \text{Bus Xfer}$$

$$\text{Time}_6(\text{1-sector read hit after a 1-sector write}) = \text{Host Delay} + \text{Bus Xfer} + \textbf{Read Hit After Write}$$

$$\text{Time}_7(\text{1-sector write hit after a 1-sector read}) = \text{Host Delay} + \textbf{Write Hit After Read} + \text{Bus Xfer}$$

$$\text{Time}_8(\text{1-sector write hit after a 1-sector write}) = \text{Host Delay} + \textbf{Write Hit After Write} + \text{Bus Xfer}$$

Media transfer for one block is computed by dividing the rotational speed by the relevant number of sectors per track. Bus transfer is obtained by comparing completion times for two different-sized READ requests that are served from the disk cache. The difference in the times is the additional bus transfer time for the larger request.

When determining the $MTBRC$ values for cache miss overheads, four different seek distances are used and appropriate seek times are subtracted. The $MTBRC$ values are averaged to determine the overhead. Including a seek in these $MTBRC$ measurements captures the effective overhead values given overlapping of command processing and mechanical positioning activities.

Compared to previous approach of Worthington et al. [1995], each overhead extraction is independent of the others, obviating the need for fragile matrix solutions. Also, cache hit times are measured directly rather than with $MTBRC$, avoiding problems of uncooperative cache algorithms (e.g., cached writes are cleared in background unless the next request arrives).

4.2.5 Scheduling algorithms

To determine the scheduling algorithm implemented by the disk firmware, DIXtrac issues multiple requests to specific locations on the media and observes their completion order. With detailed layout and mechanical delays information, the request locations are chosen such that servicing them out of the issue order would result in more efficient execution with shorter positioning delays. Based on the observed order in which requests are returned, DIXtrac determines if the scheduling algorithm implements a FIFO scheduler, a seek minimizing scheduler (a variant of SCAN), or an algorithm minimizing total positioning time (a variant of SPTF).

4.3 DIXtrac implementation

DIXtrac runs as a regular application on the Linux 2.2 operating system. In tests, raw SCSI commands are passed to the disk via the raw Linux SCSI device driver (`/dev/sg`). Each such SCSI command is composed in this buffer and sent to the disk via a `write` system call to `/dev/sg`. The results of a command are obtained via a `read` system call to `/dev/sg`. The `read` call then blocks until the disk completes the command.

DIXtrac extracts parameters in the following steps. First, it initializes the drive. Second, it performs the 4 steps of the extraction process described in Section 4.2. Third, it writes out parameter files and cleans up.

The initialization step first sets the drive to conform to the SCSI version 2 definition via the CHANGE DEFINITION command, allowing the remainder of the extraction to use this common command set. Next, it issues 50 random read and write requests which serve to "warm up" the disk. Some drives have request times which are much longer for the first few requests after they have been sitting idle for some time. This behavior is due to several factors such as thermal re-calibration or automatic head parking.

The clean up step restores the disk to its original configuration, resetting the original SCSI version and cache settings. However, this restoration does not include stored contents; the extraction steps use WRITE commands to overwrite the original contents of some sectors. A possible enhancement to DIXtrac would be to save the original contents of the blocks and restore them during clean up.

To measure elapsed time, DIXtrac uses the POSIX `gettimeofday` system call, which returns wall-clock time with a microsecond precision. The Linux implementation on Intel Pentium-compatible processors uses the processor's cycle counter to determine the time: thus the returned time has the microsecond precision defined (but not required) by POSIX.

Before doing a `write` system call to the `/dev/sg` device, the current time is obtained via the `gettimeofday` system call. `gettimeofday` is called again after the `read` system call returns with the result of the SCSI command. The execution time of the SCSI command is the difference between those two times. The time measured via `gettimeofday` includes the overheads of the `gettimeofday` and `read/write` calls and may include a sleep time during which other processes are scheduled. The advantage of using `gettimeofday` call is that the time can be measured on an unmodified kernel.

Although it is not required for proper functioning of DIXtrac, the parameter extractions reported here were performed on a kernel with a modified `sg` driver that samples the time in the kernel right before calling the low-level portion of the device

driver. The measured time is returned as a part of the `sg` device structure that is passed to the `read` and `write` call. This modification eliminates the overheads of `gettimeofday` giving more precise time measurements. The times obtained via the user-level `gettimeofday` call on the unmodified kernel are, on average, 1.5% larger, with a maximum deviation of 6.8%, compared to the time obtained via modified `sg` driver.

However, even the time obtained from the modified `sg` driver includes the PC bus, host adapter, and SCSI bus overheads. Bus and device driver overheads could be isolated by measuring time using a logical analyzer attached to the SCSI bus. DIXtrac assumes that, on average all SCSI commands incur the same bus and driver overheads. To eliminate bus contention issues, DIXtrac extracts data from a disk on a dedicated SCSI bus with no other device attached. The effects of other devices on the PC internal bus are minimized by performing extraction on an otherwise idle system.

4.4 Results and performance

DIXtrac has been fully tested on many disk models: IBM Ultrastar 18ES, Hewlett-Packard C2247, Quantum Viking, Quantum Atlas III, Quantum Atlas 10K, Atlas 10K II, Maxtor Atlas 10K III, Fujitsu MAG3091, Seagate Barracuda 4LP, Seagate Cheetah 4LP, Cheetah 9LP, Cheetah 18LP, Cheetah 73LP, Cheetah 36ES, Cheetah X15, Cheetah X15 36LP, and Seagate Hawk. This section evaluates DIXtrac in terms of extraction times and characterization accuracies and shows detailed results for the Ultrastar 18ES, Atlas III, Atlas 10K, and Cheetah 4LP disks. Similar results have been obtained for the other disks.

4.4.1 Extraction times

Table 4.1 summarizes the DIXtrac extraction times. The times are broken down to show how long each extraction step takes. With the exception of the IBM Ultrastar 18ES, an entire characterization takes less than three minutes. Extraction times could be reduced further, at the expense of accuracy, by using fewer repetitions for the timing extractions (e.g., seek, mechanical, and command processing overheads).

The extraction time for the IBM Ultrastar 18ES is longer because of the layout extraction step. The layout of this disk includes periodic unused cylinders, which causes DIXtrac to create dummy zones and repeat time-consuming, per-zone extractions (e.g., sectors per track, track skew, etc.). Extraction for this layout could certainly be optimized, but we are pleased that it worked at all given its unexpected behavior.

Vendor	IBM	Quantum		Seagate
Disk Model	Ultrastar	Atlas III	Atlas 10K	Cheetah
Capacity	9.1 GB	9.1 GB	9.1 GB	4.5 GB
Task	*Time (seconds)*			
Layout extraction	164.7 (10.6)	20.9 (0.8)	50.1 (3.9)	47.6 (0.4)
Complete seek curve	45.2 (0.1)	43.5 (0.2)	33.3 (0.3)	67.3 (0.1)
Mech. overheads	35.8 (1.3)	21.3 (2.5)	18.6 (1.5)	16.6 (1.4)
Cache parameters	25.6 (0.6)	8.1 (0.4)	12.6 (0.3)	12.3 (1.8)
Process. overheads	64.3 (2.5)	43.5 (1.5)	12.7 (0.9)	23 (2.3)
Totals	335.6 (9.2)	137.4 (3.1)	127.4 (4)	166.8 (3.4)

Table 4.1: **Break down of DIXtrac extraction times.** The times are mean values of five extractions. The values in parentheses are standard deviations. "Mech. overheads" includes the extraction of head switch, write settle, and rotation speed.

Vendor	IBM	Quantum		Seagate
Disk Model	Ultrastar	Atlas III	Atlas 10K	Cheetah
Capacity (blocks)	17916239	17783250	17783248	8887200
Defects	123	56	64	21
Translate 1 Address	2.41 ms	1.66 ms	0.86 ms	7.32 ms
Translations	36911	7081	26437	5245

Table 4.2: **Address translation details.**

Table 4.2 shows the number of address translations required by DIXtrac to characterize each disk. Note that the number of translations does not depend directly on the capacity of the disk. Instead, it depends mainly on the sparing scheme, the number of zones, and the number of defects. More translations are performed for disks with more defects, because slipped and relocated blocks obtained from the defect list are verified. Comparing the number of blocks to the number of translations provides a metric of efficiency for DIXtrac's layout discovery algorithms. Given the time required for each translation, this efficiency is important.

The disk maps obtained by the extraction process have been verified for all eight models (24 actual disks) by doing address translation of every logical block and comparing it to the disk map information. The run time of such verification ranges from almost 5 hours (Quantum Atlas 10K) to 21 hours (Seagate Barracuda). In addition to validating the extraction process, these experiments highlight the importance of translation-count-efficiency when extracting the disk layout map.

Vendor	IBM		Quantum				Seagate	
Disk Model	Ultrastar		Atlas III		Atlas 10K		Cheetah	
Trace Type	M	R	M	R	M	R	M	R
$RMS_{Overall}$ (ms)	0.20	0.07	1.14	0.14	0.30	0.19	0.27	0.43
% $\overline{T}_{Mean}$	4%	1%	18%	1%	9%	2%	5%	4%

Table 4.3: **Demetit figures (RMS).** $RMS_{Overall}$ is the overall demerit figure for all trace runs combined. The % $\overline{T}_{Mean}$ value is the percent difference of the respective RMS from the mean real disk response time. R denotes random trace and M denotes a mixed trace.

4.4.2 Validation of extracted values

Running DiskSim configured with the parameters extracted by DIXtrac allows the evaluation of the accuracy of parameter extraction. After extracting parameters from each disk drive, a synthetic trace was generated, and the response time of each request in the trace was measured on the real disk. The trace run and the extracted parameter file were then fed to DiskSim to produce simulated per-request response times. The real and simulated response times were then compared.

Two synthetic workloads were used to test the extracted parameters. The first synthetic workload was executed on each disk with both read and write caches turned off. This workload tests everything except the cache parameters. It consists of 5000 independent requests with 2/3 reads and 1/3 writes. The requests are uniformly distributed across the entire disk drive. The size of the requests is between 2 and 12 KB with a mean size of 8 KB. The inter-arrival time is uniformly distributed between 0 and 72 ms.

The second workload focuses on the cache behavior and was executed with the disk's default caching policies. This trace consists of 5000 requests (2/3 reads and 1/3 writes) with a mix of 20% sequential requests, 30% local (within 500 LBNs) requests, and 50% uniformly distributed requests. The size of the requests is between 2 and 12 KB with a mean size of 8 KB. The inter-arrival time is uniformly distributed between 0 and 72 ms.

For each disk, five extractions were performed to create five sets of disk parameters. For each set of parameters, five mixed traces and five random traces were generated and run on the real disk as well as on the DIXtrac-configured simulated disk. So, for each disk, 50 validation experiments were run. The simulated and measured response times for the four disks are shown in Figure 4.2 and Figure 4.3. Each curve is a cumulative distribution of all collected response times for the 25 runs, consisting of 125000 data points.

The difference between the response times of the real disk and the DIXtrac-configured simulator can be quantified by a demerit figure [Ruemmler and Wilkes

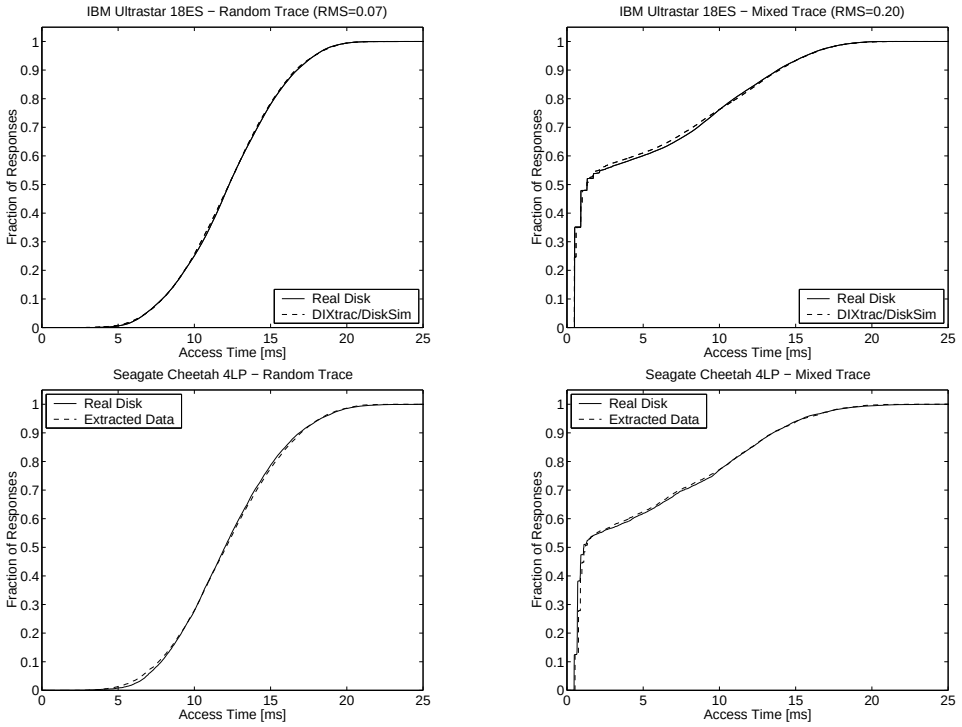

Fig. 4.2: **The comparion of measured and simulated response time CDFs for IBM Ultrastar 18ES and Seagate Cheetah 4LP disks.**

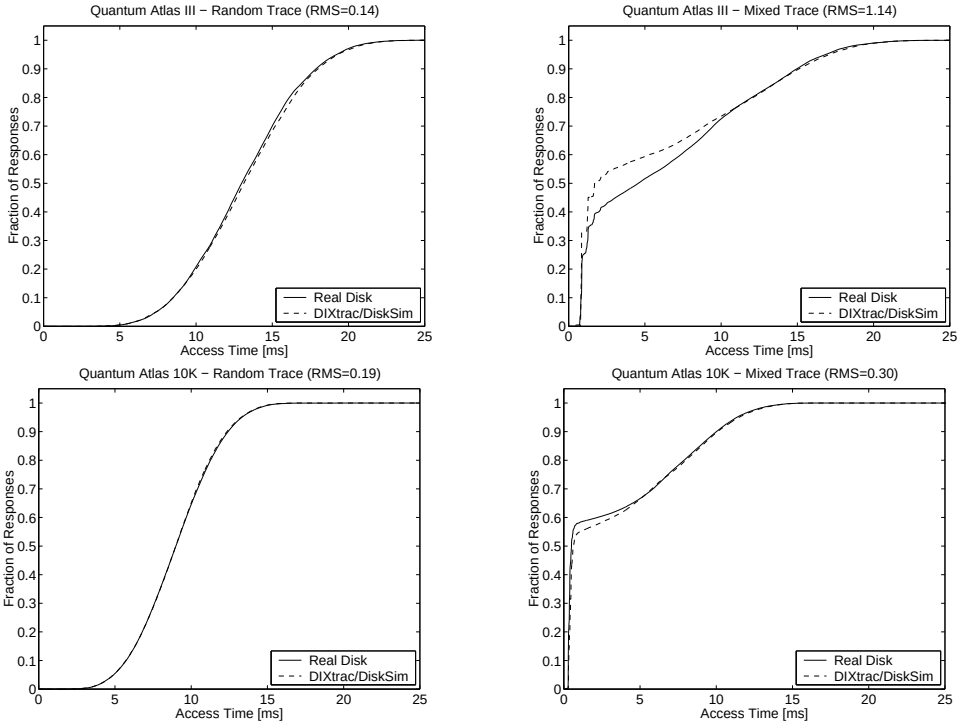

Fig. 4.3: **The comparion of measured and simulated response time CDFs for Quantum Atlas III and Atlas 10K disks.**

1993], which is the root mean square distance in the y-dimension between the two curves. The demerit figure, here referred to as the RMS, for each graph is given in Table 4.3. Most of these values compare favorably with the most accurate disk simulation models reported in the literature [Ruemmler and Wilkes 1993; Worthington et al. 1995].

However, several suboptimal values merit discussion. For the Seagate Cheetah 4LP, the simulated disk with DIXtrac-extracted parameters services requests faster than the real disk. This difference is due to smaller effective values of READ command processing overheads. Manually increasing these values by 0.35 ms results in a closer match to the real disk with RMS at 0.17 ms and 0.16 ms for the mixed and random trace respectively.

The differences in the mixed trace runs for the two Quantum disks are due to shortcomings of DiskSim. DIXtrac correctly determines that the disks use adaptive cache behavior. However, because DiskSim does not model such caches, DIXtrac configures it with average (disk-specific) values for the number and size of segments. The results show that the actual Atlas 10K disk has more cache hits than the DiskSim model configured with 10 segments of 356 blocks. Interestingly, the adaptive cache behavior of the real Atlas III disk is worse than the behavior of the simulated disk configured with 6 segments and 256 blocks per segment. Manually lowering the value of blocks per segment to 65, while keeping all other parameters the same, gives the best approximation of the real disk behavior.

These empirical validation results provide significant confidence in the accuracy of the parameters extracted by DIXtrac. For additional confidence, extracted data were compared directly with the specifications given in manufacturer's technical manuals wherever possible. In all such cases, the extracted values match the data in the documentation.

5 The Access Delay Boundaries Attribute

Storage-device-provided hints about proper I/O sizes can result in significant performance improvements to applications. The ACCESS DELAY BOUNDARIES attribute denotes groupings of contiguous logical blocks into units that yield efficient accesses. It also simplifies the task of I/O performance tuning and reduces implementation complexity; the storage manager (or a human system administrator) need not implement methods that guess efficient I/O sizes to achieve better performance.

This chapter describes the device-specific features this attribute encapsulates for disk drives, disk arrays, and MEMStores and quantifies in detail the performance gains for disk drives. It evaluates the benefits this attribute offers to block-based file systems, log-structured file systems, video servers, and database systems. Finally, it demonstrates on two implementations, the FreeBSD Fast File System [McKusick et al. 1984] and the Shore database storage manager [Carey et al. 1994], that only minimal changes to existing storage managers are needed to achieve significant performance gains for certain workloads.

5.1 Encapsulation

The ACCESS DELAY BOUNDARIES attribute encapsulates the non-linearity in access times to adjacent logical blocks in the device's address space due to device physical characteristics and LBN mappings. While the reasons for these delay boundaries are unique to each particular storage device type, they can be all expressed by this attribute, which encapsulates several device-specific characteristics.

5.1.1 Disk drive

For disk drives, delays in accessing adjacent logical blocks occur when these blocks are mapped to two adjacent tracks. Crossing a track boundary requires a disk head to move to a new location, incurring head switch delay during which no data is being transferred. On the other hand, accessing data mapped onto a single track (i.e., between two access delay boundaries) does not incur this additional delay

once the disk head is positioned. For such accesses, the data is streamed with maximum efficiency.

In addition to disk track boundaries, the ACCESS DELAY BOUNDARIES attribute also encapsulates a disk firmware feature: zero-latency access. While eliminating head switches improves access efficiency by 6%–8%, combining it with this firmware features of high-end disks provides much greater benefit as described and quantified in Section 5.3.1. For such disks, this single attribute therefore encapsulates two device-specific characteristics.

5.1.2 Disk array

Logical volumes striped across several disks in a RAID group can experience delays when either a single stripe unit spans two adjacent disk tracks, or when the logical blocks being accessed map to more than one stripe unit. For such requests, a single I/O results in several separate disk accesses. These smaller disk requests will be less efficient and therefore have a negative effect on achieved throughput and response times. The ACCESS DELAY BOUNDARIES attribute encapsulates the stripe unit boundaries which, in turn, should match the access delay boundaries of the components comprising a disk array.

The size of a stripe unit depends on several factors. Some disk array controllers set the stripe unit size to match that of their cache lines. Other controllers with caches that allow variable-size buffers may determine stripe unit size according to the individual disk characteristics. However, they require disk drives to expose their track sizes via the ACCESS DELAY BOUNDARIES attribute. As demonstrated in Section 5.7.6, RAID controllers exploiting the ACCESS DELAY BOUNDARIES attribute hints by matching stripe units to these precise values significantly outperform RAID groups whose stripe units, in the absence of additional information, merely approximate disk track sizes [Chen and Patterson 1990].

5.1.3 MEMStore

Similar to its performance in disk drives, the ACCESS DELAY BOUNDARIES attribute encapsulates the delay in accessing logical blocks mapped to adjacent tracks. When these blocks are accessed, the media sled must to come to a stop and, at minimum, reverse it direction. In the worst case, the sled must do a full strobe seek to reach the logical block mapped onto the next cylinder. As with for disk drives, it is expected that MEMStores will include in-firmware schedulers that implement position-sensitive scheduling algorithms [Schlosser et al. 2000].

5.2 System design

Access delay boundaries break up the linear LBN address space into extents of LBNs, here referred to as *ensembles*. An ensemble is thus a collection of contiguous LBNs that will provide the most efficient device accesses. Because of device-unique characteristics, ensemble size varies across devices as well as within a single device's address space. Thus, the storage manager must be able to cope with this variable size. However, for many systems, the required changes are minimal and ensembles are a natural choice for data allocation and access.

The ACCESS DELAY BOUNDARIES attribute is suitable for any system that exhibits access patterns that are, at least to some degree, regular. Such systems can allocate related data into ensembles of contiguous logical blocks, and then exploit the efficiency of the ensemble-sized I/Os that are aligned on the access delay boundary. Even though the ensemble sizes are variable, explicitly stating where these boundaries occur allows a storage manager to decide what data to allocate to which ensemble. A storage manager could also choose a particular storage device whose ensemble sizes match the workload needs.

5.2.1 Explicit contract

This attribute provides an explicit contract between the SM and a storage device:

(1) Requests that are exactly aligned on the reported boundaries and span all the blocks of a single ensemble are most efficient.

(2) Requests smaller than the preferred groupings should not, if possible, span a boundary.

The two implementations of storage manager (i.e., a block-based file system and a database storage manager) described in this dissertation demonstrate that the changes required to use the ensembles that encapsulate the ACCESS DELAY BOUNDARIES attribute require relatively minor changes to existing systems. This section discusses practical design considerations involved with these changes.

5.2.2 Data allocation and access

To utilize ensemble boundary information, the storage manager's algorithms for data placement and request generation must support variable-sized extents. Extent-based file systems, such as NTFS [Nagar 1997] and XFS [Sweeney 1996], allocate disk space to files by specifying ranges of LBNs (extents) associated with each file. Such systems lend themselves naturally to ensemble-based alignment of data: during allocation, extent ranges can be chosen to fit track boundaries. Block-based

file systems, such as Ext2 [Bovet and Cesati 2001] and FFS [McKusick et al. 1984], group LBNs into fixed-size allocation units (blocks), typically 4 KB or 8 KB.

Block-based systems can approximate track-sized extents by placing sequential runs of blocks such that they never span track boundaries. This approach wastes some space when track sizes are not evenly divisible by the block size. However, this space is usually 2–3% of total storage space and could be reclaimed by the system for storing inodes, superblocks, or fragmented blocks. Alternatively, this space can be reclaimed if the cache manager is modified to handle partially-valid and partially-dirty blocks.

Like any clustering storage system, a ensemble-based system must address aging and fragmentation and the standard techniques apply: pre-allocation [Bovet and Cesati 2001; Giampaolo 1998], on-line reallocation [Lumb et al. 2000; Rosenblum and Ousterhout 1992; Smith and Seltzer 1996], and off-line reorganization [Blackwell et al. 1995; Matthews et al. 1997]. For example, when a system determines that a large file is being written, it may be useful to reserve (preallocate) entire ensembles even when writing less than a ensemble worth of data. The same holds when grouping small files [Ganger and Kaashoek 1997; Reiser 2001]. When the file system becomes aged and fragmented, on-line or off-line reorganization can be used to re-optimize the on-disk layout. Such reorganization can also be used for retrofitting pre-existing disk partitions or adapting to a new layout of a replacement disk. The point of this dissertation is to show that ensembles are a good target layout for these techniques.

After allocation routines are modified to situate data on track boundaries, system software must also be extended to generate ensemble requests whenever possible. Usually, this will involve extending or clipping prefetch and write-back requests based on ensemble boundaries.

5.2.3 Interface implementation

The *get_ensemble(LBN)* function of the storage interface proposed in this dissertation returns access delay boundaries. Given an LBN, it returns the ensemble's boundaries, LBN_{min} and LBN_{max}, where $LBN_{min} \leq LBN \leq LBN_{max}$. The ensemble size is $|LBN_{max} - LBN_{min}|$; a request (in consecutive LBNs) of that size starting at LBN_{min} yields most efficient device access.

The `sif_ensemble()` function, whose C declaration is listed in Appendix B, implements the *get_ensemble()* function. It takes four arguments: the `lvh` is an opaque logical volume of a given storage device, the input argument `lbn` is the LBN for which an ensemble should be returned, and the `low` and `high` arguments return the LBN_{min} and LBN_{max}, respectively.

To allocate data for efficient access, a storage manager takes an `lbn` from a free block list, calls `sif_ensemble()`, and checks that none of the blocks between the `low` and `high` blocks are allocated. If data to be allocated is smaller than the returned ensemble, the storage manager can either call `sif_ensemble()` with another free `lbn` to find a more suitable free ensemble with fewer LBNs or mark the remaining LBNs in the ensemble as allocated. The data is then written to the device and all the allocation structures are updated.

To determine an I/O size that would yield efficient access (e.g., when determining how much to prefetch), the storage manager calls `sif_ensemble()` with the appropriate `lbn` to obtain the values of `low` and `high`. It then allocates a sufficiently large buffer to fit all data and issues `sif_read()`, where `lbn` equals the `low` and `cnt` equals `high - low`. The next prefetch I/O will repeat this procedure and use the value `high + 1` as the `lbn` parameter.

5.3 Evaluating ensembles for disk drives

This section examines the performance benefits of ensemble-based accesses to the disk drive, finding a 50% improvement in access efficiency and a significant reduction in response time variance. The ensemble-based access is achieved by properly sizing and aligning I/Os on disk track boundaries, which are determined by the DIXtrac tool. First, the improvements measured on actual disks are shown followed by predictions for future disk generations based on an accurate analytical model.

5.3.1 Measuring disk performance

Experimental setup

Most of the experiments described in this section were performed on two disks that support zero-latency access (Quantum Atlas 10K and Quantum Atlas 10K II) and two disks that do not (Seagate Cheetah X15 and IBM Ultrastar 18 ES). The disks were attached to a 550 MHz Pentium III-based PC. The Atlas 10K II was attached via an Adaptec Ultra160 Wide SCSI adapter, the Atlas 10K and Ultrastar were attached via an 80 MB/s Ultra2 Wide SCSI adapter, and the Cheetah via a Qlogic FibreChannel adapter. We also examined workloads with the DiskSim disk simulator [Bucy and Ganger 2003] configured to model the respective disks. Examining these disks in simulation enables us to quantify the individual components of the overall response time, such as seek and bus transfer time.

Increasing efficiency

System software attempts to maximize overall performance in the face of two competing pressures. On one hand, the underlying disk technology pushes for larger request sizes in order to maximize disk efficiency. Specifically, time-consuming mechanical delays can be amortized by transferring large amounts of data between each repositioning of the disk head. However, resource limitations and imperfect information about future accesses impose costs on the use of very large requests.

With ensemble-based access, requests can be much smaller and still achieve the same disk efficiency, as illustrated in Figure 5.1. The graphs show disk efficiency as a function of I/O size, where disk efficiency is the fraction of total access time (which includes seek and rotational latency) spent moving data to or from the media. The track-aligned and unaligned lines show disk efficiency for random, constant-sized reads within the first zone of Quantum Atlas 10K II and Seagate Cheetah X15 disks. The drop-off in efficiency for track-aligned accesses occurs just after a multiple of the first zone's track size. The dotted horizontal line represents best-case steady-state efficiency: sequential data streaming.

In Figure 5.1(a), Point B shows that reading or writing 1 MB at a time results in a 75% disk efficiency for normal (track-unaligned) access. Point A highlights the higher efficiency of track-aligned access (0.73, or 82% of the maximum) over unaligned access for a track-sized request. With I/O size four times as big at Point B, normal I/O efficiency catches up to track-aligned efficiency at Point A. The peaks in the track-aligned curve correspond to multiples of the track size.

Importance of zero-latency access

The relative increase in the efficiency of track-based access is different for the two disks depicted in Figure 5.1. This difference stems from the employment of zero-latency access. While the Quantum Atlas 10K II disk, whose firmware implements zero-latency access, experiences a 48% increase in efficiency for track-based access, the Seagate Cheetah X15, which does not have this feature, experiences only a moderate improvement of 8%.

The increase in disk efficiency for other zero-latency disks is similar to the Quantum Atlas 10K II's 48% increase. The Quantum Atlas 10K achieves 47% higher efficiency and the Maxtor Atlas 10K III 40%. These variations are due to different sizes of the disk's first zone and thus different average seek times for the random track-aligned I/Os within that zone.

Disk efficiency for track-based random I/Os increases only moderately on disks that do not support zero-latency access: 6% for the IBM Ultrastar 18ES and 8% for the Seagate Cheetah X15, depicted in Figure 5.1(b). For these disks, aligning

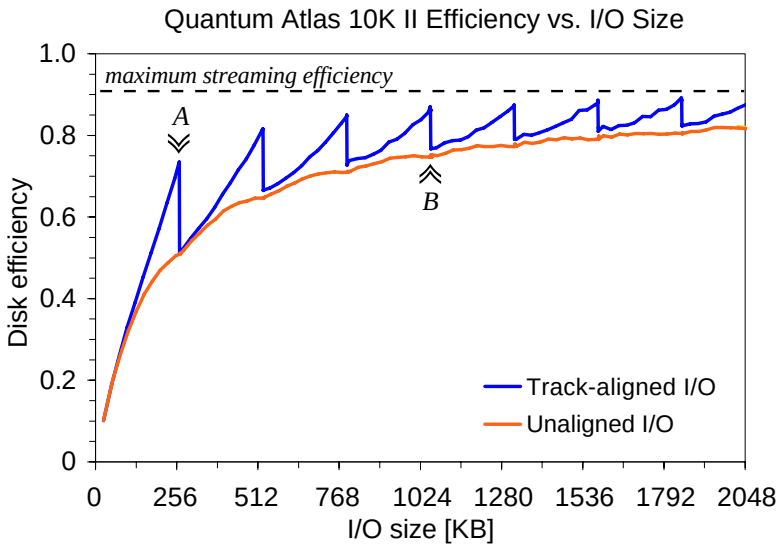

(a) **Zero-latency disk.**

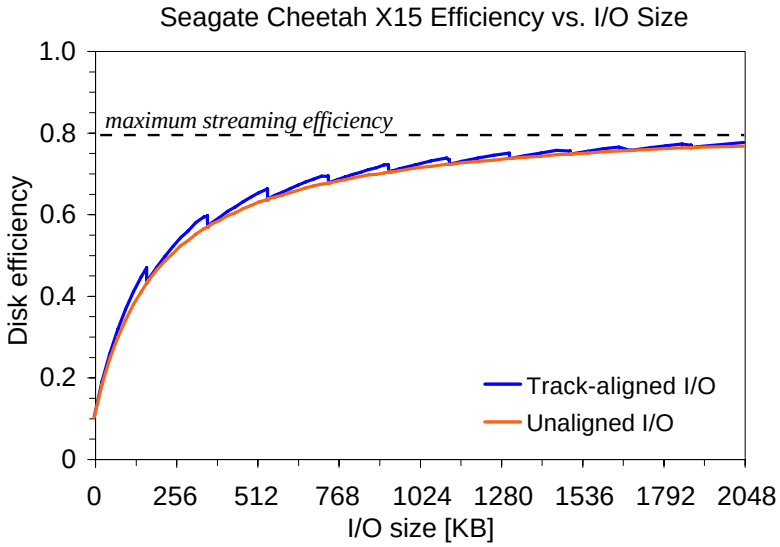

(b) **Non-zero-latency disk.**

Fig. 5.1: **Disk access efficiency.** This graph plots disk efficiency as a function of I/O size for track-unaligned and track-aligned random requests within a disk's first zone. *Disk efficiency* is the fraction of total access time (which includes seek and rotational latency) spent moving data to or from the media. The maximum streaming efficiency (i.e., sequential access without seeks and rotational latencies) is less than 1.0 due to head switches between accesses to adjacent tracks. The peaks in the track-aligned curve correspond to multiples of the track size.

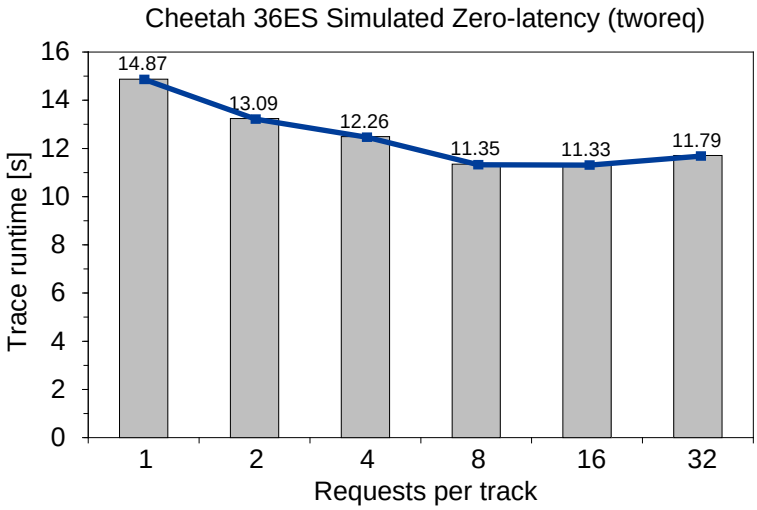

Fig. 5.2: **Getting zero-latency-disk-like efficiency from ordinary disks.** The average seek time for LBNs in the disk's first zone is 3.2 ms. The bus transfer of 738 blocks (sectors per track in the first zone) takes 2.7 ms.

accesses on track boundaries eliminates only the 0.8–1.1ms head switch time—the average rotational latencies of 4 ms (Ultrastar 18ES) and 2 ms (Cheetah X15) are still incurred.

Even though disk firmware may not implement zero-latency access, it is possible to achieve zero-latency-disk-like improvements from such disks. Taking advantage of the disk firmware scheduler and command queuing, a single track-sized request aligned on a track boundary can be broken into smaller requests that can be issued to the disk together. The disk scheduler services them so as to minimize the rotational latency. Once it selects a request rotationally closest to the current head position, all other requests will be serviced without incurring any additional rotational latency; effectively simulating zero-latency access.

Figure 5.2 shows how breaking a single track-based request into several smaller requests achieves the desired performance. The graph shows the total run time of a stream consisting of 1000 random track-sized and track-aligned requests going to the disk's first zone. One full-track request gives an average response time of 14.87 ms, which includes a seek, an average of 3 ms rotational latency, 6 ms for media access and some amount of non-overlapping bus transfer. As this track-sized request is broken into smaller requests, the average response time decreases to 11.33 ms. With smaller requests issued to the disk simultaneously, the bus transfer of data from the previous request can overlap with the media transfer of the next request. Hence, the observed 3.55 ms improvement is larger that the 3 ms expected improvement due to elimination of rotational latency.

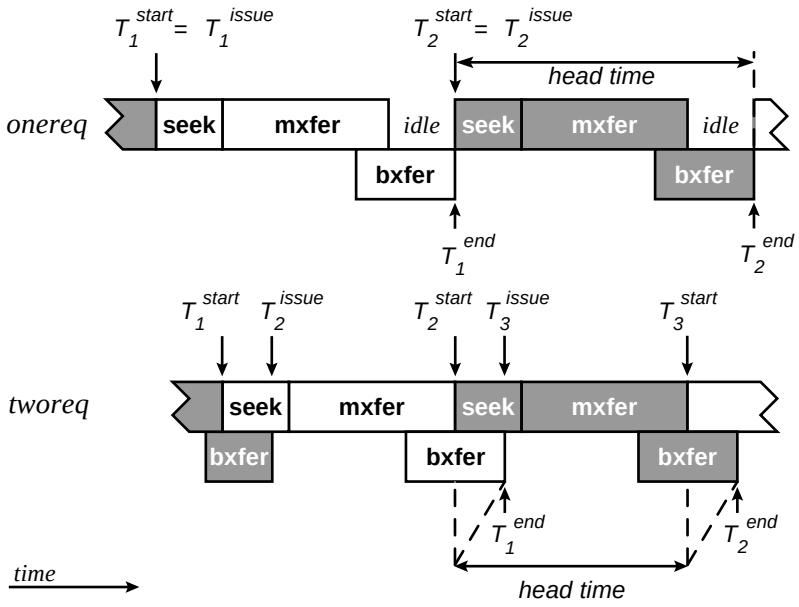

Fig. 5.3: **Expressing head time.** The head time of a *onereq* request is $T_2^{end} - T_2^{issue}$. For *tworeq*, the head time is $T_2^{end} - T_1^{end}$. T^{issue} is the time when the request is issued to the disk, T^{start} is when the disk starts servicing the request, and T^{end} is when completion is reported. Notice that for *tworeq*, T^{issue} does not equal T^{start} because of queueing at the disk.

Microbenchmark performance

Two synthetic workloads, *onereq* and *tworeq*, were used to evaluate basic track-aligned performance. Each workload consists of 5000 random requests within the first zone of the disk. The difference is that *onereq* keeps only one outstanding request at the disk, whereas *tworeq* ensures one request is always queued at the disk in addition to the one being serviced.

We compared the efficiency of both workloads by measuring the average per-request *head time*. A request's head time is the amount of time that the disk head is dedicated to that request. The average head time is the reciprocal of request throughput (i.e., I/Os per second). Therefore, higher disk efficiency will result in a shorter average head time, all else being equal. We introduced head time as a metric because it allows us to identify component delays more easily.

For *onereq* requests, head time equals disk response time as observed by the device driver, because the next request is not issued until the current one is complete. As usual, disk response time is the elapsed time from when a request is sent to the disk to when completion is reported. For *onereq* requests, the read/write head is idle for part of this time, because the only outstanding request is waiting for a bus transfer to complete. For *tworeq* requests, the head time includes

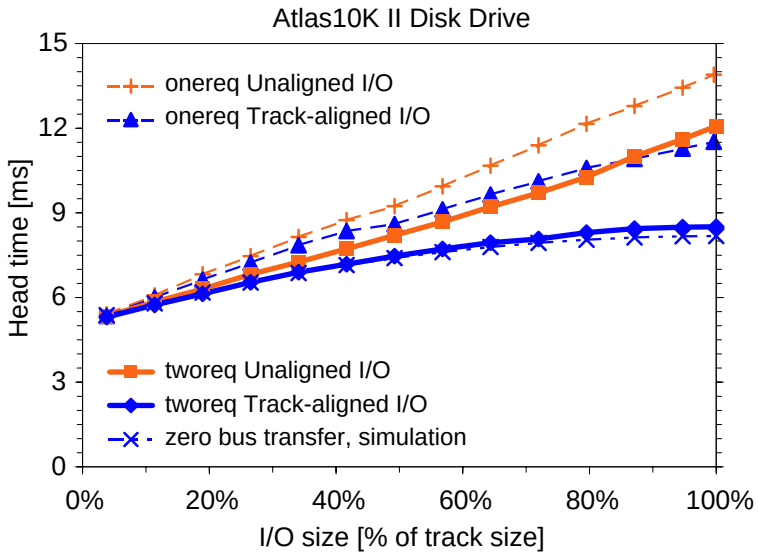

Fig. 5.4: **Average head time for track-aligned and unaligned reads for the Quantum Atlas 10K II.** The dashed and solid lines show the average of measured times for 5000 random track-aligned and unaligned reads to the disk's first zone for the *onereq* and *tworeq* workloads. Multiple runs for a subset of the points reveal little variation (<0.4%) between average head times for distinct sets of 5000 random requests. The thin dotted line represents the *onereq* workload replayed on a simulator configured with zero bus transfer time; note that it approximates *tworeq* without having to ensure queued requests at the disk.

only media access delays, since bus activity for any one request is overlapped with positioning and media access for another. The components of head times for the *onereq* and *tworeq* workloads are shown graphically in Figure 5.3.

Read performance

Figure 5.4 shows the improvement given by track-aligned accesses on the Atlas 10K II. For track-sized requests, head times for track-aligned accesses in *onereq* and *tworeq* decrease by 18% and 32% respectively, which correspond to increases of 22% and 47% in efficiency. The *tworeq* efficiency increase exceeds that of *onereq* because *tworeq* overlaps the previous request's bus transfer with the current request's media transfer.

Because bus and media transfers are overlapped, the head time for a track-aligned, track-sized request in the *tworeq* workload is 8.3 ms (calculated as shown in Figure 5.3). Subtracting 2.2 ms average seek time from the head time yields 6.1 ms. This observed value is very close to the rotation time of 6 ms, confirming that track-aligned accesses to zero-latency disks can fetch a full track in one revolution with no rotational latency.

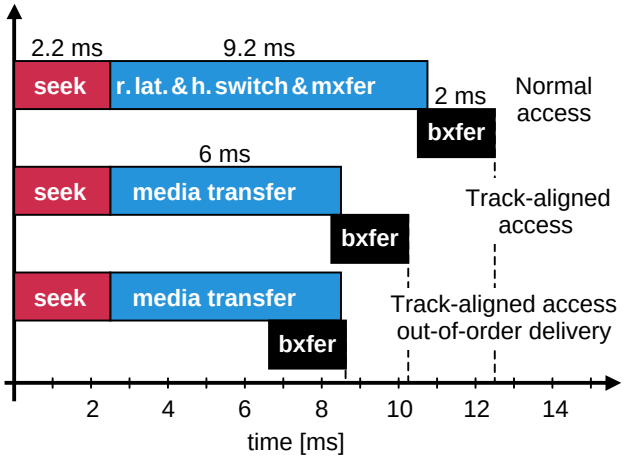

Fig. 5.5: **Breakdown of measured response time for a zero-latency disk.** "Normal access" represents track-unaligned access, including seek, rotational latency (*r.lat.*), head switch, media transfer (*mxfer*), and bus transfer (*bxfer*). For track-aligned access, the in-order bus transfer does not overlap the media transfer. With out-of-order bus delivery, overlap of bus and media transfers is possible.

The command queueing of *tworeq* is needed in current systems to address the in-order bus delivery requirement. That is, even though zero-latency disks can read data out of order, they can only send data over the bus in ascending LBN order. This results in only a 3% overlap, on average, between the media transfer and bus transfer for the track-aligned access bar in Figure 5.5. The overlap would be nearly complete if out-of-order bus delivery were used instead, as shown by the bottom bar. Out-of-order bus delivery improves the efficiency of *onereq* to nearly that of *tworeq* while relaxing the queueing requirement (shown as the "zero bus transfer" curve in Figure 5.4). Although the SCSI MODIFY DATA POINTER command enables out-of-order data delivery, none of the tested disks support it.

Write performance

Track-alignment also makes writes more efficient. For the *onereq* workload on the Atlas 10K II, the head time of track-sized writes is 10.0 ms for track-aligned access and 13.9 ms for unaligned access, a reduction of 28%. For *tworeq*, the reduction in head time is 26% (from 13.8 ms to 10.2 ms). These reductions correspond to efficiency increases of 39% and 35%, respectively.

The larger *onereq* improvement, relative to reads, occurs because the seek and bus transfer are overlapped. The disk can initiate the seek as soon as the write command arrives. While the seek is in progress, the data is transferred to the disk and buffered. Since the average seek for the *onereq* workload is 2.2 ms and the

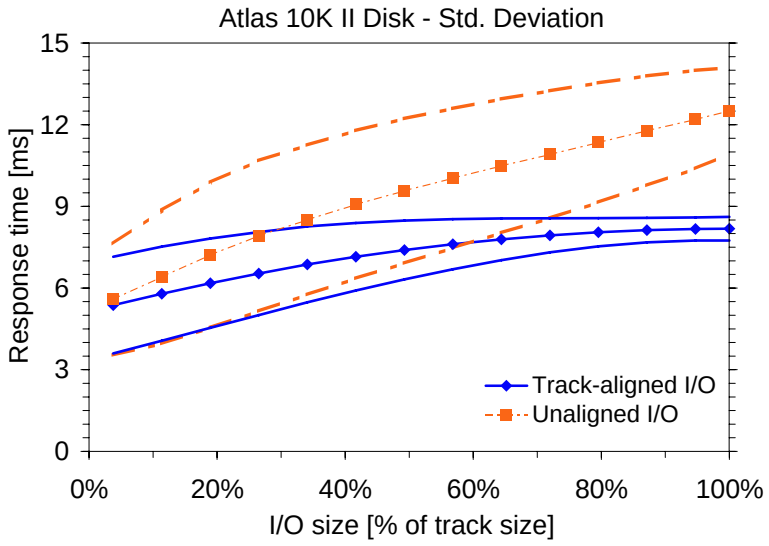

Fig. 5.6: **Response time and its standard deviation for track-aligned and unaligned disk access.** The thin lines with markers represent the average response time, and the envelope of thick lines is the response time ± one standard deviation. The data shown in the graph was obtained by running the *onereq* workload on a simulated disk configured with an infinitely fast bus to eliminate the response time variance due to in-order bus delivery.

data transfer takes about 2 ms, the data usually arrives at the disk before the seek is complete and the zero-latency write begins.

Response time variance

Track-aligned access can significantly lower the standard deviation, σ, of response time as seen in Figure 5.6. As the request size increases from one sector to the track size, $\sigma_{aligned}$ decreases from 1.8 ms to 0.4 ms, whereas $\sigma_{unaligned}$ decreases from 2.0 ms to 1.5 ms. The standard deviation of the seeks in this workload is 0.4 ms, indicating that the response time variance for aligned access is due entirely to the seeks. Lower variance makes response times more predictable, allowing soft real-time applications to use tighter bounds in scheduling, thereby achieving higher utilization. Track-based requests also have lower worst-case access times, since rotational latency and head switch time are avoided. These features bring significant improvements to real-time media servers, as shown in Section 5.6.

5.3.2 System-level benefits

For requests close to the track size (100–500 KB), the potential benefit of track-based access is substantial. A track-unaligned access to all N sectors on the track

involves four delays: seek, rotational latency, N sectors worth of media transfer, and head switch. An N-sector track-aligned access eliminates the rotational latency and head switch delays. This reduces access times for modern disks by 3–4 ms out of 9–12 ms, a 50% increase in efficiency.

Of course, the real benefit provided by track-based access depends on the workload. The greatest benefit is seen by applications with medium-sized I/Os. Streaming media services, such as video servers, MP3 servers, and CDN caches, are examples of this type of application. Other examples include storage components (e.g., Network Appliance's filers [Hitz et al. 1994], HP's AutoRAID [Wilkes et al. 1996], or EMC's Symmetrix) that map data to disk locations in mid-sized chunks. A system issuing large I/O sizes will see modest benefit, because positioning costs can be amortized over large media (the right-hand

size of graph in Figure 5.1). Finally, a workload of random small requests, (e.g., transaction processing), will experience only minimal improvement because request sizes are too small (the left-hand side of the graph in Figure 5.1). The remainder of this chapter evaluates these benefits on several concrete examples of systems.

5.3.3 Predicting improvements in response time

With the analytical model derived in the previous section, it is possible to evaluate the effects of head switch time and zero-latency firmware feature on ensemble-based access for future generations of disks. First, the analytical model is validated against the measurements described previously in Figure 5.1. It is then used to show how changes in head switch time affect the relative improvement of ensemble-based access response times.

Table 5.1 shows relative improvements in the response time of ensemble-based accesses predicted by the analytical model as compared to measurements on a real disk. For each workload, it lists the improvement of ensemble-based (track-aligned) access relative to the normal (track-unaligned) access. The analytic model results used characteristics obtained by the DIXtrac tool.

Workload *full-track* represents a synthetic workload with track-sized I/Os issued to a location randomly chosen within the disk's first zone. The I/O sizes were 334 sectors for the Quantum Atlas 10K disk (with head switch $H = 64$ sectors) and 386 sectors for the Seagate Cheetah X15 disk (with head switch $H = 74$ sectors). Workload *0.8-track* represents a workload to randomly chosen location within the disk's first zone, but I/O sizes set at 80% of first zone's track size. The I/O sizes are thus 268 and 309 blocks respectively for the Atlas 10K and Cheetah X15 disks. The measured data were obtained from the experiments described in Section 5.3.1,

Workload	Relative Improvement in Response Time			
	Quantum Atlas 10K		Seagate Cheetah X15	
	Analytic	Measured	Analytic	Measured
full-track	53%	47%	12%	8%
0.8-track	44%	41%	10%	7%

Table 5.1: **Relative response time improvement with track-aligned requests.** Notice the substantially larger improvement for the Quantum Atlas 10K disk, whose firmware implements zero-latency access, compared to the Seagate Cheetah X15 disk, which does not implement it.

and the analytic data were obtained from the model derived in Appendix A.

For the ensemble-based access of *full-track* workload, the relative improvement in response times predicted by the analytical model is 53% for the Atlas 10K disk and 12% for the Cheetah X15 disk, while the improvements measured on real disks were 47% and 8% respectively. These results confirm the importance of zero-latency access for ensemble-based access. As expected, for accesses that are less than a full track (*0.8-track* workload), the relative improvement is smaller.

The small difference between the predicted and measured values in Table 5.1 indicates the model's high accuracy. Thus, the analytical model can be used with high confidence to explore the impact of technology changes on relative improvements of ensemble-based access compared to normal (track-unaligned) access. As can be observed from the data in Table 3.1, the technology trend of the past 10 years shows that the head switch time has improved at a slower rate than rotational speed. Fortunately, as illustrated in Figure 5.7, this unfavorable trend in disk technology is mitigated by ensemble-based access.

Figure 5.7 shows the relationship between the ratio of head switch time to rotational speed and the relative improvement of ensemble-based access with zero-latency feature over traditional accesses. As head switch time becomes a more dominant factor in the overall response time, the benefit of ensemble-based access becomes larger. For example, the ratio for a typical disk in 1992 was in the 1:9 or 1:8, while disks available in 2000 fell in the 1:7–1:5 region. For 15,000 RPM disks introduced in 2000, the head switch time to rotational time ratio falls in the 1:5–1:4 range; the expected improvement in response time is between 55%–60%.

5.4 Block-based file system

We built a prototype implementation of an ensemble-aware file system in FreeBSD, called Traxtent FFS [Schindler et al. 2002]. This implementation modifies the FreeBSD Fast File System (FFS) [McKusick et al. 1984] to use the ACCESS DELAY BOUNDARIES attribute. This section reviews the the small changes needed to

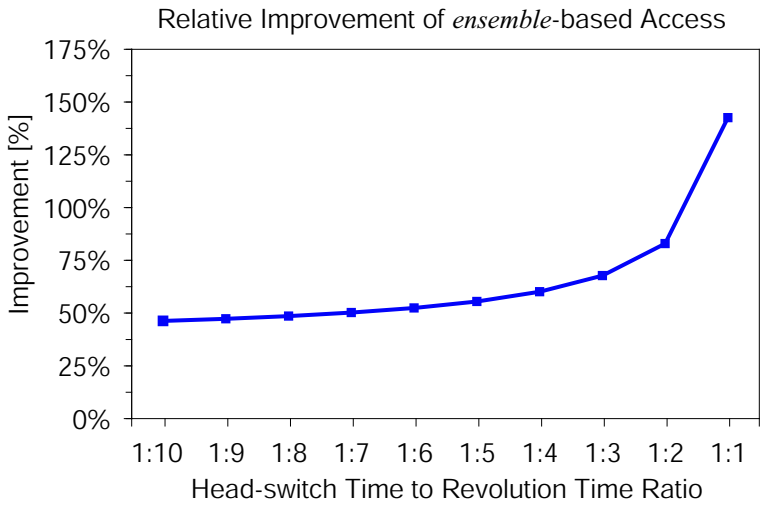

Fig. 5.7: **Relative improvement in response time for ensemble-based access over normal access in the face of changing technology.** With the ratio of head switch time to revolution time becoming larger, the ensemble-based access provides more substantial improvements for disk accesses.

implement ensemble-aware allocation and access in the FreeBSD FFS.

5.4.1 FreeBSD FFS overview

FreeBSD v. 4 assigns three identifying block numbers to buffered disk data (Figure 5.8). The `lblkno` represents the offset within a file; that is, the buffer containing the first byte of file data is identified by `lblkno` 0. Each `lblkno` is associated with one `blkno` (physical block number), which is an abstract representation of the disk addresses used by the OS to simplify space management. Each `blkno` directly maps to a range of contiguous disk *sector numbers* (LBNs), which are the actual addresses presented to the device driver during an access. (Device drivers adjust sector numbers to partition boundaries.) In our experiments, the file system block size is 8 KB (sixteen contiguous LBNs). In this section, "block" refers to a physical block.

FFS partitions the set of physical blocks into fixed-size block groups ("cylinder groups"). Each block group contains a small amount of summary information—inodes, free block map, etc.—followed by a large contiguous array of data blocks. Block group size, block allocation, and media access characteristics were once based on the underlying disk's physical geometry. Although this geometry dependence is no longer real, block groups are still used in their original form because they localize related data (e.g., files in the same directory) and their inodes, resulting in more efficient disk access. The block group size used for the experiments is 32 MB.

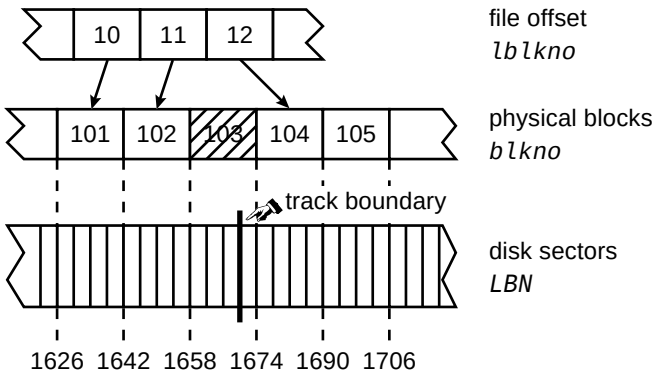

Fig. 5.8: **Mapping system-level blocks to disk sectors.** Physical block 101 maps directly to disk sectors 1626–1641. Block 103 is an *excluded* block because it spans the disk track boundary between LBNs 1669–1670.

FreeBSD's FFS implementation uses the clustered allocation and access algorithms described by McVoy and Kleiman [1991]. When newly created data are committed to disk, blocks are allocated to a file by selecting the closest "cluster" of free blocks (relative to the last block committed) large enough to store all N blocks of buffered data. Usually, the cluster selected consists of the N blocks immediately following the last block committed. To assist in fair local allocation among multiple files, FFS allows only half of the blocks in a block group to be allocated to a single file before switching to a new block group.

FFS implements a history-based read-ahead (a.k.a. prefetching) algorithm when reading large files sequentially. The system maintains a "sequential count" of the last run of sequentially accessed blocks (i.e., if the last four accesses were for blocks 17, 20, 21, and 22, the sequential count is 3). When the number of cached read-ahead blocks drops below 32, FFS issues a new read-ahead of length l beginning with the first non-cached block, where l is the lowest of (a) the sequential count, (b) the number of contiguously allocated blocks remaining in the current cluster, or (c) 32 blocks[1].

5.4.2 FreeBSD FFS modifications

Implementing ensemble-awareness into FreeBSD FFS requires a few, small changes. The implementation described here added or modified less than 100 lines of the FreeBSD C source code. This includes calls to the routines for the DIXtrac discovery tool which returns the values of the ACCESS DELAY BOUNDARIES attribute.

[1] 32 blocks is a representative default value. It may be smaller on systems with limited resources or larger on systems with custom kernels.

Excluded blocks and ensemble allocation

The concept of the *excluded* block is highlighted in Figure 5.8. Blocks that span track boundaries are excluded from allocation decisions by marking them as used in the free-block map. Whenever the preferred block (the next sequential block) is excluded, we instead allocate the first block of the closest available ensemble. When possible, mid-sized files are allocated such that they fit within a single ensemble. For example, ensembles from the Quantum Atlas 10K result in one out of every twenty blocks being excluded under the modified FFS. With increasing linear bit density, the frequency of excluded blocks decreases — only one in thirty blocks is excluded for ensembles of the Quantum Atlas 10K II disk.

Ensemble-sized access

No fundamental changes are necessary in the FFS clustered read-ahead algorithm. FFS properly identifies runs of blocks between excluded blocks as clusters and accesses them with a single I/O request. Until a non-sequential access is detected, we ignore the "sequential count" to prevent multiple partial accesses to a single ensemble; for non-sequential file sessions, the default mechanism is used. We handle the special case where there is no excluded block between contiguous ensembles by ensuring that no read-ahead request goes beyond a track boundary. At a low level, unmodified FreeBSD already supports command queuing at the device and attempts to have at least one outstanding request for each active data stream.

Data structures

When the file system is created, track boundaries are identified, adjusted to the file system's partition, and stored on disk. At mount time, they are read into an extended FreeBSD `mount` structure. We chose this mount structure because it is available everywhere ensemble information is needed.

5.4.3 FFS experiments

Building on the disk-level results, this section compares our prototype ensemble-aware Traxtent FFS to the unmodified version of FFS. We also include results for a modified FFS, here called *fast start* FFS, that aggressively prefetches contiguous blocks. The unmodified FFS slowly ramps up its prefetching as it observes sequential access to a file. The fast start FFS, on the other hand, prefetches up to 32 contiguous blocks on the first access to a file, thus approximating the behavior of the Traxtent FFS (albeit with larger requests and no knowledge of track boundaries).

FFS type	Workload					
	4GB `scan`	0.5GB `diff`	1GB `copy`	Postmark	SSH build	`head *`
unmodified	189.6 s	69.7 s	156.9 s	53 tr/s	72.0 s	4.6 s
fast start	188.9 s	70.0 s	155.3 s	53 tr/s	71.5 s	5.5 s
traxtents	199.8 s	56.6 s	124.9 s	55 tr/s	71.5 s	5.2 s

Table 5.2: **FreeBSD FFS results.** All but the `head *` values are an average of three runs. The individual run times deviate from their average by less than 1%. The `head *` value is an average of five runs and the individual runs deviate by less than 3.5%. Postmark reported the same number of transactions per second in all three runs for the respective FFS, except for one run of the unmodified FFS that reported 54 transactions per second.

Each test is performed on a freshly-booted system with a clean partition on a Quantum Atlas 10K. The tests verify the expected performance effects: small penalties for single sequential scan, substantial benefit for interleaved scans, and no effect on small file activity. The results are summarized in Table 5.2.

Single large file

The first experiment is an I/O-bound linear scan through a 4 GB file. As expected, Traxtent FFS runs 5% slower than unmodified FFS or fast start FFS (199.8 s vs. 189.6 s and 188.9 s respectively). This is because FFS is optimized for large sequential single-file accesses and reads at the maximum disk streaming rate, whereas Traxtent FFS inserts an excluded block one out of every twenty blocks (5%). This penalty could be eliminated by changing the file system cache to support buffering of partial blocks (much like IP fragments) instead of using excluded blocks in large files, giving the block-based system extent-like flexibility.

Multiple large files

The second experiment consists of the `diff` application comparing two large files. Because `diff` interleaves fetches from the two files, we expect to see a speedup from improved disk efficiency. For 512 MB files, Traxtent FFS completes 19% faster than unmodified FFS or fast start FFS. A more detailed analysis shows that Traxtent FFS performs 6724 I/Os (average size of 160 KB) in 56.6 s while unmodified FFS performs only 4108 I/Os (mostly 256 KB) but requires 69.7 s. The fast start FFS performs 4094 I/Os (all but one at 256 KB) and requires 70.0 s. Subtracting media transfer time, unmodified FFS incurs 6.9 ms of overhead (seek + rotational latency + track switch time) per request, and Traxtent FFS incurs only 2.2 ms of overhead per request. In fact, the 19% improvement in overall completion time corresponds to an improvement in disk efficiency of 23%, exactly matching the

predicted difference between single-track accesses and 256 KB unaligned accesses on an Atlas 10K disk.

The third experiment verifies write performance by copying a 1 GB file to another file in the same directory. FFS commits dirty buffers as soon as a complete cluster is created, which results in two interleaved request streams to the disk. This test shows a 20% reduction in run time for Traxtent FFS over unmodified FFS (124.9 s vs. 156.9 s). The fast start FFS finished in 155.3 s.

Small Files

Two application benchmarks are used to verify that the ensemble modifications do not penalize small file workloads. Postmark [Katcher 1997] simulates the small-file activity of busy Internet servers. Our experiments use Postmark v1.11 and its default parameters: 5–10KB files and 1:1 read-to-write and create-to-delete ratios. SSH-build [Seltzer et al. 2000] represents software development activity, replacing the Andrew benchmark. Its three phases unpack the compressed tar archive of SSH v1.2.27, generate the header files and Makefiles, and build the program executable.

As expected, we observe little difference. The SSH-build results differ by less than 0.2%, because the file system activity is dominated by small synchronous writes and cache hits. The fast start FFS performs exactly like the Traxtent FFS having an edge of 0.2% over the unmodified FFS. Postmark is 4% faster with ensembles (55 transactions/second versus 53 for both unmodified and fast start FFS), because the few track switches are avoided. Fast start is not important for Postmark, because the files consist of only 1–3 blocks.

One might view these results as a negative indication of the value of ensembles, but they are not. Recall that FreeBSD FFS does not explicitly group small files into large disk requests. Such grouping has been shown to yield 2–8× throughput increases for static web servers [Kaashoek et al. 1996], web proxy caches [Shriver et al. 2001], and software development activities [Ganger and Kaashoek 1997]. Based on our measurements, we expect that the additional 50% increase in throughput from employing ensembles would be realized given such grouping.

Worst case scenario

As expected, we observe no penalty to small file I/O and a minimal (5%) penalty to the unoptimized single stream case. For random file I/O, FFS's "sequential count" prefetch control replaces the ensemble-based fetch mechanism, preventing useless full-track reads. The one remaining worst-case scenario would be single-

block reads to the beginnings of many large files; in this case, the original FFS will fetch the first 8KB block and prefetch the second, whereas the modified FFS will fetch the entire first ensemble ($\approx$ 160 KB). To evaluate this scenario, we ran an experiment, called `head *`, that reads the first byte of 1000 200 KB files. The results show a 45% penalty for ensembles (3.6 s vs. 5.2 s), closely matching the predicted per-request service time difference (5.6 ms vs. 8.0 ms). Fortunately, this scenario is not often expected to arise in practice. Not surprisingly, the fast start FFS performs even worse than the Traxtent FFS with an average runtime of 5.5 s as it prefetches even more unnecessary data.

5.5 Log-structured file system

The log-structured file system (LFS) [Rosenblum and Ousterhout 1992] was designed to reduce the cost of disk writes. Towards this end, it remaps all new versions of data into large, contiguous regions called segments. Each segment is written to disk with a single I/O operation, amortizing the positioning cost over one large write. A significant challenge for LFS is ensuring that empty segments are always available for new data. LFS answers this challenge with an internal defragmentation operation called *cleaning*. Cleaning a previously written segment involves identifying the subset of "live" blocks, reading them into memory, and writing them into a new segment. Live blocks are those that have not been overwritten or deleted by later operations.

5.5.1 Performance tradeoff

There is a performance trade-off between write efficiency and the cost of cleaning. Larger segments offer higher write efficiency but incur larger cleaning cost since more data has to be transferred for cleaning [Matthews et al. 1997; Seltzer et al. 1995]. Additionally, the transfer of large segments hurts the performance of small synchronous reads [Carson and Setia 1992; Matthews et al. 1997]. Given these conflicting pressures, the choice of segment size must balance write efficiency, cleaning cost, and small synchronous I/O performance. Matching segments to track boundaries can yield higher write efficiency with smaller segments and thus lower cleaning costs.

To evaluate the benefit of using track-based access for LFS segments, we use the overall write cost (OWC) metric described by Matthews et al. [1997], which is a refinement of the *write cost* metric defined for the Sprite implementation of LFS [Rosenblum and Ousterhout 1992]. It expresses the cost of writes in the file system, assuming that all data reads are serviced from the system cache. The

OWC metric is defined as the product of write cost and disk transfer inefficiency:

$$\begin{aligned} OWC &= WriteCost \times TransferInefficiency \\ &= \frac{N^{new}_{written} + N^{clean}_{read} + N^{clean}_{written}}{N^{data}_{written}} \times \frac{T^{actual}_{xfer}}{T^{ideal}_{xfer}} \end{aligned}$$

where N is the number of segments written due to new data or read and written due to segment cleaning, and T is the time for one segment transfer. *WriteCost* depends on the workload (i.e., how much new data is written and how much old data is cleaned) but is independent of disk characteristics. *TransferInefficiency*, on the other hand, depends only on disk characteristics. Therefore, we can use the *WriteCost* values from Matthews et al. [1997] and apply to *TransferInefficiency* values from Figure 5.1.

Figure 5.9 shows that *OWC* is lower with track-aligned disk access and that the cost is minimized when the segment size matches the track size. Unlike our use of empirical data for *TransferInefficiency*, Matthews et al. calculate it as

$$TransferInefficiency = T_{pos} \times \frac{BW_{disk}}{S_{segment}} + 1$$

where $S_{segment}$ is the segment size (in bytes) and T_{pos} is the average positioning time (i.e., seek and rotational latency). To verify that our results are in agreement with their findings, we computed *OWC* for the Atlas 10K II based on its specifications and plotted it in Figure 5.9 (labeled "5.2 ms*40 MB/s") with the *OWC* values for the track-aligned and unaligned I/O. Because the empirical values are for the disk's first zone, the model values we used are too: 2.2 ms average seek, 3 ms average rotational latency, and peak bandwidth of 40 MB/s. As expected, the model is a good match for the unaligned case.

5.5.2 Variable segment size

As shown in Figure 5.9, the lowest write cost is achieved when the size of a segment matches the size of a track. However, different tracks may hold different numbers of LBNs. Therefore, an LFS must allow variable segment sizes in order to match segment boundaries to track boundaries. Fortunately, doing so is straightforward.

In an LFS, the segment usage table records information about each segment. In the SpriteLFS implementation [Rosenblum and Ousterhout 1992], this table is kept as an in-memory kernel structure and is stored in the checkpoint region of the file system. The BSD-LFS implementation [Seltzer et al. 1993] stores this table in a special file called the IFILE. Because of its frequent use, this file is almost always in the file system's cache.

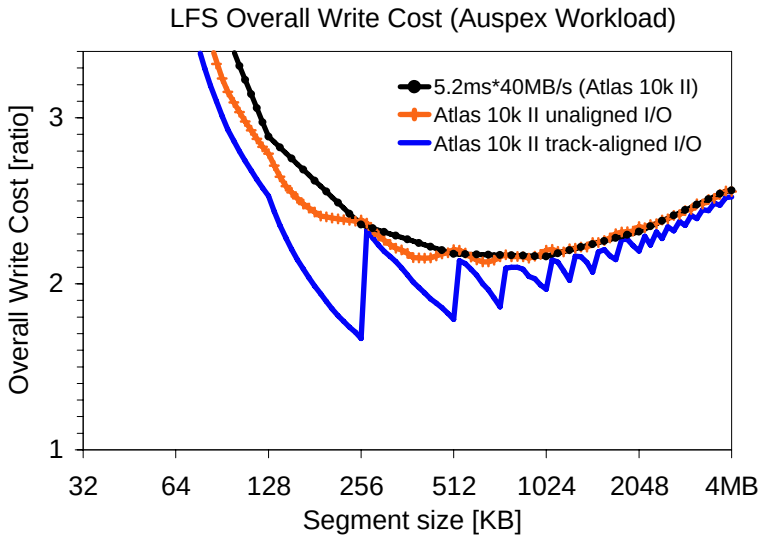

Fig. 5.9: **LFS overall write cost for the Auspex trace as a function of segment size.** The line labeled "5.2 ms*40 MB/s" is the overall write cost predicted by the transfer inefficiency model.

Variable-sized segments can be supported by augmenting the per-segment information in the segment usage table with a starting location (the LBN) and length. During the initialization, each segment's starting location and length are set according to the corresponding track boundary information. When a new segment is allocated in memory, its size is determined from the segment usage table. When the segment becomes full, it is written to the disk at the starting location given in the segment usage table. The procedures for reading segments and for cleaning are similar.

5.6 Video servers

A video server is designed to serve large numbers of video streams to clients at guaranteed rates. To accomplish this, the server first fetches one time interval of video (e.g., 0.5 s) for each stream. This set of fetches is called a *round*. Then, while the data are transferred to clients from the server's buffers, the server schedules the next round of requests. Since the per-interval disk access time is less than the round time, many concurrent streams can be supported by a single disk. Further, by spreading video streams across D disks, D times as many concurrent streams can be supported.

The per-interval disk request size, $IOsize$, is a trade-off between throughput (the number of concurrent streams) and other considerations (buffer space and

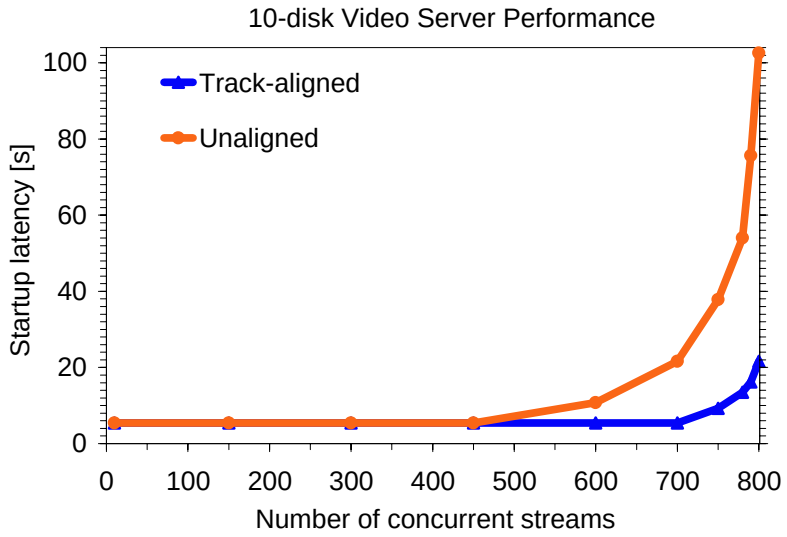

Fig. 5.10: **Worst-case startup latency of a video stream for track-aligned and unaligned accesses.** The startup latency is shown for a 10-disk array of Quantum Atlas 10K II disks, which can support up to 800 concurrent streams.

start-up latency). $IOsize$ must be large enough so that achieved disk bandwidth (disk efficiency times peak bandwidth) exceeds V times the video bit rate, where V is the number of concurrent video streams supported. As $IOsize$ increases, both disk efficiency and $Time_{perIO}$ increase, increasing both the number of supported video streams and the round time, which is defined as V times $Time_{perIO}$.

The round time determines the startup latency of a newly admitted stream. Assuming the video server spreads data across D disks, the worst-case startup latency is the round time times $(D + 1)$ [Santos et al. 2000]. The buffer space required at the server is $2 \times IOsize_{\text{disk}} \times V$. In practice, $IOsize$ is chosen to meet system goals given a trade-off between startup latency and the maximum number of supportable streams. Since track-aligned access increases disk efficiency, it enables more concurrent streams to be serviced at a given $IOsize$.

5.6.1 Soft real-time

Most video server projects, such as Tiger [Bolosky et al. 1996] and RIO [Santos et al. 2000], provide soft real-time guarantees. These systems guarantee that, with a certain probability, a request will not miss its deadline. This allows a relaxation on the assumed worst-case seek and rotational latency and results in higher bandwidth utilization for both track-aligned and unaligned access.

We evaluate two video servers (one ensemble-aware and one not), each containing 10 Quantum Atlas 10K II disks, using the same approach as the RIO video

server [Santos et al. 2000]. First, we measured the time to complete a given number of simultaneous, random track-sized requests. This measurement was repeated 10,000 times for each number of simultaneous requests from 10 to 80. (80 is the maximum number of simultaneous 4 Mb/s streams that can be supported by each disk's 40 MB/s streaming bandwidth.)

From the PDF of the measured response times, we obtained the round time that would meet 99.99% of the deadlines for the 4 Mb/s rate. Given a 0.5 s round time (which translates to a worst-case startup latency of 5.5 s for the 10-disk array), the track-aligned system can support up to 70 streams per disk. In contrast, the unaligned system is only able to support 45 streams per disk. Thus, the track-aligned system can support 56% more streams at this minimal startup latency.

To support more than 70 and 45 streams per disk for the track-aligned and unaligned systems, the I/O size must increase. This increase in I/O size causes an increase in the round time, which in turn increases the startup latency as shown in Figure 5.10. At 70 streams per disk, the startup latency for the track-aligned system is 4× smaller than for the track-unaligned system.

5.6.2 Hard real-time

Although many video servers implement soft real-time requirements, there are applications that require hard real-time guarantees. In their admission control algorithms, these systems must assume the worst-case response time to ensure that no deadline is missed. In computing the worst-case response time, one assumes the worst-case seek, transfer time, and rotational latency.

Both the track-aligned and unaligned systems have the same values for the worst-case seek. The worst-case time for V seeks is much smaller than V times a full strobe seek (seek from one edge of the disk to the other) and it decreases as the number of concurrent streams (V) increases [Reddy and Wyllie 1993]. This is because a disk scheduler can sort the requests in each round to minimize total seek distance. The worst-case seek time charged to a stream is equal to the worst-case scheduled seek route that serves all streams divided by the number of streams.

However, the worst-case rotational latency for unaligned access is one revolution, whereas track-based access suffers no rotational latency. The worst-case transfer time will be similar except that the unaligned system must assume at least one head switch will occur for each request. With a 4 Mb/s bit rate and an I/O size of 264 KB, the track-unaligned system supports 36 streams per disk whereas the track-based system supports up to 67 streams. This translates into 45% and 83% disk efficiency, respectively. With an I/O size of 528 KB, unaligned

access yields 52 streams vs. 75 for track-based access. Unaligned I/O size must exceed 2.5 MB, with a maximum startup latency of 60.5 seconds, to achieve the same efficiency as the track-aligned system.

5.7 Database storage manager

This section describes how a database storage manager, called *Lachesis*, exploits the ACCESS DELAY BOUNDARIES attribute to improve the performance and robustness of database I/O.

5.7.1 Overview

The task of ensuring optimal query execution in database management systems is indeed daunting. The query optimizer uses a variety of metrics, cost estimators, and run-time statistics to devise a query plan with the lowest cost. The storage manager orchestrates the execution of queries, including I/O generation and caching. To do so, it uses hand-tuned parameters that describe the various characteristics of the underlying resources to balance the resource requirements encapsulated in each query plan. To manage complexity, the optimizer makes decisions about other queries and modules without runtime details, trusting that its cost estimates are accurate. Similarly, the storage manager trusts that the plan for each query is indeed well-chosen and that the database administrator (DBA) has tuned the knobs correctly.

To minimize I/O costs, query optimizers and storage managers have traditionally focused on achieving efficient storage access patterns. Unfortunately, two issues complicate this task. First, the multiple layers of abstraction between the query execution engine and the storage devices complicate the evaluation of access pattern efficiency. Second, when there is contention for data or resources, efficient sequential patterns are broken up. The resulting access pattern is less efficient because accesses which were originally sequential are now interleaved with other requests, introducing unplanned-for seek and rotational delays. These two factors lead to significant degradation of I/O performance and longer execution times.

Modern database management systems typically consist of several cooperating modules; the query optimizer, the query execution engine, and the storage manager are relevant to the topic of this dissertation. As illustrated in Figure 5.11, for each query the optimizer evaluates the cost of each alternative execution plan and selects the one with the lowest cost. The execution engine allocates resources for the execution of the selected query plan, while the storage manager communicates with the storage devices as needed.

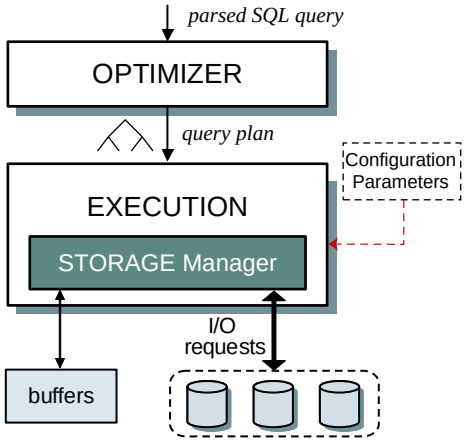

Fig. 5.11: **Query optimization and execution in a typical DBMS.**

Optimizing for I/O

Query optimizers use numerous techniques to minimize the cost of I/O operations. Early optimizers used static cost estimators and run-time statistics [Selinger et al. 1979] collected by the storage manager to estimate the number of I/O operations executed by each algorithm [Graefe 1993] (e.g., loading a page from a storage device into the buffer pool or writing a page back to the device).

Due to the physical characteristics of disk drives, random I/O is significantly slower than sequential scan. To reflect the performance difference, today's commercial database management systems (DBMS) optimizers distinguish between random and sequential I/O using cost models that take into account the data access pattern dictated by each query operator. Despite capturing this important disk performance feature, however, each query is optimized separately. In addition, the optimizer has limited knowledge of the characteristics of the underlying disk subsystem. The calculated access pattern costs are therefore not likely to be observed during execution. To maintain robust performance, the execution engine must uphold the assumed performance in the face of concurrent query execution. In particular, a storage manager must be able to maintain efficient execution of large sequential I/O access pattern even in the face of disrupting activity with small random accesses.

Tuning I/O execution efficiency

During query execution, the execution engine asks the storage manager for data from the disks. The storage manager considers factors such as resource availability and contention across concurrent queries and decides each request's size, location,

and temporal relationship to other requests. Request-related decisions are also influenced by DBA-specified parameters. For instance, IBM DB2's `EXTENTSIZE` and `PREFETCHSIZE` parameters determine the maximal size of a single I/O operation [IBM Corporation 2000], and the `DB2_STRIPED_CONTAINERS` parameter instructs the storage manager to align I/Os on stripe boundaries.

In order for the queries to be executed as planned, the storage manager must balance the competing resource requirements of the queries being executed while maintaining the access cost assumptions the query optimizer used when selecting a query plan. This balance is quite sensitive and prone to human errors. In particular, high-level generic parameters make it difficult for the storage manager to adapt to device-specific characteristics and dynamic query mixes. This results in inefficiency and performance degradation.

Exploiting observed storage characteristics

To achieve robust performance, storage managers need to exploit observed storage system performance characteristics. DBA-specified parameters are too high level to provide sufficient information to the storage manager, therefore DBAs cannot finely tune all the possible performance knobs. Current storage managers complement DBA knob settings with methods that dynamically determine the I/O efficiency of differently-sized requests by issuing I/Os of different sizes and measuring their response time. Unfortunately, such methods are unreliable and error-prone and often yield sub-optimal results.

5.7.2 Robust storage management

This section describes the new storage manager architecture, which bridges the information gap between database systems and underlying storage devices by providing the ACCESS DELAY BOUNDARIES attribute. This allows a DBMS to exploit device characteristics and achieve robust performance for queries even in the face of competing traffic. The architecture retains clean high-level abstractions between the storage manager and the underlying storage devices and leaves unchanged the interface between the storage manager and the query optimizer.

Overview

The cornerstone of the new architecture is to have a storage device (or automated extraction tool) convey to the storage manager explicit information about efficient access patterns. While the efficiency may vary for different workloads (i.e., small random I/Os are inherently less efficient than large sequential ones), this infor-

mation allows a storage manager to always achieve the best possible performance regardless of the workload mix. Most importantly, this information provides guarantees to the query optimizer that access patterns are as efficient as originally assumed when the query plan was composed.

The storage manager learns about efficient device accesses directly from the storage device, which encapsulates its performance characteristics in a few well-defined and device-independent attributes. During query execution, the storage manager uses these hints to orchestrate I/O patterns appropriately. No run-time performance measurements are needed to determine efficient I/O size.

With explicit information about access pattern efficiency, the storage manager can focus solely on data allocation and access. It groups pages together such that they can be accessed with efficient I/Os prescribed by the storage device characteristics. Such grouping meshes well with existing storage manager structures, which call these groups segments or extents [IBM Corporation 2000; Loney and Koch 2000]. Hence, implementing a storage manager that takes advantage of performance attributes requires only minimal changes, as discussed in Section 5.7.3.

Efficient I/O accesses

As shown in Figure 5.1, by the line labeled *Unaligned I/O*, disk efficiency increases as a function of the I/O size by amortizing the positioning cost over more data transfer. To take advantage of this trend, database storage managers buffer data and issue large I/O requests [IBM Corporation 1994; Loney and Koch 2000]. This, however, creates a tension between increased efficiency and higher demand for buffer space. On the other hand, utilizing the ACCESS DELAY BOUNDARIES attribute for ensemble-based access, can be much more efficient.

A database storage manager exercises several types of access patterns. Small sequential writes are used for synchronous updates to the log. Small, single-page, random I/Os are prevalent in On-line Transaction Processing (OLTP) workloads. Large, mostly sequential I/Os occur in Decision Support System (DSS) queries. When running compound workloads, there is contention for data or resources, and this sequentiality is broken. In such cases, it is important that the storage manager achieve near-streaming bandwidth when possible without unduly penalizing any of the ongoing queries.

The *Lachesis* architecture exploits the efficiency of ensemble-aligned accesses. Even with significant interleaving, it can achieve efficiency close to that of purely sequential I/O. Furthermore, it does so without using exceptionally large requests, which would require the use of more buffer space and increase interference with competing traffic.

Despite the inherent inefficiency of an OLTP workload (where disk efficiency is typically 3–5% [Riedel et al. 2000]), *Lachesis* can indirectly improve its performance when OLTP requests are interleaved with larger I/O activity. First, with large I/Os being more efficient, small random I/Os experience lower queueing times. Second, with explicit information about track boundaries, pages are always aligned. Thus, a single-page access never suffers a head switch (caused by accessing data on two adjacent tracks). Eliminating head switch (0.8 ms for the Atlas 10K disk in Table 3.1), however, provides only a limited improvement, because the small-random OLTP accesses experience head switches infrequently: instead, access costs are dominated by seek and rotational latency (averages of 5 and 3 ms respectively), as shown in Section 5.7.7.

Benefits

The database storage manager architecture using performance attributes has several advantages over current database storage managers.

Simplified performance tuning. Since a storage manager automatically obtains performance characteristics directly from storage devices, some difficult and error-prone manual configuration is eliminated. In particular, there is no need for hand-tuning such DB2 parameters as `EXTENTSIZE`, `PREFETCHSIZE`, `DB2_STRIPED_CONTAINERS` or their equivalents in other DBMS. The DBA can concentrate on other important configuration issues.

Minimal changes to existing structures. Very few changes to current storage manager structures are necessary. Most notably, the extent size must be made variable and modified according to the performance attribute values. However, decisions that affect other DBMS components, such as page size or pre-allocation for future appends of related data, are not affected; the DBMS or the DBA are free to set them as desired.

Preserving access costs across abstraction layers. The optimizer's cost estimation functions that determine access pattern efficiency are not modified. In fact, one of its major contributions is ensuring that the optimizer-expected efficiency is preserved across the DBMS abstraction layers *and* materialized at the lowest level by the storage device.

Reduced buffer space pressure. With explicit delay boundaries, a database storage manager can use smaller request sizes to achieve more efficient access. Figure 5.12 illustrates that smaller I/O requests allow smaller buffers, freeing memory for other tasks. Despite sometimes requiring additional smaller I/Os to finish the same job, the greatly increased efficiency of these smaller requests reduces the overall run time.

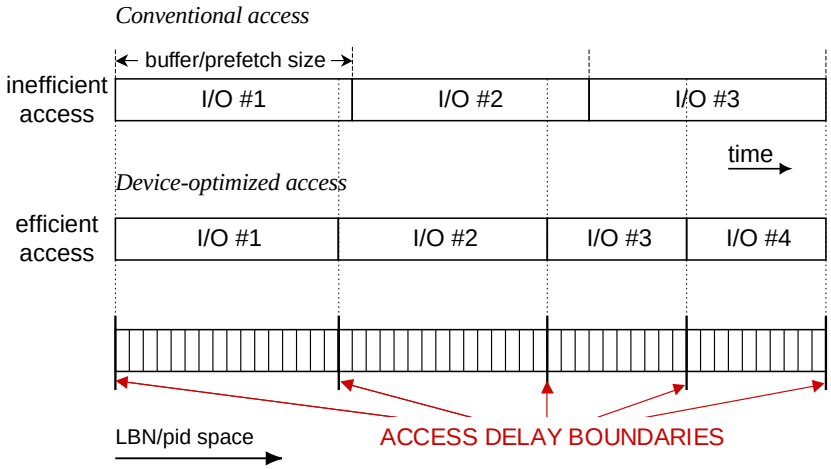

Fig. 5.12: **Buffer space allocation with performance attributes.**

Lower inter-query interference. A storage manager leveraging performance attributes consistently provides nearly streaming bandwidth for table scans even in the face of competing traffic. It can do so with smaller I/Os and still maintain high access efficiency. When there are several request streams going to the same device, the smaller size results in shorter response times for each individual request and provides better throughput for all streams (queries).

5.7.3 Implementation

This section describes the key elements of a *Lachesis* prototype in the latest supported release (interim-release-2) of the Shore storage manager [Carey et al. 1994]. Shore consists of several key components, including a volume manager for storing individual pages, a buffer pool manager, lock and transaction managers, and an ARIES-style recovery subsystem [Mohan et al. 1992]. Shore's basic allocation unit is called an extent and each extent's metadata, located at the beginning of the volume, identifies which of its pages are used.

On-disk data placement

Shore's implementation assumes a fixed number of pages per extent (8 by default) and allocates extents contiguously in a device's logical block space. Therefore, the *LBN* (logical block number) and the `extnum` (extent number) for a given page, identified by a `pid` (page identifier), can be easily computed. To match allocation and accesses to the values of the ACCESS DELAY BOUNDARIES attribute, we modified Shore to support variable-sized extents. A single extent now consists

of a number of pages and an additional unallocated amount of space, the size of which is less than one page.

Although page sizes are typically in powers of two, disk tracks are rarely sized this way (see Table 3.1). Thus, the amount of internal fragmentation (i.e., the amount of unallocated space at the end of each extent) can result in loss of some disk capacity. Fortunately, with an 8 KB page, internal fragmentation amounts to less than 2% and this trend becomes more favorable as media bit density, and hence the number of sectors per track, increases.

Now, the `extnum` and LBN values are read from a new metadata structure. This new structure contains information about how many LBNs correspond to each extent and is small compared to the disk capacity (for example, 990 KB for a 36 GB disk). Lookups do not represent significant overhead, as shown in Section 5.7.7.

I/O request generation

Shore's base implementation issues one I/O system call for each page read, relying on prefetching and buffering inside the underlying OS. We modified Shore to issue SCSI commands directly to the device driver to avoid double buffering inside the OS. We also implemented a prefetch buffer inside Shore. The new prefetch buffer mechanism detects sequential page accesses, and issues extent-sized I/Os. Thus, pages trickle from this prefetch buffer into the main buffer pool as they are requested by each page I/O request. For writes, a background thread in the base implementation collects dirty pages and arranges them into contiguous extent-sized runs. The runs, however, do not match extent boundaries; therefore, we increased the run size and divided each run into extent-sized I/Os aligned on proper extent boundaries.

Our modifications to Shore total less than 800 lines of C++ code, including 120 lines for the prefetch buffer. Another 400 lines of code implement direct SCSI access via the Linux `/dev/sg` interface.

5.7.4 Evaluation

We evaluate *Lachesis* using two sets of experiments. The first set of experiments replays modified I/O traces to simulate the performance benefits of *Lachesis* inside a commercial database system. The original traces were captured while running the TPC-C and TPC-H benchmarks [Transactional Processing Performance Council 2002a; 2002b] on an IBM DB2 relational database system. The second set of experiments evaluates the *Lachesis* implementation inside Shore using TPC-C and (a subset of) TPC-H.

The TPC-H decision-support benchmark includes 22 different queries. We ran all the queries in sequence, one at a time. Each query processes a large portion of the data. The TPC-C benchmark emulates OLTP activity, measuring the number of committed transactions per minute. Each transaction involves a few read-modify-write operations to a small number of records.

For each of the two sets of experiments, we first show the performance of the TPC-H and TPC-C benchmarks as they were run in isolation. We then look at the performance benefits *Lachesis* offers when both benchmarks are run concurrently. In particular, we consider three scenarios:

No traffic simulates a dedicated DSS setup running single-user TPC-H queries.

Light traffic simulates an environment with occasional background traffic introduced while executing the primary TPC-H workload. This represents a more realistic DSS setup with updates to data and other occasional system activity.

Heavy traffic simulates an environment with DSS queries running concurrently with a heavy OLTP workload. This represents a scenario in which decision DSS queries are run on a live production system.

Finally, we contrast the results of the experiments with simulated Lachesis-DB2 and our implementation. The same trends in both cases provide strong evidence that other DBMS implementations using *Lachesis* are likely to obtain similar benefits.

Experimental Setup

We conducted all experiments on a system with a single 2 GHz Intel Pentium 4 Xeon processor, 1 GB of RAM, and a 36 GB Maxtor Atlas 10K III disk attached to a dedicated Adaptec 29160 SCSI card with 160 MB/s transfer rate. The basic parameters for this disk are summarized in Table 3.1. The system also included a separate SCSI host bus adapter with two additional disks; one with the OS and executables and the other for database logs. We ran our experiments on RedHat 7.3 distribution under Linux kernel v. 2.4.19, modified to include an I/O trace collection facility. For DB2 runs, we used IBM DB2 v. 7.2.

5.7.5 DB2 experiments

We do not have access to the DB2 source code. To evaluate the benefits of *Lachesis* for DB2, we simulated its effect by modifying traces obtained from our DB2 setup. We ran all 22 queries of the TPC-H benchmark and captured their device-level

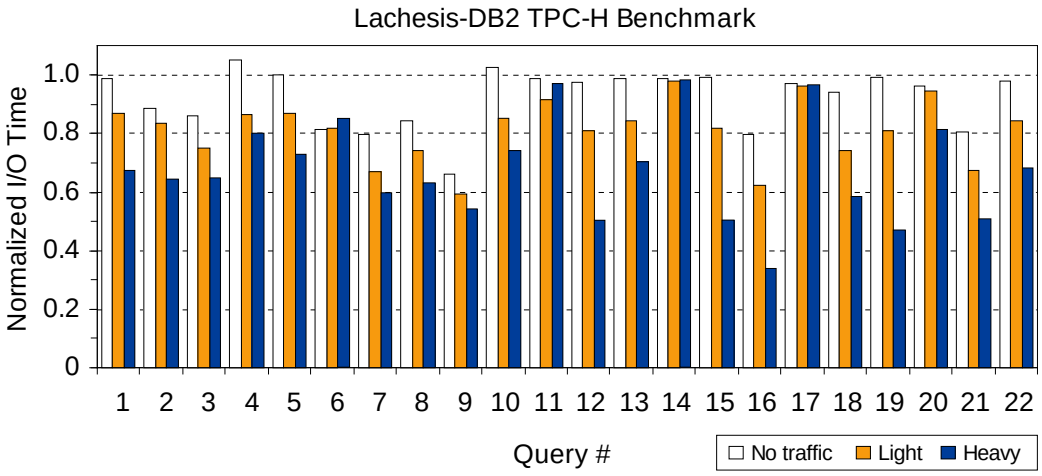

Fig. 5.13: **TPC-H I/O times with competing traffic (DB2).**

I/O traces. We then wrote a trace-replay tool and used it to replay the original captured traces. Finally, we compared the trace replay time with the DB2 query execution time. The trace-replay method is quite accurate; the measured and replayed execution times differed by at most 1.5%.

The sum of all the periods between the completion time of the last outstanding request at the device and the issue time of the next request determined the *pure CPU time* from the captured traces. It expresses the periods when the CPU is busy, while the storage device is idle. Since the goal is to study I/O efficiency, the pure CPU time was subtracted from the traces for a more direct comparison.

Having verified that the original captured TPC-H traces never had more than two outstanding requests at the disk, we replayed the no-CPU-time traces in a closed loop by always keeping two requests outstanding at the disk. This ensures that the disk head is always busy (see Section 5.7.1) and preserves the order of request issues and completions [Lumb et al. 2002]. Because of our trace replay method, the numbers reported in this section represent the query *I/O time*, which is the portion of the total query execution time spent on I/O operations.

To simulate *Lachesis* behavior inside DB2, we modified the DB2 captured traces by compressing back-to-back sequential accesses to the same table or index into one large I/O. We then split this large I/O into individual I/Os according to the values of the ACCESS DELAY BOUNDARIES attribute. Thus, the I/Os are contained within an integral number of pages that fit within two adjacent boundaries.

The resulting modified traces preserve the sequence of blocks returned by the I/Os (i.e., no out-of-order issue and completion). Allowing requests to complete out of order might provide additional performance improvements due to request

scheduling. However, we did not want to violate any unknown (to us) assumptions inside DB2 that require data to return in strictly ascending order.

The modified traces also preserve the DB2 buffer pool usage. The original DB2 execution requires buffers for I/Os of 768 blocks (determined by the `PREFETCHSIZE` parameter) whereas DB2 with *Lachesis* would generate I/Os of at most 672 blocks (a single Atlas 10K III track of the outermost zone accommodates 42 8 KB-pages).

TPC-H

We hand-tuned our DB2 configuration to give it the best possible performance on our hardware setup. We set the `PREFETCHSIZE` to 384 KB (48 pages × 8 KB page, or 768 blocks), which is comparable to the I/O sizes that would be generated by *Lachesis* inside DB2 running on the disk we used for our experiments[2]. We also turned on `DB2_STRIPED_CONTAINERS` to ensure proper ramp-up and prefetching behavior of sequential I/Os. We configured the DB2 TPC-H kit with the following parameters: a scaling factor of 10 (10 GB total table space), a page size of 8 KB, and a 768 MB buffer pool. We put the TPC-H tablespace on a raw device (a partition of the Atlas 10K III disk) to avoid double buffering inside Linux kernel.

The results of the TPC-H experiments are shown in Figure 5.13 by the bars labeled *No traffic*. For each TPC-H query, the bar shows the resulting I/O time of the Lachesis-simulated trace normalized to the I/O time of the original trace.

With the exception of queries 4 and 10, whose run times were respectively 4% and 1% longer, all queries benefited. Queries that are simple scans of data (e.g., queries 1, 4, 15) in general do not benefit; the original DB2 access pattern already uses highly efficient large sequential disk accesses thanks to our manual performance tuning of the DB2 setup. The minor I/O size adjustments of these sequential accesses cause small changes in performance (e.g., a 1% improvement for queries 1 and 15 and a 4% slowdown for query 4). On the other hand, queries that include multiple nested joins, such as query 9, benefited much more (i.e., a 33% shorter execution time or a 1.5× speedup) because of inherently interleaved access patterns. Interestingly, such queries are also the most expensive ones. On average, the 22 queries in the workload experienced an 11% speedup. When weighted by each query's run time the average improvement is 19%, indicating that the longest running queries see the most improvement.

The access pattern of query 10 is dominated by runs of 2–4 sequential I/O accesses (sized at `EXTENTSIZE` of 768 blocks). At the end of each run, the disk head

[2] `PREFETCHSIZE` setting of 512 KB triggers a Linux kernel "feature": a single `PREFETCHSIZE`-d I/O to the raw device generated by DB2 was broken into two I/Os of 1023 and 1 block. Naturally, this results in highly inefficient accesses. Therefore, we chose 768 instead.

seeks to another nearby location a few cylinders away and performs another short sequential run. The *Lachesis*-simulated trace, however, transforms the sequential runs into 3–5 I/Os (the track size is at most 686 blocks) with the last being less than a full track in size. Hence the modified trace executes more I/Os, not all of them being track-sized.

Because of data dependencies in queries with several nested joins (e.g., queries 9 and 21), the I/O accesses were not purely sequential. Instead, they contained several interleaved data and index scans. Even when executing such queries one at a time, these interleaved sequential accesses in effect interfered with each other and caused additional seek and rotational delays. *Lachesis* mitigated these adverse effects, resulting in significant performance improvements.

The plans for queries 17 and 20 include two nested-loop joins and index scans. Hence, most I/Os are small random requests of 1–2 pages; the limited performance improvement of *Lachesis* comes from the elimination of head-switches with delay boundary-aligned accesses, just like in the OLTP experiments described below.

TPC-C

Since *Lachesis* targets track-sized I/Os, we do not expect any benefit to small random I/Os stemming from an OLTP workload. To ensure that *Lachesis* does not hurt TPC-C performance we captured I/O traces on our DB2 system running the TPC-C benchmark, applied the same transformations as for the TPC-H workload, and measured the trace replay time. Eliminating CPU time was not necessary because there were no storage device idle periods in the trace.

The DB2 configuration for the TPC-C benchmark is identical to the one described in Section 5.7.5 (8 KB pages, a 768 MB buffer pool, a raw device partition of the Atlas 10K III disk holding the TPC-C data and indexes). We used the following parameters for the TPC-C benchmark: 10 warehouses (approximately 1 GB of initial data), 10 clients per warehouse, and zero keying/think time. As expected, the experiments showed that *Lachesis* does not adversely affect TPC-C performance. Using our setup, we achieved a throughput of 309.3 transactions per minute (TpmC). The original TPC-C trace replay took 558.2 s and the Lachesis-modified trace took 558.6 s.

Compound workload

To demonstrate *Lachesis*' ability to increase I/O efficiency under competing traffic, we simulated the effects of running TPC-C simultaneously with TPC-H queries by injecting small 8 KB random I/Os (a reasonable approximation of TPC-C traffic) into the disk traffic during the TPC-H trace replay. We used a Poisson arrival

process for the small-random I/O traffic and varied the arrival rate between 0 and MAX arrivals per second. With the hardware setup, MAX was determined to be 150 by measuring the maximal throughput of 8 KB random I/Os.

The results are shown in Figure 5.13. As in the *No traffic* scenario, we normalize the *Lachesis* runs to the base case of replaying the no-CPU-time original traces. However, since there is additional traffic at the device, the absolute run times increase (see Section 5.7.7 for details). For the *Light traffic* scenario, the arrival rate λ was 25 arrivals per second, and for the *Heavy traffic* scenario λ was 150. Under *Heavy traffic*, the original query I/O times varied between 19.0 and 1166.2 s, yielding an average 2.6× increase in I/O time compared to *No traffic*.

The Lachesis-modified traces exhibit substantial improvement in the face of competing traffic. Further, this relative value grows as the amount of competing traffic increases, indicating the *Lachesis*' robustness in the face of competing traffic. On average, the improvement for the *Light traffic* and *Heavy traffic* scenarios was 21% (or 1.3× speedup) and 33% (1.5× speedup) respectively. Query 16 experienced the greatest improvement, running 3 times faster in the *Heavy traffic* scenario. With the exception of queries 6, 11, 14, and 17, which showed little or no benefit, all other queries benefit the most under the *Heavy traffic* scenario.

5.7.6 RAID experiments

To evaluate the benefit of having explicit performance attributes from disk arrays, we replayed the captured DB2 traces against a disk array simulated by a detailed storage subsystem simulator, called DiskSim [Bucy and Ganger 2003]. We created a logical volume on a RAID5 group with 4 disks configured with validated Atlas 10K III characteristics [Schindler and Ganger 1999].

In the base case scenario, called *base-RAID*, we set the stripe unit size to 256 KB (or 512 disk blocks) and fixed the I/O size to match the stripe unit size. This value approximates the 584 sectors per track in one of the disk's zones and, as suggested by Chen and Patterson [1990], provides the best performance in the absence of exact workload information. In the second scenario, called *ensemble-RAID*, both the RAID controller and the database SM can explicitly utilize the precise track-size; both the stripe unit and I/O sizes are equal to 584 blocks.

The resulting I/O times of the 22 TPC-H queries, run in isolation without any competing traffic, are shown in Figure 5.14. The graph shows the *ensemble-RAID* time normalized to the *base-RAID*. Comparing this with the TPC-H runs on a single disk, we immediately notice a similar trend. Queries 17 and 20 do not get much improvement. However, most queries enjoy more significant improvement (on average 25%, or 1.3× speedup) than in the single disk experiments.

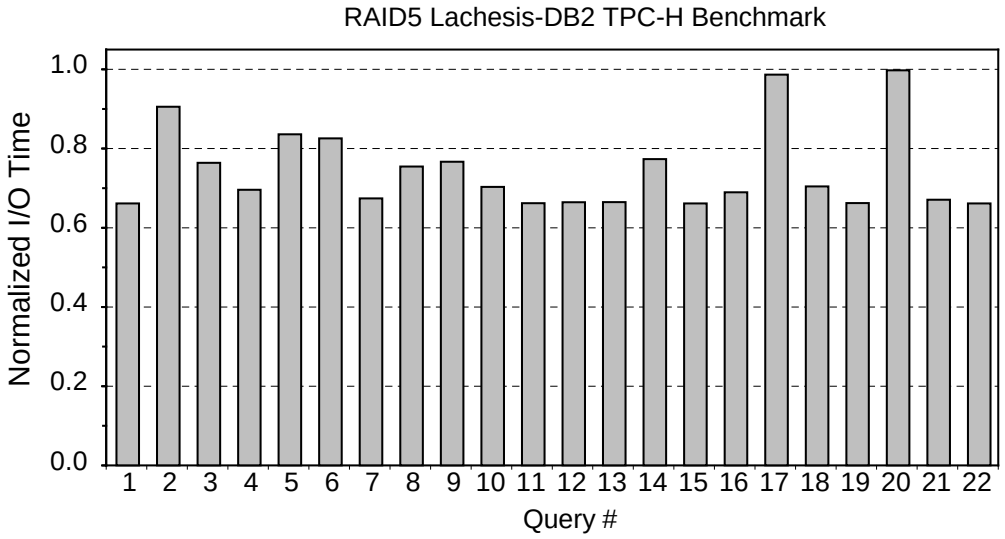

Fig. 5.14: **TPC-H trace replay on RAID5 configuration (DB2).**

The performance benefits in the RAID experiments are larger because the parity stripe, which rotates among the four disks, causes a break in sequential access to each individual's disk in the *base-RAID*. This is not a problem, however, in the *ensemble-RAID* case, which achieves efficiency close to streaming bandwidth with ensemble-sized stripe units.

5.7.7 Shore experiments

We compared the performance of our implementation, called *Lachesis-Shore* and described in Section 5.7.3, to that of baseline Shore. For fair comparison, we added (one-extent) prefetching and direct SCSI to the Shore interim-release 2 and call it *Basic-Shore*. Unless stated otherwise, the numbers reported in the following section represent an average of 5 measured runs of each experiment.

TPC-H

The Shore TPC-H kit (obtained from earlier work [Ailamaki et al. 2001]) implements queries 1, 6, 12, and 14. We used a scaling factor of 1 (1 GB database) with data generated by the `dbgen` program [Transactional Processing Performance Council 2002b]. We used an 8 KB page size, a 64 MB buffer pool, and the default 8 pages per extent in Basic-Shore. The Lachesis-Shore implementation matches an extent size to the device characteristics, which, given the location of the volume on the Atlas 10K III disk, varied between 26 and 24 pages per extent (418 and 396

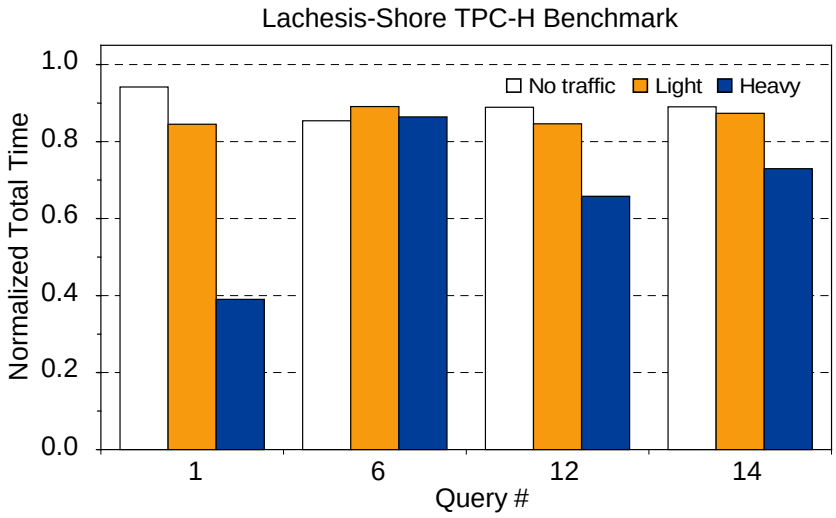

Fig. 5.15: **TPC-H queries with competing traffic (Shore).**

disk blocks). Figure 5.15 shows the normalized total run time for all four TPC-H queries implemented by the TPC-H kit. *Lachesis* improved run times between 6% and 15% in the *No traffic* scenario.

TPC-C

To ensure that *Lachesis* does not hurt the performance of small random I/Os in OLTP workloads, we compared the TPC-C random transaction mix on our Basic- and Lachesis-Shore implementations configured as described in Section 5.7.7. We used 1 warehouse (approximately 100 MB of initial data) and varied the number of clients per warehouse. We set the client keying/think time to zero and measured the throughput of 3000 transactions. As shown in Table 5.3, our implementation had minimal effect on the performance of the standalone TPC-C benchmark.

Compound workload

We modeled competing device traffic for DSS queries of the TPC-H benchmark by running a TPC-C random transaction mix. Due to the limitations of the Shore TPC-H and TPC-C kit implementations, we could not run the TPC-H and TPC-C benchmarks in the same instance. Thus, we ran two instances whose volumes were located next to each other on the same disk. Because the volumes occupied a small part of the disk, this experiment approximates the scenario of OLTP and DSS workloads accessing the same database.

The TPC-H instance was configured as described in Section 5.7.7 while the

	Basic Shore		*Lachesis Shore*	
Clients	**TpmC**	**CPU**	**TpmC**	**CPU**
1	844	34%	842	33%
3	1147	46%	1165	45%
5	1235	50%	1243	49%
8	1237	53%	1246	51%
10	1218	55%	1235	53%

Table 5.3: **TpmC (transactions-per-minute) and CPU utilization.** The slightly better throughput for the Lachesis-Shore implementation is due to proper alignment of pages to track boundaries.

TPC-C instance was configured with 1 warehouse and 1 client per warehouse, which ensured that no transactions were aborted. We varied the amount of background OLTP traffic by changing the keying/think time of the TPC-C benchmark to achieve a rate of 0 to TpmC_{MAX} (maximum transactions per minute).

Figure 5.15 shows the performance results for Lachesis-Shore, normalized to the Basic-Shore execution time. As with the DB2 trace replay experiments, *Lachesis* provides greater speedups in the face of competing traffic, than under the *No traffic* scenario. Additional experiments show that *Lachesis*' relative improvement increases as a function of the amount of competing traffic. The average improvement for the four TPC-H queries under the *Light traffic* and *Heavy traffic* scenarios was 14% (or a 1.2× speedup) and 32% (a 1.5× speedup) respectively.

An important result of this experiment is shown in Figure 5.16. This figure compares the absolute run times for each query as a function of increasing transactional throughput. The two Shore implementations achieve different TpmC_{MAX}. While for the Basic-Shore implementation TpmC_{MAX} was 426.1, Lachesis-Shore achieved a 7% higher maximal throughput (456.7 transactions per minute). Thus, *Lachesis* not only improves the performance of the TPC-H queries alone, but also improves the performance of the TPC-C workload under the *Heavy traffic* scenario.

Extent lookup overhead

Since a *Lachesis* implementation uses variable size extents, we also wanted to evaluate the potential overhead of `extnum` and LBN lookup. Accordingly, we configured our Lachesis-Shore implementation with extents of uniform size (128 blocks) to match the default 8-page extent size in the Basic-Shore implementation and ran the four TPC-H queries. In all cases, the difference was less than 1% of the total runtimes. Thus, explicit lookup, instead of a simple computation from the page `pid` in Basic-Shore, does not result in a noticeable slowdown.

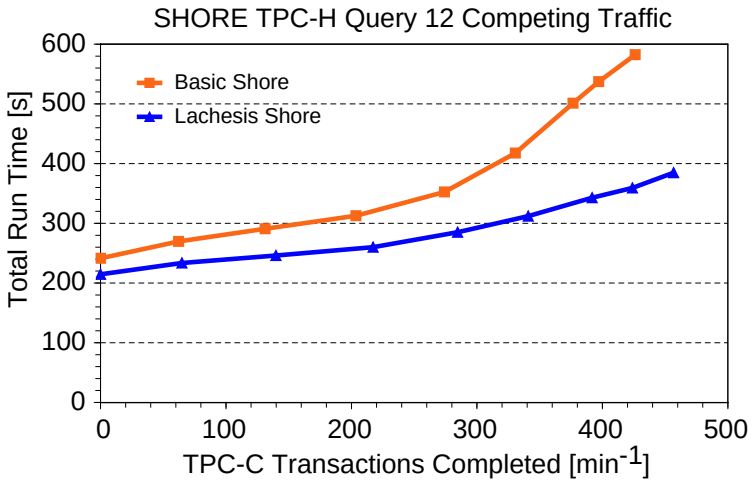

Fig. 5.16: **TPC-H query 12 execution time as a function of TPC-C competing traffic (Shore).**

Comparison to DB2 experiments

The results for compound workloads with the Lachesis-Shore implementation and the Lachesis-modified DB2 traces show similar trends. For example, as the competing traffic to queries 1 and 12 increases, the relative performance benefit of *Lachesis* increases as well. Similarly, the relative improvement for query 6 remained stable (around 20%) under the three scenarios for both DB2 and Shore.

Two important differences between the DB2 and Shore experiments warrant a closer look. First, under the *No traffic* scenario, Lachesis-Shore experienced a larger speedup. This is because the Basic-Shore accesses are less efficient than the accesses in the original DB2 setup. Basic-Shore uses 8-page extents, spanning 128 blocks, compared to *Lachesis*' variable-sized extents of 418 and 396 blocks (the track sizes of the two inner-most zones). DB2, on the other hand, prefetched 768 disk blocks in a single I/O, while the *Lachesis*-modified traces used at most 672 blocks (the outer-most zone has 686 sectors). Consequently, the base case for DB2 issues more efficient I/Os relative to its Shore counterpart, and hence the relative improvement for Lachesis-Shore is higher.

Second, TPC-H query 14 with the DB2 trace replay did not improve much, whereas Lachesis-Shore's improvement grew with increasing traffic. The reason lies in the different access patterns resulting from different join algorithms. While DB2 used a nested-loop join with an index scan and intermediate sort of one of its inputs, Lachesis-Shore used a hash-join. Thus, Lachesis-Shore saw a higher improvement, whereas in the DB2 trace replay, the improvement did not change.

Finally, to demonstrate that both experimental setups yield the same quali-

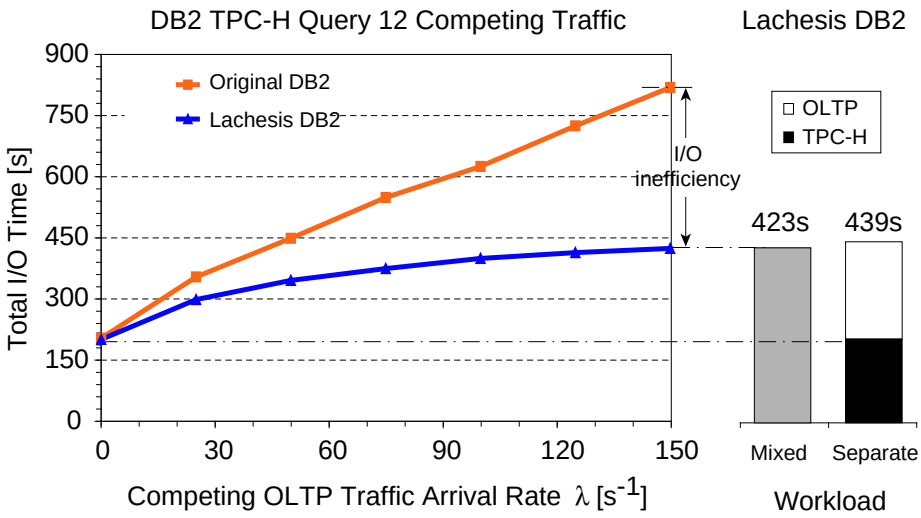

Fig. 5.17: **TPC-H query 12 execution (DB2)** The graph on the left shows the amount of time spent in I/O operations as a function of increasing competing OLTP workload, simulated by random 8 KB I/Os with arrival rate λ. The I/O inefficiency in the original DB2 case is due to extraneous rotational delays and disk head switches when running the compound workload. The two bars illustrate the robustness of *Lachesis*; at each point, both the TPC-H and OLTP traffic achieve their best-case efficiency. The **Mixed** workload bar in the right graph corresponds to the $\lambda = 150$ Lachesis-DB2 datapoint of the left graph. The **Separate** bar shows the total I/O time for the TPC-H and the OLTP-like workloads when run separately.

tative results, we compared the run times for TPC-H query 12 on Lachesis-Shore (shown in Figure 5.16) vs. Lachesis-DB2 (shown in Figure 5.17). This query first scans through the LINEITEM table applying all predicates, and then performs a join against the ORDERS table data. Although the x-axes use different units, and hence the shapes of the curves are different, the trends in those two figures are the same. With small amounts of competing traffic, the relative improvement of *Lachesis* is small. However, as the amount of competing traffic increases, the speedup grows to 1.5× for Shore and 2× for DB2 under the *Heavy traffic* scenario.

Executing with maximum efficiency

Figure 5.17 demonstrates the effect of *Lachesis* on the performance of a DSS workload as a function of competing OLTP I/O traffic. The graph on the left plots the time spent in I/O operations during TPC-H query 12 execution on DB2 as a function of increasing competing OLTP workload. As the amount of competing traffic increases (simulated as before by random 8 KB I/Os with arrival rate λ), the execution time of the original DB2 increases. This increase comes from I/O inefficiency in the original DB2 stemming from extraneous rotational delays and disk head switches when running the compound workload.

The graph on the left shows the amount of time spent in I/O operations as a function of an increasing amount of competing OLTP workload. The two bars on the right illustrate how *Lachesis* uses storage device resources with maximum efficiency allowed by the workload. Even with the largest contention for the storage device (the bar labeled Mixed), *Lachesis* achieves as good a performance as if it were executing the two workloads separately. The bar on the right, labeled Separate, adds the runtimes of the OLTP and TPC-H workloads run separately.

Even though the mostly-sequential accesses of the TPC-H workload are broken by the small random I/Os of the OLTP workload, the efficient ensemble-based accesses guarantee the expected performance of the TPC-H workload running in isolation. Naturally, the total runtime is larger since the device is doing more work, but it does deliver the same efficiency to the TPC-H workload under both scenarios. The 4% performance improvement in the Mixed workload comes from the disk firmware built-in scheduler. With more requests outstanding, it can schedule requests more efficiently.

6 The Parallelism Attribute

Several classes of applications, such as scientific computing or data mining, can greatly benefit from exploiting internal parallelism of a storage device. While parallelism in disk arrays, for example, reduces latency by spreading load across multiple individual disks and improves data throughput by being able to deliver the aggregate bandwidth of individual disks, traditional systems do not expose the bindings of logical blocks to the individual disks. As a consequence, a storage manager issues several requests at once expecting them to be serviced in parallel. With no knowledge of how these requests map to individual disks, however, they may produce I/Os competing for the same device rather than proceeding in parallel, utilizing only a fraction of the available resources.

With explicit knowledge of (i) the proper level of parallelism and (ii) the mappings of individual logical blocks to parallel-accessible locations, a storage manager can partition its work to most effectively utilize all available resources. The PARALLELISM attribute, which conveys both notions, not only improves the utilization of the available resources, but also simplifies storage administration. For example, today's database systems use an administrator tunable parameter describing how many disks comprise a logical volume [IBM Corporation 2000]. This parameter is used to determine the level of parallelism for sort and join algorithms [Graefe 1993]. With explicit information, this parameter need not be exposed; a database system can automatically tune to the storage device-provided parameter.

This chapter describes device-specific features of disk arrays and MEMStores the PARALLELISM attribute encapsulates and shows how applications with parallel accesses to two-dimensional data structures can benefit from this explicit knowledge. It describes a design and implementation of a disk array logical volume manager, called *Atropos*, that provides a new layout leveraging disk-specific features for efficient parallel access. The benefits of this efficient parallel access to two-dimensional structures are shown for database management systems (DBMS) performing selective table scans. The evaluation uses two implementations of parallel-accessible storage systems: *Atropos* disk array logical volume manager and emulated MEMStore [Griffin et al. 2002].

6.1 Encapsulation

The PARALLELISM attribute encapsulates the ability of the device to access efficiently (i.e., in parallel) separate areas of the media mapped to disjoint LBNs of the device's address space. Such access is possible thanks to either device's internal configuration (e.g., logical volumes consisting of several disks) or specific technology of a single physical device such as MEMStore.

Any system that allocates data to disjoint LBNs and then accesses them together frequently can benefit from the PARALLELISM attribute. In particular, device-specific characteristics encapsulated within ensure efficient access to two-dimensional data structures that are mapped to a linear address space of fixed-size LBNs. It allows a storage manager to turn regular access patterns in both dimensions (i.e., row- and column-major accesses) into efficient I/Os (possibly proceeding in parallel), even though they may map to disjoint LBNs.

6.1.1 Access to two-dimensional data structures

Figure 6.1 uses a simple example to illustrate the benefits of exposing PARALLELISM attribute to storage managers and applications and contrasts it with the conventional systems that stripe data across disks in fixed-size stripe units. The example depicts a two-dimensional data structure (e.g., a table of a relational database) consisting of four columns, numbered $1, \ldots, 4$, and rows, labeled $a, \ldots, f$. For simplicity, the example assumes that each element of this two dimensional structure (e.g., a_1), maps to a single LBN of the storage device, which consists of two independent disks. For the remainder of the discussion, the number of disks is referred to as the level of parallelism, p.

To map this two-dimensional structure into a linear space of LBNs, conventional systems decide a priori which order (i.e., column- or row-major) is likely to be accessed most frequently [Copeland and Khoshafian 1985]. Using the unwritten contract stating that sequential access is efficient, they then map a portion of the data along the frequently-accessed-major to a range of contiguous LBNs to ensure efficient execution of the most likely access pattern.

The example in Figure 6.1 chose a column-major access to be most prevalent, and hence assigned the runs of $[a_1, b_1, \ldots, f_1]$, $[a_2, b_2, \ldots, f_2]$, $[a_3, b_3, \ldots, f_3]$, and $[a_4, b_4, \ldots, f_4]$ to contiguous LBNs. The mapping of each element to the LBNs of the individual disks is depicted in Figure 6.1(b) in a layout called *Naïve*. When accessing a column, the disk array uses (i) sequential access within each disk and (ii) parallel access to both disks, resulting in maximum efficiency.

With the a priori decision of organizing data in column-major order, accessing data in the other major (i.e., row-major) results in accesses to disjoint LBNs.

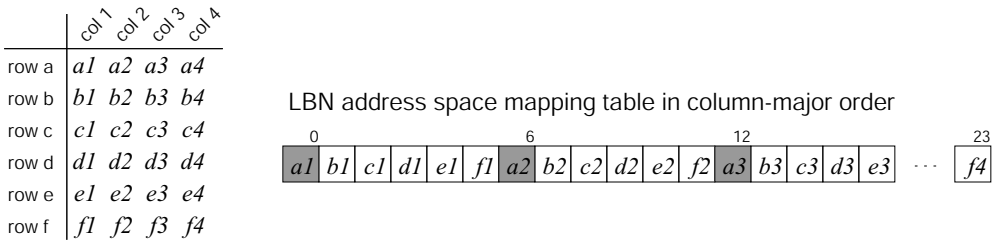

(a) Mapping two-dimensional data structure into linear LBN space.

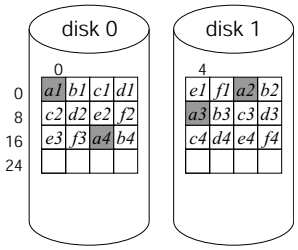

(b) Naïve.

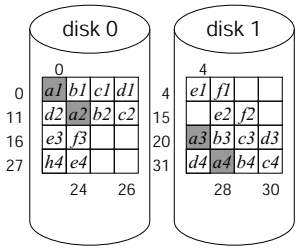

(c) Parallel-efficient.

Fig. 6.1: **Example describing parallel access to two-dimensional data structures.**

Hence, a row-major access to a single row of $[a_1, a_2, a_3, a_4]$ is carried out by four separate, and less efficient, I/Os. As shown in Figure 6.1(b), where the disks of the disk array map four LBNs per track, a_1 and a_4 will be read from disk 0, while a_2 and a_3 will be read from disk 1. This access pattern is inefficient; it includes a high positioning cost of a small (random) access to fetch each element from the disk. The inefficiency of this access pattern stems from the lack of information in conventional systems; one column is blindly allocated after another within the LBN address space.

Even if the dimensions of the table do not naturally fit the characteristics of the disks, it is possible to achieve efficient access in both majors with an alternative layout depicted in Figure 6.1(c). This layout, called *Parallel-efficient*, utilizes both the knowledge of stripe unit sizes (i.e., the ACCESS DELAY BOUNDARIES attribute) and the number of parallel-accessible disks, p, to map columns 1 and 2 such that their respective first row elements start on disk 0, while the first row elements of columns 3 and 4 are mapped to disk 1. Such grouping of columns is referred to as the layout depth, d. In this example, d equals two.

The *Parallel-efficient* layout still gives efficient column-major access, just like the *Naïve* layout. When reading the row $[a_1, a_2, a_3, a_4]$, the first two elements are

accessed from disk 0, and the other two from disk 1. Compared to the *Naïve* layout, however, these accesses are much more efficient; instead of having two random accesses, d elements of the row are accessed diagonally, incurring much smaller positioning cost than the *Naïve* layout. Section 6.3 describes why this diagonal access, called *semi-sequential*, is efficient. Additionally, the load is balanced across disks and accesses to a_1 and a_2 on disk 0 proceed in parallel with accesses to a_3 and a_4 on disk 1.

The efficient access in both dimensions comes at a small cost of some wasted space. As shown in Figure 6.1(c), some LBNs are not allocated so as to preserve access efficiency. However, the amount of wasted space is not as severe as this contrived example might suggest. As shown in Section 6.3.6, this space amounts to less than 2% of the total disk capacity. Additionally, the results in Figure 5.1 of Chapter 5 show that the apparent break in sequential access caused by skipping over a few sectors lowers the efficiency of sequential access by at most 1%.

6.1.2 Equivalence class abstraction

The PARALLELISM attribute encapsulates two parameters, p and d, that respectively denote the number of (possibly disjoint) LBNs that can be accessed in parallel and the number of disjoint LBNs that can be accessed efficiently. Exposing these two parameters alone, however, is not sufficient for storage managers to realize parallel and efficient access. Thus, to explicitly convey the LBNs that can be accessed in parallel and/or efficiently, a storage device also exposes sets of LBNs, called *equivalence classes*.

A grouping of LBNs into one equivalence class indicates which p LBNs can be accessed in parallel and grouping into another equivalence class indicates which d disjoint LBNs can be accessed efficiently (but not necessarily in parallel). Unlike the ACCESS DELAY BOUNDARIES attribute, which defines a set of *contiguous* LBNs, the PARALLELISM attribute denotes a set of disjoint LBNs that can be accessed efficiently. The access efficiency for these disjoint LBNs is at most as high, but no higher, as the efficiency for any set of contiguous LBNs expressed by the ACCESS DELAY BOUNDARIES attribute. Using the example of Figure 6.1(c), which maps all elements of row a to LBNs in the set of $\{0, 8, 24, 28\}$, LBN 0 forms a parallel-accessible equivalence class with LBNs 24 or 28 (parameter p) and another equivalence class with LBN 8 for efficient access to the same disk (parameter d).

6.1.3 Disk array

For disk arrays, the PARALLELISM attribute exposes the mapping of logical volume LBNs onto blocks of individual disks (i.e., striping) and the number of disks, p,

that can independently position their heads. With such information, a storage manager can simultaneously issue p I/Os to appropriately selected disjoint logical volume LBNs. Internally, these I/Os are issued to the p disks of the same group that can service, in parallel, one request each.

Exposing just the p parameter without the LBNs of an equivalence class is not sufficient. Requests to p disjoint LBNs mapped to a single disk, but intended to be serviced in parallel, will utilize only $1/p$ of the available resources (disks). On the other hand, explicitly knowing the members of an equivalence class (i.e, mapping of stripe units to individual disks) enables the storage manager to issue I/Os to all p disks.

With conventional disk arrays, the mapping of LBNs to different disks could be calculated from the stripe unit and RAID group size. However, the equivalence class construct has much more expressive power than simple exposure of the stripe unit size and the RAID group size and organization; the LBNs may have arbitrary values with no apparent relationship. As shown in Section 5.7.6, matching stripe units sizes individual disk's track sizes yields the highest access efficiency. With zoned disk geometries, where different tracks have different number of sectors (that are rarely powers of two), the parallel-accessible LBNs do not follow regular strides. Knowing individual disks' track size, which are conveyed via the ACCESS DELAY BOUNDARIES attribute, a disk array volume manager can simply determine the proper equivalence class members and expose them to a storage manager.

The equivalence class construct and the d parameter of the PARALLELISM attribute also encapsulates a unique concept of efficient access to disjoint LBNs mapped to a single disk. The efficient semi-sequential access to adjacent tracks exploits two characteristics unique to disk drives: data layout with track skews, caused by track switches, and firmware request scheduler. Both of these characteristics are detailed in Section 3.2. Exploiting these two characteristics that are encapsulated in the d parameter is instrumental in providing efficient access to two-dimensional data structures in both row- and column-major orders.

Even though different disk array characteristics influence the values of the d and p parameters, there exists a direct relationship between them. The parameter d puts an upper bound on how many disjoint LBNs can be accessed from a single disk in time equivalent to a single revolution, as shown in Section 6.3.3. With requests issued to all p disks, a disk array can thus service at most $d \times p$ blocks in a given amount of time. Issuing more requests will only increase access latency with no improvement to access efficiency. As the service time for a semi-sequential access to a single disk is determined by track switch time, issuing more than d requests in a batch to one disk, only increase the latency. With just d requests in the queue, the firmware scheduler can determine an optimal service order that

eliminates all of rotational latency. Issuing more than p batches will negate the effect of parallel access.

6.1.4 MEMStore

For MEMStores, the PARALLELISM attribute exposes the mapping of logical blocks to the locations on the media sled that can be accessed as a result of single positioning movement of the media sled relative to the read/write tips. Once the position is determined, a (sub)set of the available read/write tips can access several LBNs in parallel.

For each LBN, there exists an equivalence class of LBNs that can be potentially accessed in parallel. The members of the set are determined by the LBN's position within device's virtual geometry. The size of the set is determined by the number of read/write tips in the device. Only a subset (e.g., 5–10%) of the equivalence class can actually be accessed in parallel, as determined by the power budget of the device. If read/write tips share components, then there will be constraints on which LBNs from the set can be accessed together. Both of these constraints, however, are hidden behind the storage interface.

Given a single LBN, a two-step algorithm [Schlosser et al. 2003] can calculate all the LBNs belonging to one equivalence class. The algorithm uses four virtual device geometry parameters, listed in Table 3.3: the number of parallel-accessible squares in the x-dimension, N_x, in the y-dimension, N_y, and the number of sectors per track, S_T, and per cylinder, S_C. Once the equivalence class is known, a storage manager can choose any (sub)set of p sectors from that class. These sectors are guaranteed to be accessed in parallel.

For MEMStores, parallel access to p LBNs is realized by a set of read/write tips that can access media together for a given sled position. The efficient access to d LBNs is then realized by using a different set of read/write tips and hence proceeding in parallel as well. Thus, the distinction between p and d LBNs is only caused by the device's geometry and LBN mappings. For MEMStores with square virtual geometry (i.e., when $N_x = N_y$), two values are equal; the same number of locations can be accessed by turning either a row or a column of the tips. Using the example MEMStore device in Figure 3.8, $p = d = 3$ and the LBN 33 forms an equivalence class $\{33, 34, 35\}$ with p LBNs and another equivalence class $\{33, 36, 51\}$ with d LBNs. With a virtual geometry that is not square, or for devices with additional power or shared-component constraints, d may be different from p.

6.2 System design

The PARALLELISM attribute is intended to facilitate efficient accesses to disjoint LBNs. Given a two-dimensional data structure, a storage manager still allocates data sequentially along the most-likely access major. With the equivalence class abstraction, however, it can determine which LBNs of this sequence can be accessed in parallel as well as how to allocate data to disjoint LBN to provide efficient access in the other major.

6.2.1 Explicit contract

The PARALLELISM attribute provides the following explicit contract between a storage manager and a storage device:

(1) A set of p (potentially disjoint) LBNs forms an equivalence class E_p, where $p = |E_p|$. All LBNs of E_p can be always accessed in parallel.

(2) A subset of d specific (disjoint) LBNs forms an equivalence class E_d, where $d = |E_d|$. All LBNs of E_d can be always accessed most efficiently, provided the requests are issued to the device together. Accessing fewer than d LBNs may not be as efficient as accessing all of them together.

(3) Accessing together d disjoint LBNs from the set E_d may potentially be as efficient as accessing an equal number of sequential LBNs (denoted by the ACCESS DELAY BOUNDARIES attribute) but is not guaranteed to be so. However, accessing d LBNs from the E_d set is more efficient that accessing d randomly chosen LBNs not belonging to the same equivalence class.

6.2.2 Data allocation and access

The abstraction of disk parallelism in the PARALLELISM attribute with its equivalence classes assures that appropriately chosen disjoint blocks i.e., LBNs that are members of the same equivalence class, can be always accessed in parallel. Given an LBN mapped to a particular disk and, say, two disks comprising a logical volume, *any* LBN mapped to a different disk is parallel-accessible and the number of equivalence classes for that LBN equals the total number of blocks on that disk.

When the choice of a particular equivalence class E_{LBN} is unconstrained i.e., when the application has no preference which LBNs are chosen, the PARALLELISM attribute has no clear advantage. Simply partitioning the address space of a logical volume consisting of two disks into two halves, and exposing the individual device boundaries, as done for example by ExRAID [Denehy et al. 2002], is sufficient. The PARALLELISM attribute, however, is advantageous to applications with

regular accesses to ordered data such as two-dimensional data structures that put constraints on how data are mapped and accessed.

By virtue of mapping two-dimensional structures (e.g., large non-sparse matrices or database tables) into a linear LBN space, efficient accesses in conventional storage systems that do not expose additional information to storage managers are possible only in either row-major or column-major order. Hence, a data layout that optimizes for the most common access method is chosen with the understanding that accesses along the other major axis are inefficient [Ramamurthy et al. 2002].

To make accesses in both dimensions efficient, one can create two copies of the same data; one copy is then optimized for row order access and the other for column order access [Ramamurthy et al. 2002]. Unfortunately, not only does this double the required space, but updates must propagate to both replicas to ensure data integrity. With proper data layout that uses the PARALLELISM attribute, it is possible to achieve efficient accesses in both dimensions with only one copy of the data.

The explicit grouping of LBNs encapsulated in the PARALLELISM attribute allows a storage manager to properly allocate rectangular data and access them efficiently along both dimensions using the same data organization. As illustrated in Figure 6.1(c), two-dimensional data is mapped into a contiguous run of LBNs along its one dimension. These contiguous LBNs can be accessed in parallel with p efficient (e.g., ensemble-sized) I/Os. For the other dimension, the data is allocated to the d LBNs. The access along this other dimension is also efficient; up to p sets of LBNs (equivalence classes), each with d distinct LBNs, can be retrieved with a single positioning cost.

For accesses to regular structures, the choice of parallel-accessible LBNs is much more constrained and both the number and cardinality of the equivalence classes a storage device exposes to a storage manager can be much smaller. Given the example in Figure 6.1(c), the equivalence class for LBN 0 can only list LBNs 20 and 28 as being parallel-accessible (i.e., positionally equivalent), instead of listing all LBN mapped to disk 1 as parallel-accessible (e.g., LBNs 4 through 7, 12 through 15, 20 through 23, and 28 through 31).

6.2.3 Interface implementation

The storage interface includes a *get_parallelism()* function, which returns the number of blocks, p, that can be accessed by the storage device in parallel and the number of blocks, d that can be accessed efficiently. The *get_equivalent(LBN)* returns a set of disjoint LBNs in the equivalence class. The *batch()* command explicitly groups a collection of READ or WRITE commands. For storage devices

that do not provide the same level of parallelism across its entire address space, the *get_parallelism()* function called with an with the LBN parameter can return values of p and d parameters, together with the appropriate equivalence classes, relevant to the provided LBN.

The C declaration of the functions and relevant data structures exposing the PARALLELISM attribute are listed in Appendix B. These functions and structures are used in the prototypes described later in the Chapter. The *get_parallelism()* function is implemented by `sif_inquiry()`, which returns an `lv_options` data structure describing a logical volume `lvh`. The `parallelism` member is the p parameter, `depth` is the d parameter, `capacity` is the total capacity of the logical volume in LBNs, and `volume_block_size` is the number of physical blocks mapped to a single logical volume LBN.

The *get_ensemble()* function is implemented by `sif_equivalent()` that, given an `lbn`, returns an array,`lbns`, with `cnt` elements. This array is the the which is a union of all possible equivalence classes E_p and E_d, formed by the original LBN. To illustrate how a storage manager parses the information, suppose a storage device with a logical volume with $p = 2$ and $d = 4$. Given `lbn`=0, a call to the `sif_equivalent()` would return 8 LBNs in the `lbns` array (`cnt` = 8): 0, 200, 400, 600, 800, 1000, 1200, 1400. In this set, p consecutive elements form a single equivalence class E_p : {0, 200}, {400, 600}, {800, 1000}, {1200, 1400}. Similarly, every p-th element forms an equivalence class E_d containing d elements: {0, 400, 800, 1200} and {200, 600, 1000, 1400}. For clarity, it may help to show the members as a two-dimensional structure:

0	200
400	600
800	1000
1200	1400

where columns form the E_d equivalence classes and rows the E_p equivalence classes.

To allocate data for parallel access, a storage manager chooses any of the four E_p's. To figure out how many consecutive blocks can be accessed in parallel, the storage manager would call `sif_ensemble()` function. For example, given parallel-accessible LBNs 400 and 600, the `sif_ensemble(400)` would return LBNs 400 and 599 for `low` and `high`, while `sif_ensemble(600)` would return LBNs 600 and 799. Hence, the storage device could access in parallel up to 200 LBNs, each with the most efficient access. Section 6.4.3 details how the functions are used for data allocation of two-dimensional data structures. For efficient access (that might not occur in parallel), the storage manager can map data up to four LBN that form one of the two E_d's. However, no efficient access to more than one consecutive LBN could be achieved.

Since non-consecutive LBNs can form an equivalence class, the interface also provides `sif_batch_read()` and `sif_batch_write()` functions. The function arguments include an array of LBNs, `*lbn[]`, an array of each I/O's size, `*bcnt[]`, an array of `iovec`-tors, `*data[]`, which designates memory locations where the data should be read/written to, and `num` which is the count of I/Os in a batch. Using `iovec`-tors allows a storage manager to place data into consecutive memory locations even though they are accessed from disjoint LBN at the storage device.

6.3 Atropos logical volume manager

This section describes a new disk array logical volume manager, called *Atropos*. It exploits disk-specific characteristics to construct a new data organization and exposes information about explicit grouping of non-contiguous logical blocks (LBNs) mapped across multiple disks. This information is encapsulated into the PARALLELISM attribute. Combined with the ACCESS DELAY BOUNDARIES attribute, these two attributes offer applications efficient access to two-dimensional data structures in *both* dimensions, here referred to as row- and column-majors. By utilizing (i) features built into disk firmware and (ii) a new data layout, *Atropos* delivers the aggregate bandwidth of all disks for accesses in both majors, without penalizing small random I/O accesses. Additionally, unlike any other layout previously described, *Atropos* can also facilitate an access to a rectangular portion of data i.e., a subset of columns and rows.

6.3.1 Atropos design

As illustrated in Figure 6.2, *Atropos* lays data across p disks in basic allocation units called quadrangles. A quadrangle is a collection of (non-contiguous) logical volume LBNs, here referred to as $VLBN$s, mapped to a single disk. Each successive quadrangle is mapped to a different disk, much like a stripe unit of an ordinary RAID group.

A quadrangle consists of d consecutive disk tracks, with d referred to as the quadrangle's *depth*. Hence, a single quadrangle is mapped to a contiguous range of a single disk's logical blocks, here referred to as $DLBN$s. The $VLBN$ and $DLBN$ sizes may differ; a single $VLBN$ consists of b $DLBN$s, with b being the block size of a single logical volume block. For example, a $VLBN$ size can match match application's allocation units (e.g., an 8 KB database block size or a 4 KB file system block size), while a $DLBN$ is typically 512 bytes.

Each quadrangle's dimensions are $w \times d$ logical blocks ($VLBN$s), where w is the quadrangle width and equals the number of $VLBN$s mapped to a single track. In Figure 6.2, both d and w are four. Section 6.3.3 describes the relationship

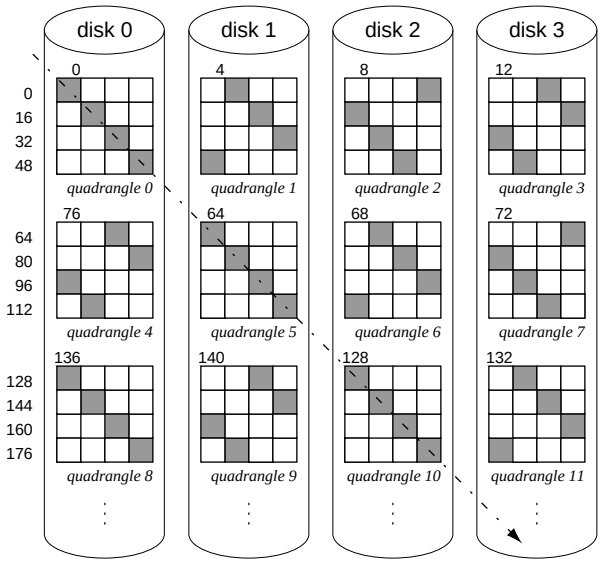

Fig. 6.2: ***Atropos* quadrangle layout.** The numbers to the left of disk 0 are the $VLBN$s mapped to the gray disk locations connected by the arrow and not the first block of each quadrangle row. The arrow illustrates efficient access in the other-major.

between quadrangle dimensions and the mappings to individual logical blocks. The mapping of $VLBN$s to quadrangles ensures maximal efficiency for accesses in both majors. Access in one major proceeds sequentially in the $VLBN$ space and achieves the aggregate streaming bandwidth of all disks. Access in the other-major uses non-contiguous $VLBN$s mapped diagonally across quadrangles located on all p disks. This access is referred to as semi-sequential and it is symbolized by the dashed arrow in Figure 6.2.

Atropos stripes contiguous $VLBN$s across quadrangles on all disks. Much like ordinary disk arrays, which map LBNs across individual stripe units, one quadrangle row contains a contiguous run of $VLBN$s and this row is mapped to a contiguous run of single disk's $DLBN$ that are located on a single track. Hence, this sequential access naturally exploits the high efficiency of ensemble-based access explained in Chapter 5. For example, in Figure 6.2, an access to 16 sequential blocks starting at $VLBN$ 0, will be broken to four sequential disk I/Os executing in parallel and fetching full tracks with $VLBN$s 0–3 from disk 0, $VLBN$s 4–7 from disk 1, $VLBN$s 8–11 from disk 2, and 12–15 from disk 3.

Efficient access in the other-major is achieved by accessing semi-sequential $VLBN$s. Requests to the semi-sequential $VLBN$s in a single quadrangle are all issued together in a batch. The disk's internal scheduler then chooses the request that will incur the smallest positioning cost (the sum of seek and rotational latency) and services it first. Once the first request is serviced, servicing all other

requests will incur only a track switch to the adjacent track. Thanks to the semi-sequential layout, no rotational latency is incurred for any of the subsequent requests, regardless of which request was serviced first.

Naturally, the sustained bandwidth of semi-sequential access is smaller than that of sequential access. However, semi-sequential access is more efficient than reading d effectively-random $VLBN$s spread across d tracks, as would be the case in a normal striped disk array. Accessing random $VLBN$s will incur rotational latency, averaging half a revolution per access. In the example of Figure 6.2, the semi-sequential access, depicted by the arrow, proceeds across $VLBN$s $0, 16, 32, \ldots, 240$ and occurs on all p disks, achieving the aggregate semi-sequential bandwidth of the disk array.

6.3.2 Quantifying access efficiency

To demonstrate the benefits of the quadrangle layout, this section quantifies the efficiency of accesses in both majors and shows that the efficiencies surpass or equal those of traditional systems. This higher efficiency is achieved without paying substantial penalty for random accesses. As before, access efficiency is defined as the fraction of total access time (which includes seek, rotational latency, and head switches) spent reading/writing data from/to the media. Hence, the maximum streaming efficiency (i.e., sequential access without seeks and rotational latencies) is less than 1.0 due to head switches between accesses to adjacent tracks.

The efficiencies and response times described in the following sections are for a single disk. With p disks in a group, each disk will experience the same efficiency while accessing data in parallel, achieving an aggregate bandwidth of all p disks.

Efficient access in both majors

Figure 6.3 shows the access efficiency of quadrangle layout as a function of I/O size. The I/O size is determined as the product of quadrangle depth, d, and the number of consecutive $DLBN$s, b, accessed at each track. For $d = 4$, an I/O of a given size S is split into four I/Os each of size $S/4$. Efficiency is then calculated as the ratio between the time it takes to rotate around the S sectors (I/O size divided by rotational speed), and the measured total response time, which also includes an average seek of 2.46 ms and, possibly, some rotational latency.

The data in the graph was obtained by measuring the response times of requests issued to a random $DLBN$ within Maxtor Atlas 10K III's outer-most zone with 686 sectors per track (343 KB) and aligned on track boundary. Hence, the drop in sequential access efficiency at the 343 KB mark is due to an additional head switch when the I/O size is larger than track size.

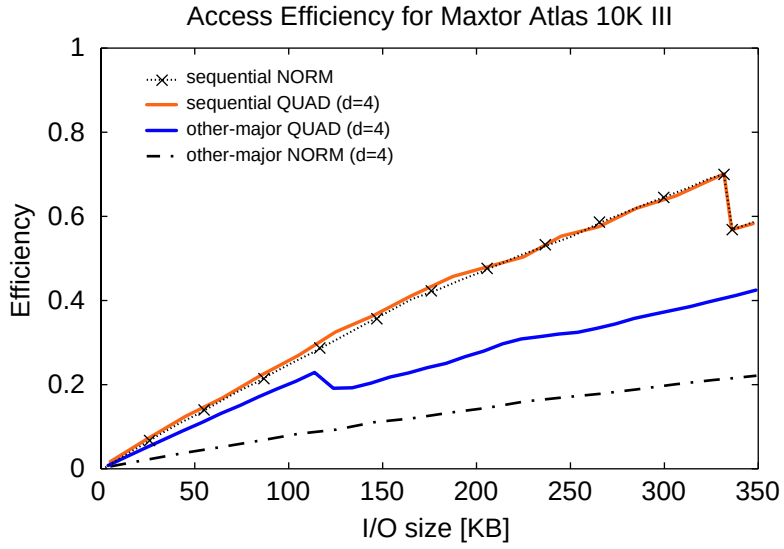

Fig. 6.3: **Comparison of access efficiencies.**

In *Atropos*, a large sequential access in the $VLBN$ space is broken into individual I/Os along acess delay boundaries (disk track boundaries), with each I/O going to a different disk. Thus, a single disk will access at most 343 KB and the drop in efficiency past the 343 KB mark, caused by head switch, is not experienced, provided the original request size was at most p times w $DLBN$s.

The efficiency of sequential access in $VLBN$ space with quadrangle layout (labeled "sequential QUAD") is identical to the efficiency of traditional layout that stripes data across disks in track-sized units. The efficiency of semi-sequential quadrangle access (labeled "other-major QUAD") with I/O sizes below 124 KB is only slightly smaller than that of the efficiency of the sequential quadrangle layout. The efficiency of the other-major quadrangle access ("other-major QUAD") with I/O sizes below 124 KB is only slightly smaller than sequential access. Past this point, the efficiency drops and then increases at a rate slower than the sequential access efficiency. Section 6.3.3 details why this drop occurs.

The continuing increase in efficiency past the 124 KB mark is due to amortizing the cost of a seek by larger data transfer. This increase in efficiency, however, comes at a cost of longer request response time; to access more than 124 KB will now require multiple revolutions. Finally, for all I/O sizes, the other-major access efficiency with quadrangles is much larger than for traditional layout.

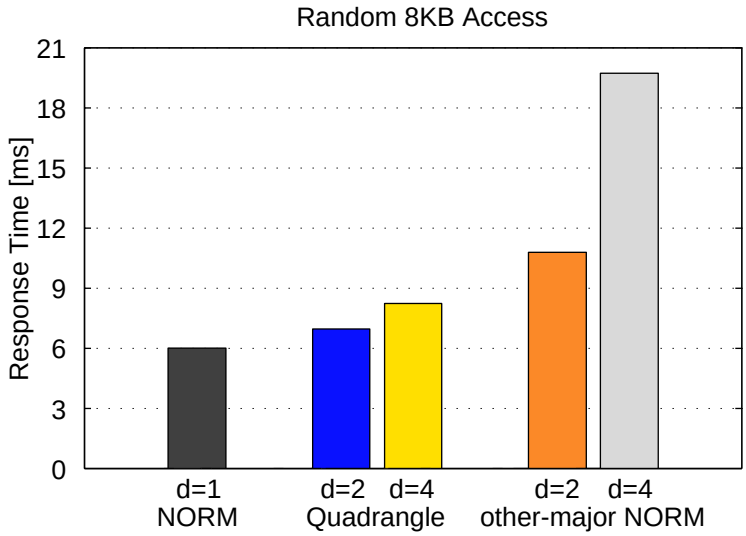

Fig. 6.4: **Comparison for response times for random access.**

Random access time

Figure 6.4 compares access times for a random 8 KB chunk of data with different data layouts. In traditional systems (labeled "NORM"), when this data is mapped to consecutive LBNs, such access incurs an average seek of 2.46 ms and an average rotational latency of half a revolution followed by an 8 KB media access.

When the requested 8 KB are spread across non-contiguous $VLBN$s on d tracks (e.g., when accessing a single row in the *Naïve* layout of Figure 6.1), each access to one $VLBN$ incurs a seek and half a revolution rotational latency. This results in large response time (bar labeled "other-major NORM"). In contrast, quadrangle layout incurs smaller average rotational latency (thanks to efficient scheduling). However, this smaller penalty is offset by one (for $d = 2$) or three (for $d = 4$) head switches. Because the cost of a head switch is much smaller than the cost of the average rotational latency of half a revolution, the quadrangle layout response time is much smaller. In addition, the quadrangle access average response time can be bounded by the choice of d, as described in Section 6.3.3. Intuitively, the smaller the d, the lower the bound on average response time for small random access.

6.3.3 Formalizing quadrangle layout

The parameters that define efficient quadrangle layout depend on disk characteristics described by two parameters. The parameter N describes the number of sectors, or $DLBN$s, per track and the parameter H describes the track skew in

Symbol	Name	Units
Quadrangle layout parameters		
p	Parallelism	# of disks
d	Quadrange depth	# of tracks
b	Block size	# of $DLBN$s
w	Quadrange width	# of $VLBN$s
Disk physical parameters		
N	Sectors per track	
H	Head switch	in $DLBN$s

Table 6.1: **Parameters used by *Atropos*.**

the mapping of $DLBN$s to physical sectors. Track skew is a property of disk data layouts as a consequence of track switch time. When data is accessed sequentially on a disk beyond the end of a track, the disk must switch to the next track to continue accessing. Switching tracks takes some amount of time, during which no data can be accessed. While the track switch is in progress, the disk continues to spin, of course. Therefore, sequential LBNs on successive tracks are physically skewed so that when the switch is complete, the head will be positioned over the next sequential LBN. This skew is expressed as the parameter H which is the number of $DLBN$s that the head passes over during the track switch time[1]. The layout and disk parameters are summarized in Table 6.1.

This section first derives equations that determine the expected response time and access efficiency for normal layout (i.e., RAID striping). It then derives equations that determine the same metrics for the quadrangle layout given its b and d parameters.

Figure 6.5 shows a sample quadrangle layout and its parameters. The top two pictures show how quadrangle $VLBN$s map to $DLBN$s. Along the x-axis, a quadrangle contains w $VLBN$s, each of size b $DLBN$s. In the example, one $VLBN$ consists of two $DLBN$s, and hence $b = 2$. As illustrated in the picture, a quadrangle does not always use all $DLBN$s when the number of sectors per track, N, is not divisible by b. In that case, there are R $DLBN$s that are not assigned. The third picture shows the physical locations of each b-sized $VLBN$ on individual tracks, accounting for track skew, which is 3 sectors (H= 3 $DLBN$s).

[1]Some disks map $DLBN$s to adjacent tracks on the same surface, causing a single-cylinder seek instead of head switch during sequential access. This seek takes equal or less time than head switch. Therefore, the value of the parameter H is corresponds to the greater of the head switch or single-cylinder seek times.

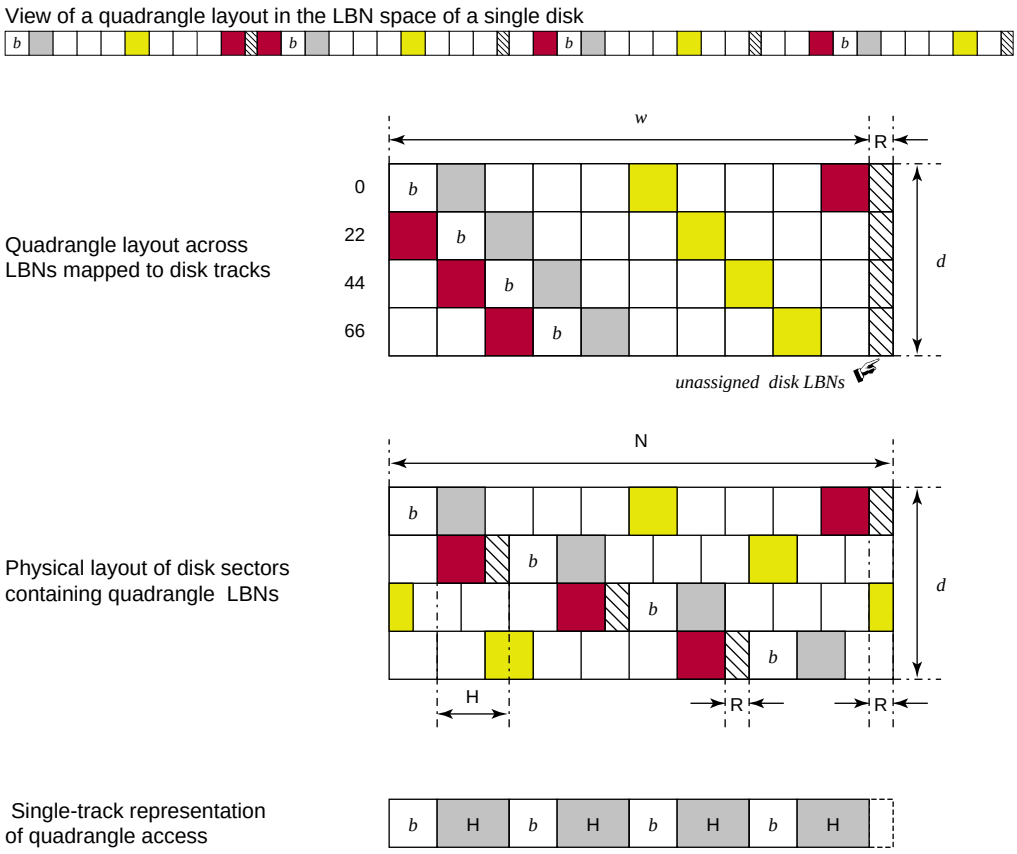

Fig. 6.5: **Single quadrangle layout.**

6.3.4 Normal access

Expected response time

Ignoring seek, the time to access and read data from a disk drive is determined by a firmware feature called zero-latency access. Let's call this time $T_n(N, K)$, which expresses the access time for a request of K sectors that fit onto a single track of a disk with N sectors per track. For disks that do implement this feature, this time is equal to time T_{zl}, which is calculated as

$$T_{zl}(N, K) = \frac{(N - K + 1)(N + K)}{2N^2} + \frac{K - 1}{N} \tag{6.1}$$

For disks that do not implement this feature the time is equal to is

$$T_{nzl}(N, K) = \frac{N - 1}{2N} + \frac{K}{N} \tag{6.2}$$

These expressions are derived in Appendix A.

Access efficiency

We can express access efficiency as the ratio between the raw rotational speed and the time it takes to read $S = kN$ sectors for some large k. Hence,

$$\begin{aligned} E_n &= \frac{kT_{rev}}{T_n(N, N) + (k - 1)(T_{hs} + T_{rev})} \\ E_n &\approx \frac{kT_{rev}}{k\,(T_{hs} + T_{rev})} \end{aligned}$$

where $T_n(N, N)$ is the time to read data on the first track, and $(k-1)(T_{hs}+T_{rev})$ is the time spent in head switches and accessing the remaining tracks. In the limit, the access efficiency is

$$E_n(N, H) = 1 - \frac{H}{N} \tag{6.3}$$

which is the maximal efficiency attainable from a disk. Note that it is less than one because of a disk's physical characteristics; due to head switches, there is a period of time when data is not transferred from the media.

6.3.5 Quadrangle access

Expected response time

Assume we want to read S sectors in a quadrangle where $S = db$ for some integer d, b sectors are located on a single track, and H is the number of sectors that pass

by the head during a head switch. As illustrated in Figure 6.5, the locations of the b blocks on each track are chosen to ensure most efficient access. Accessing b on the next track can commence as soon as the disk head finishes reading on the previous track and repositions itself above the new track. During the repositioning, H sectors pass under the heads.

To bound the response time for reading the S sectors, we need to find suitable values for b and d to ensure that the entire request, consisting of db sectors, is read in at most one revolution. Hence,

$$\frac{db}{N} + \frac{(d-1)\,H}{N} \leq 1 \tag{6.4}$$

where db/N is the media access time needed to fetch the desired S sectors and $(d-1)\,H/N$ is the fraction of time spent in head switches when accessing all d tracks. Then, as illustrated at the bottom of Figure 6.5, reading db sectors is going to take the same amount of time as if we were reading $db + (d-1)H$ sectors on a single track of a zero-latency access disk.Using Equation 6.1 and setting $K = db + (d-1)H$, the expected time to read $S = db$ sectors is

$$T_q(N, S) = T_{zl}\,(N, db + (d-1)H) \tag{6.5}$$

The maximal number of tracks, d, from which at least one sector each can be read in a single revolution is bound by the number of head switches that can be done in a single revolution, so

$$d \leq \left\lfloor \frac{N}{H} \right\rfloor - 1 \tag{6.6}$$

If we fix d, the number of sectors, b, that yield the most efficient access (i.e., reading as many sectors on a single track as possible before switching to the next one) can be determined from Equation 6.4 to get

$$b \leq \frac{N+H}{d} - H \tag{6.7}$$

Alternatively, if we fix b, the maximal depth, called D_{max}, can be expressed from Equation 6.4 as

$$D_{max} \leq \frac{N+H}{b+H} \tag{6.8}$$

For certain values of N, db sectors do not span a full track. In that case, $db+(d-1)\,H < N$ and there are R residual sectors, where $R < b$, as illustrated in Figure 6.5. These sectors are skipped to maintain the invariant that db quadrangle sectors can be accessed in at most one revolution.

Access efficiency

The maximal efficiency of semi-sequential quadrangle access is simply

$$E_q(N,H) = \frac{T_{rev}}{T_q(N,S)} = \frac{T_{rev}}{T_{zl}\,(N, db+(d-1)H)} \tag{6.9}$$

with $d = \lfloor N/H \rfloor - 1$ and b set accordingly.

Relaxing the one-revolution constraint

The previous section assumed a constraint that all db sectors are to be accessed in at most one revolution. Even though relaxing this constraint might seem to achieve better efficiency, this section shows that this intuition is wrong.

Suppose that a quadrangle with some large d is accessed such that

$$\frac{db}{N} + \frac{(d-1)\,H}{N} > 1$$

With probability $1/N$, a seek will finish with disk heads positioned exactly at the beginning of the b sectors mapped to the first track (the upper left corner of the quadrangle in Figure 6.6). In this case, the disk will access all db sectors with maximal efficiency (only incurring head switch of H sectors for every b-sector read).

However, with probability $1 - 1/N$, the disk heads will land somewhere "in the middle" of the b sectors after a seek, as illustrated by the arrow in Figure 6.6. Then, the access will incur a small rotational latency to access the beginning of the nearest b sectors, which are, say, on the k-th track. After this initial rotational latency, which is, on average, equal to $(b-1)/2N$, the $(d-k)b$ sectors mapped onto $(d-k)$ tracks can be read with maximal efficiency of the semi-sequential quadrangle access.

To read the remaining k tracks, the disk heads will need at be positioned to the beginning of the b sectors on the first track. This will incur a small seek and

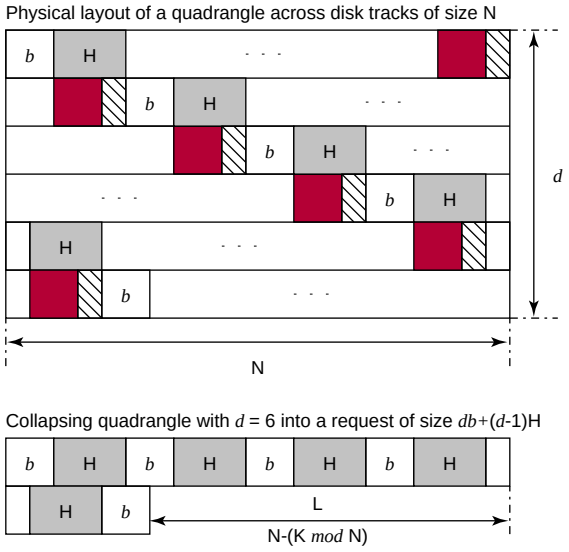

Fig. 6.6: **An alternative representation of quadrangle access.**

additional rotational latency of L/N. Hence, the resulting efficiency is much lower than when the one-revolution constraint holds.

We can express the total response time for quadrangle access without the one-revolution constraint as

$$T_q(N,S) = \frac{b-1}{2N} + \frac{K}{N} + P_{lat}\frac{L}{N} \tag{6.10}$$

where $P_{lat} = (N - H - b - 1)/N$ is the probability of incurring the additional rotational latency after reading k out of d tracks, $K = db - (d-1)H$ is the effective request size, $L = N - (K \bmod N)$, and $S = db$ is the original request size. To understand this equation, it may be helpful to refer to the bottom portion of Figure 6.6.

The efficiencies of the quadrangle accesses with and without the one-revolution constraint are approximately the same when the time spent in rotational latency and seek for the unconstrained access equals to the time spent in rotational latency incurred during passing over dR residual sectors. Hence,

$$\frac{dR}{N} = \frac{N-1}{N}\left(\frac{N-1}{2N} + Seek\right)$$

Ignoring seek and approximating $N-1$ to be N, this occurs when $R \neq 0$ and

$$d \approx \frac{N}{2R}.$$

Thus, in order to achieve the same efficiency for the non-constrained access, we will have to access at least d $VLBN$s. However, this will significantly increase I/O latency. If $R = 0$ i.e., when there are no residual sectors, the one-revolution constraint already yields the most efficient quadrangle access.

6.3.6 Implementing quadrangle layout

The characteristics of a particular disk, described by two parameters N and H, determine the maximal quadrangle depth, D_{max}, as shown in Equation 6.6. Thus, the smaller the head switch time relative to the rotational speed, the deeper the quadrangle can be in order to read all d blocks of size b in at most one revolution. As described in Section 6.3.5, accessing more than D_{max} tracks, is detrimental to the overall performance unless d is some multiple of D_{max}. In that case, the service time for such access is a multiple of one-revolution time.

With d chosen, the maximal number, b, of $DLBN$s that can be accessed on a single track is determined as shown in Equation 6.7. Again, b depends on the size of head switch time relative to the revolution time. The smaller the head switch time, the larger b can be, given a particular value of d.

Once both d and b are determined, the quadrangle width is

$$w = \left\lfloor \frac{N}{b} \right\rfloor$$

and the number of residual $DLBN$s on each track not mapped to quadrangle is

$$R = N \bmod w$$

Hence, given the number of sectors per track, N, and some b and d, the fraction of space that is wasted is R/N.

Access performance analysis

Using parameters derived in Section 6.3.3 and the analytical model described in Appendix A, we can express the expected response time for a quadrangle access and compare it with measurements taken from a real disk. Even though this section presents data for accessing a single disk, the same results apply for an array of p disk, since all disks are accessing their quadrangles in parallel.

Figure 6.7 plots response times for quadrangle accesses to the disk's outer-most zone as a function of I/O request size, S, and compares the values obtained from the analytic model to measurements from a real disk. The close match between these data sets confirms the validity of the analytical model. The data is shown

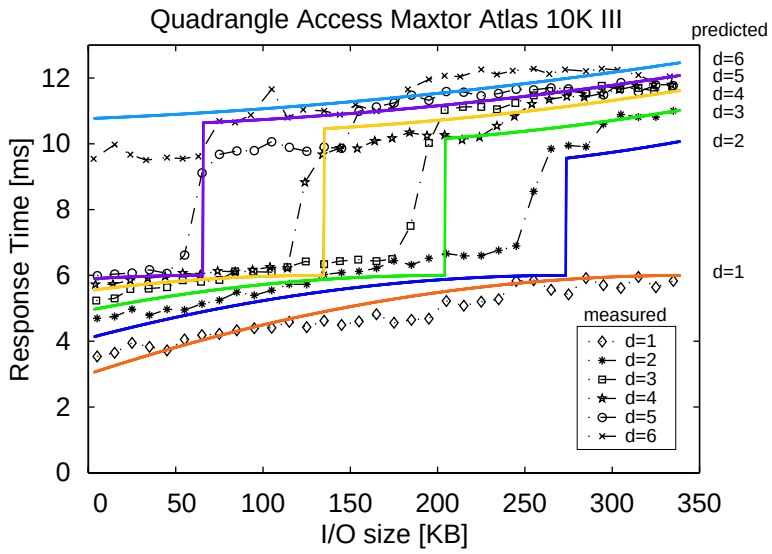

Fig. 6.7: **Comparison of measured and predicted response times.** The solid lines show the predictions made by the quadrangle access model. The dashed lines show measurements taken from a real disk. To stress the importance of rotational latency, the plotted response times do not include seek time, which was 2.46 ms. Including it would simply shift the lines up.

for the Atlas 10K III disk: $N = 686$, $H = 139$, and 6 ms revolution time.

The plotted response time does not include seek time; adding it to the response time would simply shift the lines up by an amount equivalent to the average seek time. The total I/O request size, S, shown along the x-axis is determined as $S = db$. With $d = 1$, quadrangle access reduces to normal disk access. Thus, the expected response time grows from 3 to 6 ms. For $d = 6$, the response time is at least 10.8 ms, even for the smallest possible I/O size; $D_{max} = 5$ for the given disk.

The most prominent features of the graph are the steps from the 6 ms to 10–12 ms regions. This abrupt change in response time shows the importance of the one-revolution constraint. If this constraint is violated by an I/O size that is too large, the penalty in response time is significant.

The data measured on the real disk (dashed lines in Figure 6.7) match the predicted values. To directly compare the two sets of data, the average seek value was subtracted from the measured values. The small differences occur because the model does not account for bus transfer time, which does not proceed entirely in parallel with media transfer.

Quadrangle sizes across disk generations

The data in Figure 6.7 showed the relationship between quadrangle dimensions and disk characteristics of one particular disk for which the one-constraint resulted

Disk	Year	D_{max}	b	R
HP C2247	1992	7	1	0
IBM Ultrastar 18 ES	1998	7	5	0
Quantum Atlas 10K	1999	6	2	0
Quantum Atlas 10K II	2000	6	5	3
Seagate Cheetah X15	2000	6	4	2
Seagate Cheetah 36ES	2001	6	7	3
Maxtor Atlas 10K III	2002	5	26	10
Seagate Cheetah 73LP	2002	7	8	2

Table 6.2: **Quadrangle parameters across disk generations.** For each disk the amount of space not utilized due to residual $DLBN$s is less than 1% with the exception of the Atlas 10K III, where it is 1.5%.

in $D_{max} = 5$. To determine how characteristics of disks affect quadrangle layout, we use the derived model, to study different disks. As shown in Table 6.2, the quadrangle dimensions remain stable across different disks of the past decade with $D_{max} = \langle 5, 7 \rangle$. The smaller D_{max} for the Atlas 10K III is due to an unfortunately chosen track skew/head switch of $H = 139$. With $H = 136$, $D_{max} = 6$.

Table 6.2 also shows that, with d set to D_{max}, the number of $DLBN$s, b, accessed at each disk track remains below 10 (with the exception of the Maxtor Atlas 10K III disk). Intuitively, this is because of small improvements of head switch time relative to rotational speeds. The data also reveals another favorable trend. The small value of the parameter R (number of $DLBN$s on each track not mapped to $VLBN$s) for all disks results in a modest capacity tradeoff for large performance gains. For all but the Atlas 10K III disk, less than 1% of the capacity is wasted. For the Atlas 10K III, it is 1.5%.

6.3.7 Practical system integration

Building the *Atropos* logical volume out of p disks is not difficult thanks to regular geometry of each quadrangle. *Atropos* collects a set of disks with the same characteristics and selects a disk zone with the desired number of sectors per track, N. Using the abstractions introduced in this dissertation, a zone is a collection of ensembles, defined by the ACCESS DELAY BOUNDARIES attribute, that have the same size.

The $VLBN$ size, b, is set according to the application needs and it determines the access granularity. For example, it may correspond to a file system block size or database page size. With b, known, *Atropos* validates b against disk parameters and sets the resulting $d \leq D_{max}$. Once d is validated, the volume is ready for use.

In practice, this can be accomplished in a two-step process. First, a storage

manager issues a format command with desired values of volume capacity, level of parallelism p, and quadrangle parameters d and b. Internally, *Atropos* selects appropriate set of disks out of a pool of spare ones, and formats the logical volume. Once, it is done, the actual parameters for the logical volume are returned by the *get_parallelism()* command.

Single quadrangle layout

Mapping $VLBN$s to the $DLBN$s of a single quadrangle is straightforward. Each quadrangle is identified by $DLBN_Q$, which is the lowest $DLBN$ of the quadrangle and is located at the quadrangle's top-left corner. The $DLBN$s that can be accessed semi-sequentially are easily calculated from the N and b parameters. As illustrated in Figure 6.5, given $DLBN_Q = 0$ and $b = 2$, the set $\{0, 24, 48, 72\}$ contains blocks that can be accessed semi-sequentially. To maintain rectangular appearance of the layout to an application, these $DLBN$s are mapped to $VLBN$s $\{0, 10, 20, 30\}$ when $b = 2$, $p = 1$, and $VLBN_Q = DLBN_Q = 0$.

With no media defects, *Atropos* only needs to know the $DLBN_Q$ of the first quadrangle. The $DLBN_Q$ for all other quadrangles can be calculated from the N, d, and b parameters. With media defects handled via slipping (e.g., the primary defects that occurred during manufacturing), certain tracks may contain fewer $DLBN$s. If the number of such defects is less than R, that track can be used; if it is not, the $DLBN$s on that track must be skipped. If any tracks are skipped, the starting $DLBN$ of each quadrangle row must be stored.

To avoid the overhead of keeping a table to remember the $DLBN$s for each quadrangle row, *Atropos* could reformat the disk and instruct it to skip over any tracks that contain one or more bad sectors. By examining twelve Seagate Cheetah 36ES disks, we found there were, on average, 404 defects per disk; eliminating all tracks with defects wastes less than 5% of the disk's total capacity. The techniques for handling grown defects still apply.

Zoned disk geometries

With zoned-disk geometries, the number of sectors per track, N, changes across different zones, which affects both the quadrangle width, w, and depth, d. The latter changes because the ratio of N to H may be different for different zones; the track switch time does not change, but the number of sectors that rotate by in that time does. By using disks with the same geometries (e.g., same disk models), we opt for the simple approach: quadrangles with one w can be grouped into one logical volume and those with another w (e.g., quadrangles in a different zone) into a different logical volume. Since modern disks have fewer than 8 zones, the

size of a logical volume stored across a few 72 GB disks would be tens of GBs.

Data protection

Data protection is an integral part of disk arrays and the quadrangle layout lends itself to the protection models of traditional RAID levels. Analogous to the parity unit, a set of quadrangles with data can be protected with a parity quadrangle. To create a RAID5 homologue of a parity group with quadrangles, there is one parity quadrangle unit for every $p - 1$ quadrangle stripe units, which rotates through all disks. Similarly, the RAID 1 homologue can be also constructed, where each quadrangle has a mirror on a different disk. Both protection schemes are depicted in Figure 6.8.

6.4 Database storage manager exploiting parallelism

This section describes a method for exploiting the explicit knowledge of storage device's inherent parallelism to provide efficient access to database tables mapped to a linear LBN space. It shows how such efficient access to tables in DBMS can significantly improve performance of queries doing selective table scans. These selective table scan can request (i) a subset of columns (restricting access along the x-dimension), (ii) a subset of rows (restricting access along the y dimension), or (iii) a combination of both.

6.4.1 Database tables

Database systems (DBMS) use a scan operator to sequentially access data in a table. This operator scans the table and returns the desired records for a subset of attributes (table fields). Internally, the scan operator issues page-sized I/Os to the storage device, stores the pages in its buffers, and reads the data from buffered pages. A single page (typically 8 KB) contains a fixed number of complete records and some page metadata overhead.

The page layout prevalent in commercial DBMS, called N-ary storage model (NSM), stores a fixed number of records for all n attributes in a single page. Thus, when scanning a table to fetch records of only one attribute (i.e., column-major access), the scan operator still fetches pages with data for *all* attributes, effectively reading the entire table even though only a subset of the data is needed. To alleviate the inefficiency of a column-major access in this data layout, an alternative page layout, called decomposition storage model (DSM), vertically partitions data to pages with a fixed number of records of a *single* attribute [Copeland and Khoshafian 1985]. However, record updates or appends require writes to n different

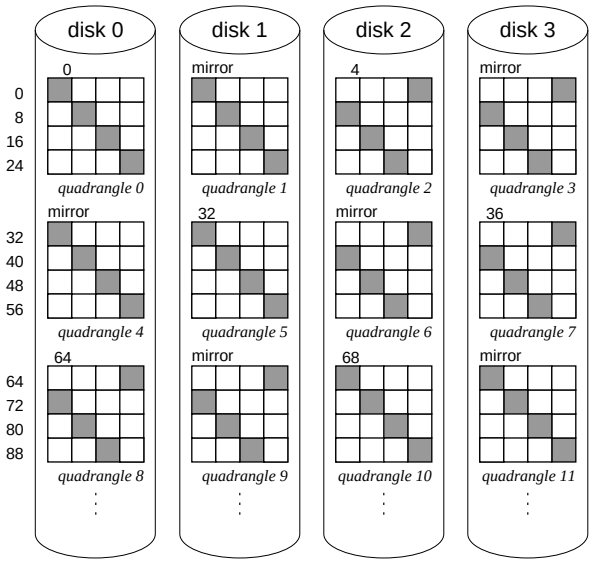

(a) RAID 1 (Mirrored pair) layout.

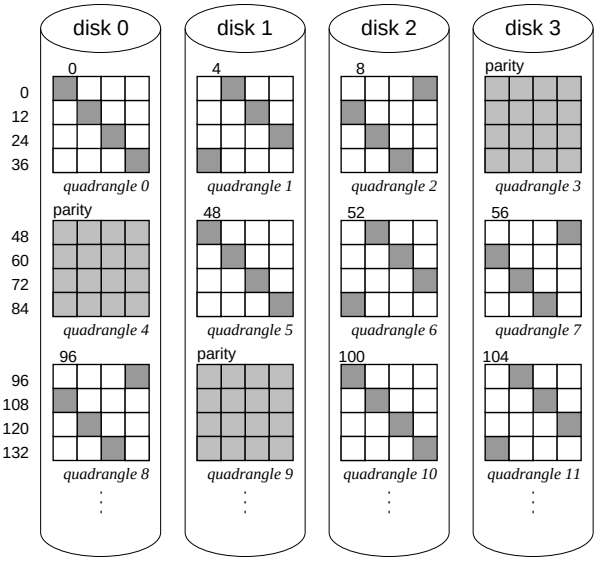

(b) RAID 5 layout.

Fig. 6.8: ***Atropos*** **quadrangle layout for different RAID levels.**

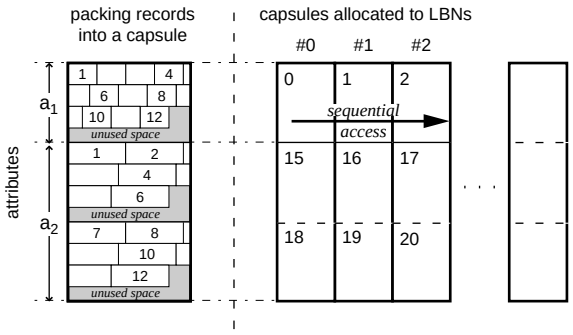

Fig. 6.9: **Data allocation with capsules.** The capsule on the left shows packing of 12 records for attributes a_1 and a_2 into a single capsule. The numbers within denote record number. The 12-record capsules are mapped such that each attribute can be accessed in parallel and data from a single attribute can be accessed sequentially, as shown on the right. The numbers in the top left corner are the LBNs of each block comprising the capsule.

locations, making such row-order access inefficient. Similarly, fetching full records requires n single-attribute accesses and $n-1$ joins to reconstruct the entire record.

With proper allocation of data, one or more attributes of a single record can be accessed in parallel. Given a degree of parallelism, p, accessing a single attribute yields higher bandwidth, by accessing more data in parallel. When accessing a subset of $k+1$ attributes, the desired records can exploit the internal storage device parallelism to fetch records in lock-step, eliminating the need for fetching the entire table.

6.4.2 Data layout

To exploit parallel data accesses in both row- and column-major orders, we define a *capsule* as the basic data allocation and access unit. A single capsule contains a fixed number of records for all table attributes. As all capsules have the same size, accessing a single capsule will always fetch the same number of complete records. A single capsule is laid out such that reading the whole record (i.e., row order access) results in parallel access to all of its LBNs.

The capsule's individual LBNs are assigned such that they belong to the same equivalence class, offering parallel access to any number of attributes within. If a relation includes variable sized-attributes, all fixed-size attributes are put into one capsule and the variable size ones are put into separate ones. To reconstruct the entire record, the attributes from these capsules will be joined on record identifiers. However, this access is still more efficient than complete record access in DSM; fewer joins are needed unless all attributes have variable size.

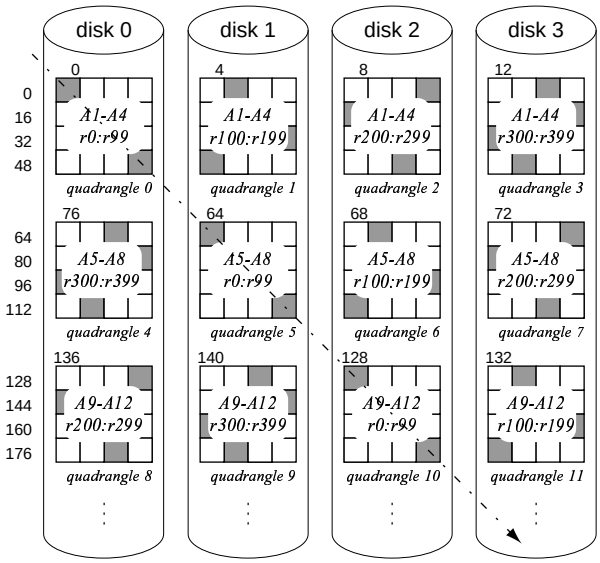

Fig. 6.10: **Mapping of a database table with 16 attributes onto *Atropos* logical volume.**

Adjacent capsules are laid next to each other such that records of the same attribute in two adjacent capsules are mapped to sequential LBNs. Such layout ensures that reading sequentially across capsules results in repositioning only at the end of each track or cylinder. Furthermore, this layout ensures that sequential streaming of one attribute is realized at the storage device's aggregate bandwidth.

A simple example that lays records within a capsule and maps contiguous capsules into the LBN space is illustrated in Figure 6.9. It depicts a capsule layout with 12 records consisting of two attributes a_1 and a_2, which are 1 and 2 units in size, respectively. It also illustrates how adjacent capsules are mapped into the LBN space of the three-by-three MEMStore example from Figure 3.8.

Finding the (possibly non-contiguous) LBNs to which a single capsule should be mapped, as well as the location for the logically next LBN, is done by calling the *get_equivalent()* and *get_ensemble()* functions. In practice, once a capsule has been assigned to an LBN and this mapping is recorded, the locations of the other attributes can be computed from the values returned by the interface functions.

The mapping of database tables into capsules spread across the $VLBN$ space of the *Atropos* logical volume is depicted in Figure 6.10. It shows the mapping of a single capsule containing 100 records of a table with 16 attributes of equal size. The capsule is mapped to the gray $VLBN$s marked with the dashed arrow. To fetch the entire capsule, *Atropos* issues 4 semi-sequential I/Os to each of the four disks.

6.4.3 Allocation

Data allocation is implemented by two routines that call the storage interface functions described in Section 6.2.3. These routines do not perform the calculations described in this section. They simply lookup data returned by the *get_equivalent()* and *get_ensemble()* functions. The `CapsuleResolve()` routine determines an appropriate capsule size using attribute sizes. The degree of parallelism, p, determines the offsets of individual attributes within the capsule. A second routine, called `CapsuleAlloc()`, assigns a newly allocated capsule to free LBNs and returns new LBNs for the this capsule. The LBNs of all attributes within a capsule can be found according to the pattern determined by the `CapsuleResolve()` routine.

The `CapsuleAlloc()` routine takes an LBN of the most-recently allocated capsule, l_{last}, finds enough unallocated LBNs in its equivalence class E_{last}, and assigns the new capsule to l_{new}. By definition, the LBN locations of the capsule's attributes belong to E_{new}. If there are enough unallocated LBNs in E_{last}, $E_{last} = E_{new}$. If no free LBNs in E_{last} exist, E_{new} is different from E_{last}. If there are some free LBNs in E_{last}, some attributes may spill into the next equivalence class. However, this capsule can still be accessed sequentially.

Allowing a single capsule to have LBNs in two different equivalence classes does not waste any space. However, accessing all attributes of these split capsules is accomplished by two separate parallel accesses, the latter being physically sequential to the former. Given capsule size in LBNs, c, there is one split capsule for every $|E| \mod cp$ capsules. If one wants to ensure that *every* capsule is always accessible in a single parallel operation, one can waste $1/(|E| \mod cp)$ of device capacity. These unallocated LBNs can contain indexes or database logs.

Because of the layout, l_{new} is not always equal to $l_{last} + 1$. This discontinuity occurs at the end of each track. Calling *get_ensemble()* determines if l_{last} is the last LBN of the current track. If so, the `CapsuleAlloc()` simply offsets into E_{last} to find the proper l_{new}. The offset is a multiple of p and the number of blocks a capsule occupies. If l_{last} is not at the end of the track, then $l_{new} = l_{last} + 1$.

Figure 6.11 illustrates the allocation of capsules with two attributes a_1 and a_2 of size 1 and 2 units, respectively, to the LBN space of a G2 MEMStore using the sequential-optimized layout. The depicted capsule stores a_1 at capsule offset 0, and the two blocks of a_2 at offsets p and $2p$. These values are offset relative to the capsule's LBN position within E_{LBN}.

6.4.4 Access

For each capsule, a DBMS storage manager maintains its starting LBN from which it can determine the LBNs of all attributes in the capsule. This is accomplished

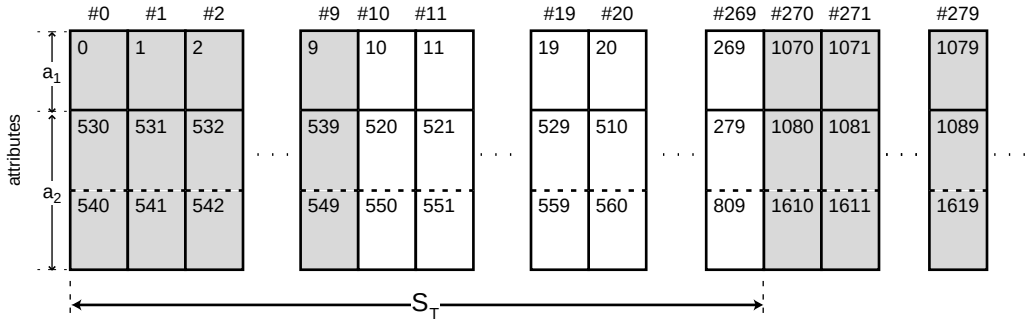

Fig. 6.11: **Capsule allocation for the G2 MEMStore.** This picture shows capsules with two attributes a_1 and a_2 whose sizes are 8 and 16 bytes, respectively. Given an LBN size of 512 bytes, and a level of parallelism, $p = 10$, a single capsule contains 64 records and maps to three LBNs. Note that each row for capsules 0 through 269 contains contiguous LBNs of a single track: a_1 spans track 0-269, and a_2 spans two tracks with LBN ranges 270-539 and 540-809. The shaded capsules belong to the same equivalence class. Thanks to the *get_equivalent()* and *get_ensemble()* functions, a database system does not have to keep track of all these complicated patterns. Instead, it only keeps the capsule's starting LBN. From this LBN, all other values are found by the storage interface function calls.

by calling the *get_equivalent()* function. Because of the allocation algorithm, the capsules are laid out such that sequential scanning through records of the attribute a_1 results in sequential access in LBN space as depicted in Figure 6.11. This sequential access in LBN space is realized by p batched reads executing in parallel. When accessing both a_1 and a_2, up to p/c capsules can be accessed in parallel where capsule size $c = size(a_1 + a_2)$.

Streaming a large number of capsules can be also accomplished by pipelining reads of S_T sequential LBNs of attribute a_1 followed by $2S_T$ sequential LBNs of a_2. Setting a scatter-gather list for these sequential I/Os ensures that data are put into proper places in the buffer pool. The residual capsules that span the last segment smaller than S_T are then read in parallel using batched I/Os.

6.4.5 Implementation details

The parallel scan operator is implemented as a standalone C++ application. It includes the allocation and layout routines described in Section 6.4.3 and allows an arbitrary range of records to be scanned for any subset of attributes. The allocation routines and the scan operator use the interface functions described in Section 6.2.3. These functions are exported by linked-in stub, which communicates via a socket to another process. This process, called *devman*, implements the code of the *Atropos* logical volume manager and emulates the functionality of MEMStore device manager running firmware code.

The *devman* process accepts I/O requests through a socket. For the *Atropos* logical volume manager, it determines how these requests are broken into individual disk I/Os and issues them directly to the attached SCSI disks via raw Linux SCSI device. For MEMStore, it runs the requests through the DiskSim simulator configured with the G2 MEMStore parameters. Similar to the timing-accurate storage emulator [Griffin et al. 2002], The *devman* process synchronizes DiskSim's simulated time with the wall clock time and uses main memory for data storage.

6.4.6 Experimental setup

The experiments are conducted on a two-way 1.7 GHz Pentium 4 Xeon workstation running Linux kernel v. 2.4.24 and RedHat 7.1 distribution. The machine for the disk array experiment has 1024 MB memory and is equipped with two Adaptec Ultra160 Wide SCSI adapters, each controlling two 36 GB Seagate Cheetah 36ES disks (ST336706LC). An identical machine configuration is used for the MEMStore experiments; it has 2 GB of memory, with half used as data store.

Atropos setup

The *Atropos* LVM exports a single 35 GB logical volume created from the four disks in the experimental setup and maps it to the blocks on the disks' outermost zone. Unless stated otherwise, the volume was configured as RAID 0 with $d = 4$ and $b = 1$ ($VLBN = DLBN = 512$ bytes).

Simulating MEMStore

Our experiments rely on simulation because real MEMStores are not yet available. A detailed model of MEMS-based storage devices has been integrated into the DiskSim storage subsystem simulator [Bucy and Ganger 2003]. For the purposes of this work, the MEMStore component was augmented to service requests in batches. As a batch is serviced by DiskSim, as much of its data access as possible is done in parallel given the geometry of the device and the level of parallelism it can provide. If all of the LBNs in the batch are parallel-accessible, then all of its media transfer will take place at once.

Using the interface described in Section 6.2.3, a database storage manager can generate parallel-accessible batches of I/Os during table access. Internally, the MEMStore device interface uses the virtual geometry parameters, described in Section 3.3.1, to calculate equivalence classes with LBNs.

For the experiments below, the four basic device parameters are set to represent a realistic MEMStore. The parameters are based on the G2 MEMStore

p	Level of parallelism	10
N	Number of squares	100
S_x	Sectors per square in X	2500
S_y	Sectors per square in Y	27
M	Degree of micropositioning	0
N_x	Number of squares in X	10
N_y	Number of squares in Y	10
S_T	Sectors per track	270
S_C	Sectors per cylinder	2700

Table 6.3: **Device parameters for the G2 MEMStore.** The parameters given here take into account the fact that individual 512 byte LBNs are striped across 64 read/write tips each.

from [Schlosser et al. 2000], and are shown in Table 6.3. The G2 MEMStore has 6400 probe tips, and therefore 6400 total squares. However, a single LBN is always striped over 64 probe tips so N for this device is $6400/64 = 100$. We have modified the G2 model to allow only 640 tips to be active in parallel rather than 1280 to better reflect the power constraints outlined in Section 3.3.1, making $p = 10$. Therefore, for a single LBN, there are 100 LBNs in an equivalence class, and out of that set any 10 LBNs can be accessed in parallel.

Each physical square in the G2 device contains a 2500×2500 array of bits. Each 512 byte LBN is striped over 64 read/write tips. After striping, the virtual geometry of the device works out to a 10×10 array of virtual squares, with sectors laid out vertically along the Y dimension. After servo and ECC overheads, 27 512-byte sectors fit along the Y dimension, making $S_y = 27$. Lastly, $S_x = 2500$, the number of bits along the X dimension. The total capacity for the G2 MEMStore is 3.46 GB. It has an average random seek time of 0.56 ms, and has a sustained bandwidth of 38 MB/s.

6.4.7 Scan operator results

To quantify the advantages of the parallel scan operator, this section compares the times required for different table accesses. It contrasts their respective performance under three different layouts on a *Atropos* logical volume consisting of four disks and on a single G2 MEMStore device. The first layout, called NSM, is the traditional row-major access optimized page layout. The second layout, called DSM, corresponds to the vertically partitioned layout optimized for column-major access. The third layout, called CSM, uses the capsule layout and access described in Section 6.4.3. We compare in detail the NSM and CSM cases.

Our sample database table consists of 4 attributes a_1, a_2, a_3, and a_4 sized at 8, 32, 15, and 16 bytes respectively. The NSM layout consists of 8 KB pages that

Operation	Data Layout	
	normal	*capsule*
entire table scan	5.19 s	5.34 s
a_1 scan	5.19 s	1.06 s
$a_1 + a_2$ scan	5.19 s	3.20 s
100 records of a_1	5.56 ms	5.37 ms

Table 6.4: **Database access results for *Atropos* logical volume manager.** The table shows the runtime of the specific operation on the 10,000,000 record table with 4 attributes for the NSM and CSM. The rows labeled a_1 scan and $a_1 + a_2$ represent the scan through all records when specific attributes are desired. the last row shows the time to access the data for attribute a_1 from 100 records.

include 115 records. The DSM layout packs each attribute into a separate table. For the given table header, the CSM layout produces capsules consisting of 9 pages (each 512 bytes) with a total of 60 records. The table size is 10,000,000 records with a total of 694 MB of data.

Atropos results

Table 6.4 summarizes the parallel scan results for the NSM and CSM cases. Scanning the entire table takes respectively 5.19 s and 5.34 s for the NSM and CSM cases. The run time difference is due to the amount of actual data being transfered. Compared to the CSM, the NSM layout can pack data more tightly into its 8 KB page. Given the attribute sizes and the 8 KB page size, the overhead for the NSM layout is 2.8%, resulting in total transfer of 714 MB. The CSM layout creates, in effect, 512-byte pages which waste more space due to internal fragmentation. This results in an overhead of 10.6% and total transfer of 768 MB. Given the total run time of the experiment and the amount of data transferred, the achieved user-data bandwidth is respectively 132.9 MB/s and 137.3 MB/s for the NSM and CSM layouts. *Atropos* achieves larger sustained bandwidth of user data thanks to more efficient ensemble-based access.

As expected, CSM is highly efficient when only a subset of the attributes are required. A table scan of a_1 or $a_1 + a_2$ in the NSM case always takes 5.19 s, since entire pages including the undesired attributes must be scanned. The CSM case only requires a fraction of time corresponding to the amount of data for each desired attribute. Figure 6.12 compares the runs of a full table scan for all attributes against four scans of individual attributes.

The total runtime of four individual-attribute scans in the CSM case takes only 1.5× more time as the full table scan. In contrast, the four successive scans take four times as long as the full table scan with the NSM layout. A scan of a single

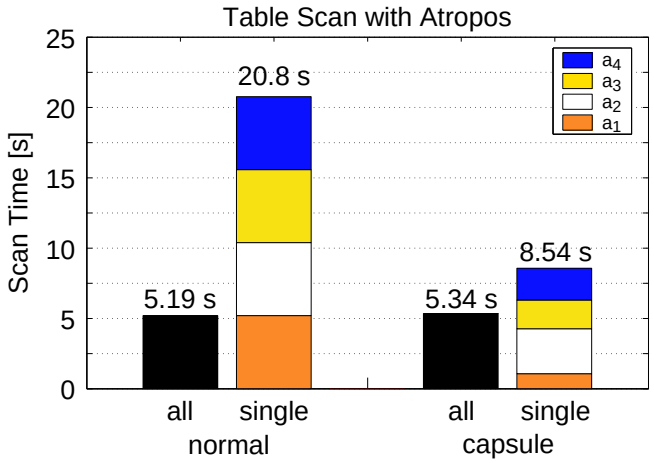

Fig. 6.12: **Table scan on *Atropos* disk array with different number of attributes.** This graph shows the runtime of scanning 10,000,000 records. For each of the two layouts the left bar, labeled all, shows the runtime of the entire table with 4 attributes. The right bar, labeled single, is composed of four separate scans of each successive attribute, simulating the situation where multiple queries access different attributes. Since the CSM layout takes adavantage of available parallelism, each attribute scan runtime is proportional to the amount of data occupied by that attribute. The NSM, on the other hand, must read the entire table to fetch one of the desired attributes.

attribute a_1 in the CSM case takes only 20% (1.06 s vs. 5.34 s) of the full table scan. On the other, scanning the full table in the NSM case requires a transfer of 9 times as much data.

Short scans of 100 records (e.g., in queries with high selectivity) correspond to small random, one-page I/Os. For NSM, this access involves a random seek and rotational latency of half a revolution, resulting in access time of 5.56 ms. For CSM, this access includes the same penalties, but only 1 KB of data is fetched, instead of the whole 8 KB page. This result is in accord with random record access under the three different scenarios shows an interesting behavior. The CSM case gives an average access time of 8.32 ms, the NSM case 5.56 ms, and the DSM case 21.3 ms. The difference is due to different access patterns.

The CSM access includes a random seek to the capsule's location followed by 9 batched accesses to one equivalence class proceeding in parallel. Six of these requests are serviced by one disk with semi-sequential access, since $d = 6$, and the remaining three are serviced in parallel by another disk. The NSM access involves a random seek followed by a sequential access to 16 LBNs. Finally, the DSM access requires four accesses, each including a random seek.

Operation	Data Layout	
	normal	*capsule*
entire table scan	22.44 s	22.93 s
a_1 scan	22.44 s	2.43 s
a_1 + a_2 scan	22.44 s	12.72 s
100 complete records	1.58 ms	1.31 ms

Table 6.5: **Database access results for G2 MEMStore.** The table shows the runtime of the specific operation on the 10,000,000 record table with 4 attributes for the NSM and CSM. The rows labeled a_1 scan and $a_1 + a_2$ represent the scan through all records when specific attributes are desired. the last row shows the time to access the data for attribute a_1 from 100 records.

MEMStore results

Table 6.5 summarizes the table scan results for the NSM and CSM cases. Scanning the entire table takes respectively 22.44 s and 22.93 s for the NSM and CSM cases and the corresponding user-data bandwidth is 30.9 MB/s and 30.3 MB/s. The run time difference is due to the amount of actual data being transfered. Since the NSM layout can pack data more tightly into its 8 KB page, it transfers a total of 714 MB at a rate of 31.8 MB/s from the MEMStore. The CSM layout creates, in effect, 512-byte pages which waste more space due to internal fragmentation. Despite transferring 768 MB, it achieves a sustained bandwidth of 34.2 MB/s, or 7% higher than NSM. While both methods access all 10 LBNs in parallel most of the time, the data access in the CSM case is more efficient due to smaller repositioning overhead at the end of a cylinder.

Similar to the *Atropos* results, CSM is highly efficient when only a subset of the attributes are required. A table scan of a_1 or $a_1 + a_2$ in the NSM case always takes 22.44 s, since entire pages including the undesired attributes must be scanned. The CSM case only requires a fraction of the time corresponding to the amount of data for each desired attribute. Figure 6.13 compares the runs of a full table scan for all attributes against four scans of individual attributes. The total runtime of four individual-attribute scans in the CSM case takes the same amount of time as the full table scan. In contrast, the four successive scans take four times as long as the full table scan with the NSM layout.

Most importantly, a scan of a single attribute a_1 in the CSM case takes only one ninth (2.43 s vs. 22.93 s) of the full table scan since all ten parallel accesses read records of a_1. On the other, scanning the full table in the NSM case requires a transfer of 9 times as much data and uses the parallelism p to access.

Short scans of 100 records (e.g., in queries with high selectivity) are 20% faster for CSM since they fully utilize the MEMStore's internal parallelism. Furthermore, the latency to the first record is shorter due to smaller access units, compared to

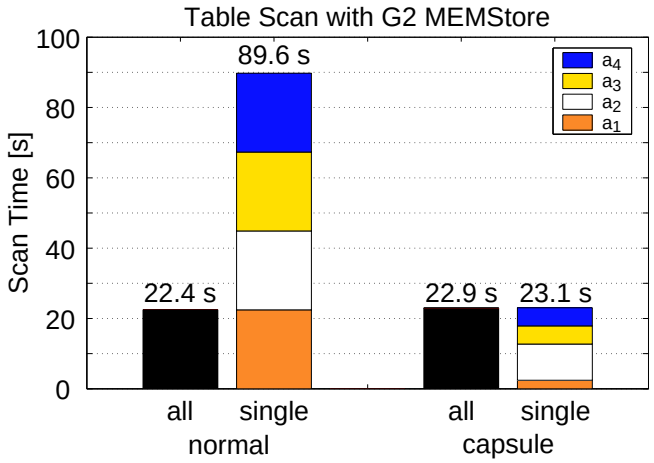

Fig. 6.13: **Table scan on G2 MEMStore with different number of attributes.** This graph shows the runtime of scanning 10,000,000 records. For each of the two layouts the left bar, labeled all, shows the runtime of the entire table with 4 attributes. The right bar, labeled single, is composed of four separate scans of each successive attribute, simulating the situation where multiple queries access different attributes. Since the CSM layout takes adavantage of MEMStore's parallelism, each attribute scan runtime is proportional to the amount of data occupied by that attribute. The NSM, on the other hand, must read the entire table to fetch one of the desired attributes.

NSM. Compared to DSM, the access latency is also shorter due to the elimination of the join operation. In our example, the vertically partitioned layout must perform two joins before being able to fetch an entire record. This join, however, is not necessary in the CSM case, as it accesses records in lock-step, implicitly utilizing the available MEMStore internal parallelism. The DSM case exhibits similar results for individual attribute scans as the CSM case. In contrast, scanning the entire table requires additional joins on the attributes.

Comparing the latency of accessing one complete random record under the three different scenarios shows an interesting behavior. The CSM case gives an average access time of 1.385 ms, the NSM case 1.469 ms, and the DSM case 4.0 ms. The difference is due to different access patterns. The CSM access includes a random seek to the capsule's location followed by 9 batched accesses to one equivalence class proceeding in parallel. The NSM access involves a random seek followed by a sequential access to 16 LBNs. Finally, the DSM access requires 4 accesses each consisting of a random seek and one LBN access.

6.4.8 Database workloads

We now evaluate the benefits of exposing the PARALLELISM attribute to a database storage manager on three database workloads: On-line Transaction Processing

(OLTP), Decision Support System (DSS) queries, and compound workloads running both types concurrently.

The evaluation is done on a prototype implementation of a database storage manager called *Clotho* [Shao et al. 2004]. In addition to using the row-major optimized NSM and column-major optimized DSM page layouts, *Clotho* can run database queries with the CSM page layout that takes advantage of the PARALLELISM attribute exposed by a storage device (e.g., *Atropos* logical volume manager or MEMStore). The *Clotho* storage manager is based on the Shore database storage manager [Carey et al. 1994] and it leverages both the ACCESS DELAY BOUNDARIES and PARALLELISM attributes for page allocation and data access. The details of *Clotho* implementation are described elsewhere [Shao et al. 2004].

With NSM and DSM page layouts, it is sufficient to take advantage of only the ACCESS DELAY BOUNDARIES attribute (as described in Section 5.7) to achieve efficient accesses in the respective optimized orders. However, the accesses in the other order are inefficient. The CSM also leverages the PARALLELISM attribute in order to achieve efficient accesses in both dimensions. Hence, the CSM targets environments where both access patterns are equally likely to occur.

Another page layout, called PAX, targets the same environments where both types of accesses are likely to occur. It offers efficient execution of both access patterns at the CPU-cache memory level [Ailamaki et al. 2001]. A single PAX page contains all attributes, but partitions them across the page to avoid unnecessary data fetches into CPU-cache when only a subset of attributes are needed. However, from the prospective of the storage device, a PAX page is just like an NSM page and therefore exhibits similar performance to NSM at the storage device level.

DSS workload performance

To compare the DSS workload performance for different layouts we run a subset of the TPC-H decision support benchmark on our *Clotho* prototype. Each layout uses an 8 KB page size. The TPC-H dataset is 1 GB and the buffer pool size is 128 MB. Figure 6.14 shows execution times relative to NSM for four representative TPC-H queries. Q1 and Q6 are sequential scans through the largest table in the TPC-H benchmark while Q12 and Q14 execute joins across two relations. The left group of bars shows TPC-H execution on *Atropos*, whereas the right group shows queries run on a simulated MEMStore. NSM performs the worst by a factor of 1.24× – 2.0× (except for DSM in Q1) because they must access all attributes.

The performance of DSM, compared to NSM, is better for all queries except Q1 because of its high projectivity (i.e., number of attributes constituting query payload). CSM performs best because it benefits from projectivity and avoids

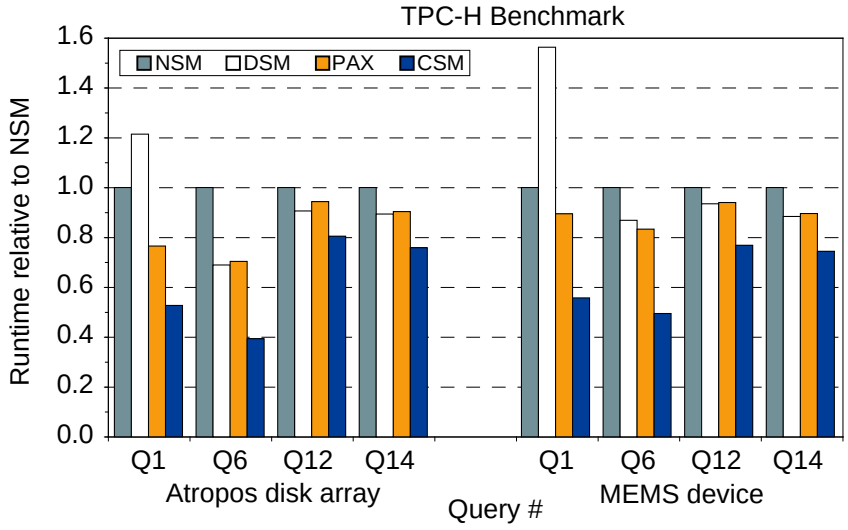

Fig. 6.14: **TPC-H performance for different layouts.** Performance is shown relative to NSM.

the cost of the joins that DSM must do to reconstruct records. As expected, the TPC-H benchmark performance for DSM and CSM is comparable, since both storage models can efficiently access data, requesting only the attributes that constitute the payload for the individual queries (7 attributes for Q1 and 5 for Q6). DSM, however, must perform additional joins to reconstruct records, which is not necessary when using CSM. NSM must fetch pages that contain full records which results in the observed 1.24× to 2× worse performance. Not surprisingly, PAX performs better than NSM but not as well as CSM; all attributes still have to be fetched from a storage device into main memory. Its improvements over NSM are due to more efficient memory access. Results with MEMStore exhibit the same trends.

OLTP workload performance

The queries in a typical OLTP workload access a small number of records spread across the entire database. In addition, OLTP applications have several insert and delete statements as well as point updates. With NSM page layout, the entire record can be retrieved by a single-page random I/O, because these layouts map a single page to consecutive LBNs. *Clotho* spreads a single capsule across non-consecutive LBNs of the logical volume, enabling efficient sequential access when scanning a single attribute across multiple records and less efficient semi-sequential scan when accessing full records.

Layout	TpmC
NSM	1063
PAX	1090
DSM	140
CSM	1002

Table 6.6: **TPC-C benchmark results with *Atropos* disk array LVM.** The table shows the transactional throughput of the TPC-C benchmark.

The TPC-C benchmark approximates an OLTP workload on our *Clotho* prototype with all four data layouts using 8 KB page size. TPC-C is configured with 10 warehouses, 100 users, no think time, and 60 seconds warm-up time. The buffer pool size if 128 KB, so it only caches 10% of the database. The completed transactions per minute (TpmC) throughput is repeatedly measured over a period of 120 seconds.

Table 6.6 shows the results of running the TPC-C benchmark. As expected, DSM yields much lower throughput compared to NSM. Despite the less efficient semi-sequential access, CSM observes only 6% lower throughput than NSM. The frequent point updates inherent in the the TPC-C benchmark penalize CSM's performance: the semi-sequential access needs to to retrieve full records. This penalty is in part compensated by the ability of the *Clotho*'s buffer pool manager to create and share pages containing only the needed data.

Compound OLTP/DSS workload

Benchmarks involving compound workloads are important in order to measure the impact on performance when different queries access the same logical volume concurrently. With CSM, the performance degradation may be potentially worse than in other page layouts. The originally efficient semi-sequential access to disjoint LBNs (i.e., for OLTP queries) could be disrupted by competing I/Os from the other workload creating inefficient access. This problem does not occur for other layouts that map the entire page to consecutive LBNs that can be fetched in a single media access.

We simulate a compound workload with a single-user DSS (TPC-H) workload running concurrently with a multi-user OLTP workload (TPC-C) against our *Atropos* disk LVM and measure the differences in performance relative to the isolated workloads. The respective TPC workloads are configured as described earlier. In previous work [Schindler et al. 2003], we demonstrated the effectiveness of track-aligned disk accesses on compound workloads; here, we compare all of the page layouts using these efficient I/Os to achieve comparable results for TPC-H.

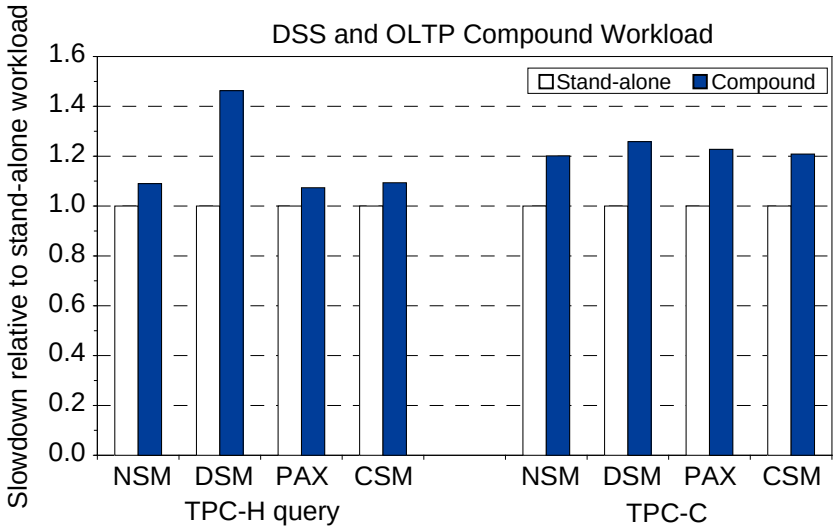

Fig. 6.15: **Compound workload performance for different layouts.** This figure expresses the slowdown of TPC-H query 1 runtime when run concurrently with TPC-C benchmark relative to the base case when running in isolation.

As shown in Figure 6.15, undue performance degradation does not occur: CSM exhibits the same or lesser relative performance degradation than the other layouts. The figure shows indicative performance results for TPC-H query 1 (others exhibit similar behavior) and for TPC-C, relative to the base case when OLTP and DSS queries run separately. The larger performance impact of compound workloads on DSS with DSM shows that small random I/O traffic aggravates the impact of seeks necessary to reconstruct a DSM page.

6.4.9 Results summary

The results for both MEMStore and the *Atropos* disk array demonstrate that exposing performance attributes to database storage managers improves performance of database workloads. For environments with only one workload type, the ACCESS DELAY BOUNDARIES attribute is sufficient. The storage manager can choose a page layout optimized for the workload type and achieve efficient accesses by utilizing the explicit information. Naturally, the benefit of using the ACCESS DELAY BOUNDARIES attribute is much larger for DSS workloads. Most DSS queries can exploit ensemble-based access, while OLTP, dominated by small random I/O, sees only minimal improvements.

The PARALLELISM attribute enables efficient execution for a new type of environment with compound workloads exhibiting both row- and column-major accesses. A database system taking advantage of the PARALLELISM attribute can

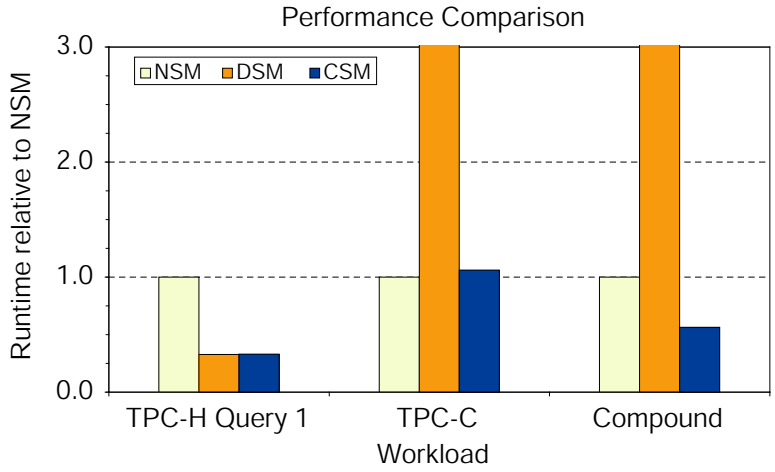

Fig. 6.16: **Comparison of three database workloads for different data layouts.** The workload runtime is shown relative to NSM, which is the page layout prevalent in commercial database systems. The TPC-C workload expresses the time to complete the same number of transactions for the three different workloads. The compound workload measures the total runtime of TPC-H query 1 executed simultaneously with the TPC-C benchmark completing a fixed number of transactions with no think time. Note that for DSM the runtime is respectively 7.5× and 4.5× larger for the TPC-C and Compound workloads.

use one data organization (CSM) for all three workload types (DSS, OLTP, and compound workload of DSS/OLTP). In all three cases, CSM performance is equal to or within 6% of the performance achieved with the respective layout optimized for only one workload, as shown in Figure 6.16. This characteristic is important for environments where workloads change over time (e.g., on-line retailers with predominantly OLTP workload running DSS during off-peak hours). Using CSM eliminates the need to use two replicas of data to run both workloads efficiently and also reduces the total cost of ownership — only one set of hardware is required.

The PARALLELISM attribute abstraction can hide device-specifics. With a few simple storage interface constructs, described in Appendix B, a storage manager can work seamlessly across devices with vastly different performance characteristics such as MEMStore and disk arrays, yet experience the same quantitative improvements.

6.4.10 Improving efficiency for a spectrum of workloads

To extrapolate how performance attributes improve efficiency across a spectrum of access patterns, Figure 6.17 compares access in current systems using state-of-the art techniques and systems that exploit performance attributes. It extrapolates from the database experiments results described in Chapter 5 and 6 and data

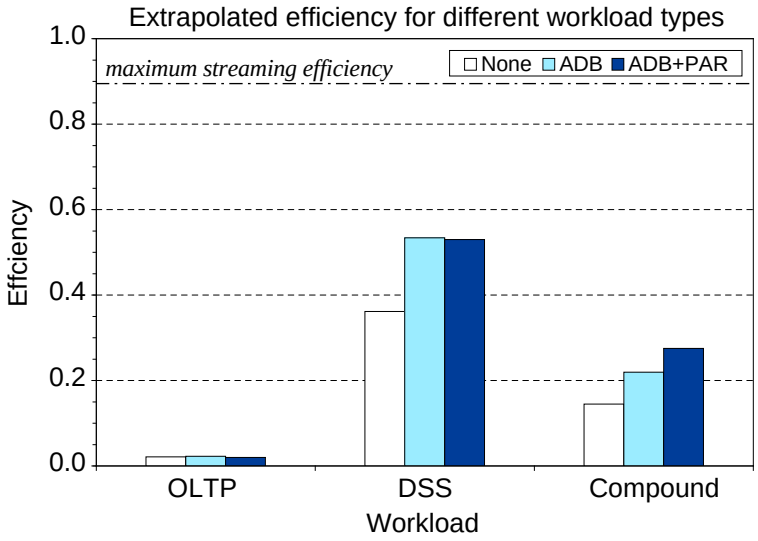

Fig. 6.17: **Comparison of disk efficiencies for three database workloads.**

collected from raw disk accesses. It expresses the results in terms of disk access efficiency of each individual disk of a four-disk logical volume. Disk efficiency is defined in Chapter 5 and Figure 5.1 as the ratio between media access time (time spent doing useful work) and total I/O service time, which also includes positioning time. The results also take into account how much data is requested by the system vs. how much is actually needed by the application.

The graph in Figure 6.17 compares for each workload type the disk access efficiency of the (i) current best approach that does not use any information from storage devices (labeled None), (ii) one that uses only the ACCESS DELAY BOUNDARIES attribute (labeled ADB), and (iii) one that uses both the ACCESS DELAY BOUNDARIES and the PARALLELISM attributes (labeled ADB+PAR). The efficiency of the base case for the OLTP workload is assessed from measurements of response times and using DiskSim models to break response time into individual components: seek, rotational latency, and media transfer. The results for the DSS and compound workloads are assessed from experimental measurements on scenario (iii) and the efficiencies for the other two scenarios are extrapolated from data in Figure 5.1 and I/O traces for the respective workloads.

For the OLTP workload, the disk efficiency of scenario (i) is expressed for a system using an 8 KB NSM page. Scenario (ii) also uses the NSM page layout with 8 KB pages allocated in extents matching ACCESS DELAY BOUNDARIES, as described in Section 5.7.3. Scenario (iii) uses the CSM page layout, described in Section 6.4.2. As can be seen, performance attributes do not significantly improve

disk efficiency. The ADB case, however, improves overall workload performance by almost 7% compared to the base scenario. The slightly lower efficiency for the ADB+PAR scenario stems from using CSM instead of NSM — semi-sequential access, instead of sequential, is used when fetching a single page. The overall efficiency for all three scenarios is 0.21, 0.23, and 0.20 respectively.

The achieved access efficiencies are much lower than the best possible case of maximum streaming efficiency for the following reason: OLTP workload is dominated by random accesses to individual pages that are only 8 KB in size. Hence disk access time is dominated by seeks and rotational latencies, while the time for useful data transfer is negligible compared to the positioning time.

For the DSS workload, the data represents the average across the 22 TPC-H queries. Scenario (i) expresses access efficiency of a system with 8 KB DSM page layout and issuing I/Os that match stripe unit size approximating track size (256 KB for the Maxtor Atlas 10k III disks). Scenario (ii) also uses 8 KB DSM pages, but I/O sizes match as close as possible the ACCESS DELAY BOUNDARIES attribute. Scenario (iii) uses the CSM page layout.

In contrast to the OLTP workload, performance attributes significantly improve disk efficiency. The slightly lower efficiency for the ADB+PAR case compared to the ADB is due to different page layout; CSM is slightly less efficient when packing records into a single page. The achieved access efficiency for the DSS workload is closer to the maximum streaming efficiency of the disk than for the OLTP workload. For a given I/O, seeks are still present, but (for the majority of the TPC-H benchmark queries), the performance attributes are able to significantly reduce rotational latency and achieve media transfers from the majority of the disk's track. The only way to increase access efficiency is through reduction of seek times. However, this can only be possible by employing a workload (query)-specific layout, which could shorten the seek distance and hence reduce seek time, or by improving disk's characteristics.

For the compound DSS/OLTP workload, the data shown represents the disk efficiency averaged over all I/Os in the workload. Recall that the workload exhibits both small 8 KB I/Os (coming from the OLTP workload) and much larger I/Os (coming from the DSS workload). Both scenarios (i) and (ii) use the NSM page layout, which is prevalent in commercial DBMS, and scenario (iii) uses CSM. The I/O sizes of each workload are the same as for the respective stand-alone workloads described in the preceding two paragraphs. As can be seen from the graph, this workload type benefits from utilizing both performance attributes.

7 Conclusions and Future Work

7.1 Concluding remarks

This dissertation demonstrates that storage managers in conventional computer systems have insufficient information about storage device performance characteristics. As a consequence, they utilize the available storage device resources inefficiently. This results in undue application performance degradation, especially when competing workloads contend for the same storage device. A few high-level, device-independent static hints about storage device performance characteristics can achieve significant I/O performance gains for workloads exhibiting regular access patterns.

The two examples of performance attributes proposed in this dissertation serve as these high-level, device-independent static hints. They can capture unique device characteristics to allow storage managers to automatically tune their access patterns to the given device. These attributes do not break established storage interface abstractions and for certain systems, as illustrated on the example of database systems, simple abstractions are restored. In particular, these attributes allow a storage manager to maintain the assumptions about access efficiencies made by other parts of the system regardless of the dynamic workload changes. And most importantly, they greatly simplify, or completely eliminate, the difficult and error-prone task of performance tuning.

For database systems, explicit performance attributes allow a database storage manager to specialize to particular storage devices and provide more robust performance in the presence of concurrent query execution. In particular, it can support high I/O concurrency without disrupting planned sequential I/O performance. It also eliminates the need for several (previously DBA-specified) parameters, thereby simplifying DBMS configuration and performance tuning. Explicitly stated characteristics restore the validity of the assumptions made by the query optimizer about the relative costs of different storage access patterns.

Since a storage manager is any system component that translates requests for data to the underlying mechanism for storing this data, the findings of this disser-

tation are applicable at many levels of the I/O path. In addition to file systems, database systems, and logical volume managers (whose implementations are detailed in this dissertation), the same mechanisms can be used in other systems as well. For example, object-based storage systems can use the described mechanisms to efficiently store and access objects on the underlying storage device.

Performance hints mesh well with existing system software data structures and algorithms. Thus, computer systems need minimal changes to incorporate them and can use unmodified existing storage devices. The three different storage manager implementations described in this dissertation made no changes to storage device hardware in order to enjoy the documented performance gains.

The evaluation of access efficiencies for state-of-the-art disk drives reveals a few noteworthy points. Zero-latency access is an important firmware feature that yields large improvements with track-based access. A storage manager that exploits these accesses (such as the ones described in this dissertation) can greatly benefit. When combined with out-of-order data delivery (which is defined in the SCSI specification, it yields additional 10% improvement in access efficiency. All disk vendors should implement both of these features and thus create an opportunity for storage managers to exploit them.

The ACCESS DELAY BOUNDARIES attribute can achieve significant increase in access efficiency (within 82% of the maximum efficiency) for random accesses that are appropriately sized and aligned on ensemble boundaries. A variety of systems such as disk array logical volume managers, file systems, or database systems can match their access patterns to utilize this access efficiency. The PARALLELISM attribute offers efficient access to two dimensional data structures. Compared to traditional systems that, in order to achieve better access efficiency, fetch extraneous data that is dropped, a data layout taking advantage of this attribute allows applications to request only the data that is needed.

The proposed mechanism for providing explicit performance hints by attribute annotation represents only one possible solution. The focus of this dissertation is on identifying *what* device-specific characteristics should be exposed to allow better utilization of the available storage device resources rather than on *how* the information should be conveyed.

7.2 Directions for future research

This dissertation encompasses a broad range of storage and computer systems. There are many interesting topics it touched upon that are worth exploring in more detail.

The obvious next step is the research of more attributes that can potentially provide benefit to storage managers. This dissertation presents two examples of attributes, namely the ACCESS DELAY BOUNDARIES and PARALLELISM, that encapsulate a variety of unique storage device characteristics. It also discusses the fault-isolation boundary attribute proposed by related research [Denehy et al. 2002]. Studying if other attributes can potentially capture additional important device performance characteristics and evaluating by how much they improve application performance should provide interesting insights.

The performance hints described in this dissertation are static in their nature. They prescribe to the storage manager how to exercise its access patterns to obtain the best possible efficiency at any level of device utilization. Because of this invariant, the hints need not quantify device performance. It can be simply observed by the storage manager which can decide if it is sufficient for the application needs. Capturing and quantifying dynamic behavior by performance attributes may provide additional benefits. However, it will also require more substantial changes to the storage interface and system software behavior.

Sufficient information about device performance characteristics given to a storage manager can significantly improve application performance. The chosen method of annotating device's linear address space with attributes described in this dissertation gets this job done. The thesis of this dissertation provides an interesting basis for exploring alternative and more expressive storage interfaces. Evaluating the tradeoff between these new interfaces and the effort required to modify existing systems to adapt them warrants more research.

Performance characteristics discovery tools are specialized to one type of a storage device. The DIXtrac tool described in this dissertation works with disk drives. Building upon its methods, similar tools could be potentially built to automatically characterize disk arrays, which have more complicated internal structure. This characterization would be useful for other applications such as capacity planning and storage outsourcing with different service-level agreements.

Bibliography

Ailamaki, A., DeWitt, D. J., Hill, M. D., and Skounakis, M. 2001. Weaving relations for cache performance. In *International Conference on Very Large Databases*. Morgan Kaufmann Publishing, Inc., 169–180.

Ailamaki, A., DeWitt, D. J., Hill, M. D., and Wood, D. A. 1999. DBMSs on a modern processor: where does time go? In *International Conference on Very Large Databases*. Morgan Kaufmann Publishing, Inc., 266–277.

Anderson, D., Dykes, J., and Riedel, E. 2003. More than an interface—SCSI vs. ATA. In *Conference on File and Storage Technologies*. USENIX Association.

Arge, L., Procopiuc, O., and Vitter, J. S. 2002. Implementing i/o-efficient data structures using tpie. In *European Symposium on Algorithms*. 88–100.

Arpaci-Dusseau, A. and Arpaci-Dusseau, R. 2001. Information and control in gray-box systems. In *ACM Symposium on Operating System Principles*. 43–56.

Arpaci-Dusseau, R. H., Anderson, E., Treuhaft, N., Culler, D. E., Hellerstein, J. M., Patterson, D., and Yelick, K. 1999. Cluster I/O with River: making the fast case common. In *Workshop on Input/Output in Parallel and Distributed Systems*.

Bailey, D. H., Barszcz, E., Dagum, L., and Simon, H. D. 1993. NAS parallel benchmark results 10-93. Tech. Rep. RNR–93–016, NASA Ames Research Center, Mail Stop T045-1, Moffett Field, CA 94035.

Baker, M. G., Hartman, J. H., Kupfer, M. D., Shirriff, K. W., and Ousterhout, J. K. 1991. Measurements of a distributed file system. In *ACM Symposium on Operating System Principles*. 198–212.

Bitton, D. and Gray, J. 1988. Disk shadowing. In *International Conference on Very Large Databases*. 331–338.

Blackwell, T., Harris, J., and Seltzer, M. 1995. Heuristic cleaning algorithms in log-structured file systems. In *USENIX Annual Technical Conference*. USENIX Association, 277–288.

Bolosky, W. J., Barrera, J. S., Draves, R. P., Fitzgerald, R. P., Gibson, G. A., Jones, M. B., Levi, S. P., Myhrvold, N. P., and Rashid, R. F. 1996. The Tiger video fileserver. Tech. Rep. MSR–TR–96–09, Microsoft Corporation.

Boncz, P. A., Manegold, S., and Kersten, M. L. 1999. Database architecture optimized for the new bottleneck: memory access. In *International Conference on Very Large Databases*. Morgan Kaufmann Publishers, Inc., 54–65.

Bovet, D. P. and Cesati, M. 2001. *Understanding the Linux kernel*. O'Reilly & Associates.

Brown, A. D., Mowry, T. C., and Krieger, O. 2001. Compiler-based I/O prefetching for out-of-core applications. *ACM Transactions on Computer Systems 19,* 2, 111–170.

Bucy, J. S. and Ganger, G. R. 2003. The DiskSim simulation environment version 3.0 reference manual. Tech. Rep. CMU–CS–03–102, Department of Computer Science Carnegie-Mellon University, Pittsburgh, PA.

Burnett, N. C., Bent, J., Arpaci-Dusseau, A. C., and Arpaci-Dusseau, R. H. 2002. Exploiting gray-box knowledge of buffer-cache contents. In *USENIX Annual Technical Conference*. 29–44.

Carey, M. J., DeWitt, D. J., Franklin, M. J., Hall, N. E., McAuliffe, M. L., Naughton, J. F., Schuh, D. T., Solomon, M. H., Tan, C. K., Tsatalos, O. G., White, S. J., and Zwilling, M. J. 1994. Shoring up persistent applications. In *ACM SIGMOD International Conference on Management of Data*. 383–394.

Carley, L. R., Ganger, G. R., and Nagle, D. F. 2000. MEMS-based integrated-circuit mass-storage systems. *Communications of the ACM 43,* 11, 73–80.

Carson, S. and Setia, S. 1992. Optimal write batch size in log-structured file systems. In *USENIX Workshop on File Systems*. 79–91.

Chang, E. and Garcia-Molina, H. 1996. Reducing initial latency in a multimedia storage system. In *International Workshop on Multi-Media Database Management Systems*. 2–11.

Chang, E. and Garcia-Molina, H. 1997. Effective memory use in a media server. In *International Conference on Very Large Databases*. Morgan Kaufmann Publishers, Inc., 496–505.

Chao, C., English, R., Jacobson, D., Stepanov, A., and Wilkes, J. 1992. Mime: high performance parallel storage device with strong recovery guarantees. Tech. Rep. HPL-92-9, HPL-92-9.

Chen, P. M., Lee, E. K., Gibson, G. A., Katz, R. H., and Patterson, D. A. 1994. RAID: high-performance, reliable secondary storage. *ACM Computing Surveys 26,* 2, 145–185.

Chen, P. M. and Patterson, D. A. 1990. Maximizing performance in a striped disk array. In *ACM International Symposium on Computer Architecture*. 322–331.

Chen, S., Gibbons, P. B., Mowry, T. C., and Valentin, G. 2002. Fractal prefetching B+-trees: optimizing both cache and disk performance. In *ACM SIGMOD International Conference on Management of Data*. ACM Press, 157–168.

Copeland, G. P. and Khoshafian, S. 1985. A decomposition storage model. In *ACM SIGMOD International Conference on Management of Data*. ACM Press, 268–279.

Corbett, P. F. and Feitelson, D. G. 1994. Design and implementation of the Vesta parallel file system. In *Scalable High-Performance Computing Conference*. 63–70.

Cormen, T. H. 1993. Fast permuting on disk arrays. *Journal of Parallel and Distributed Computing 17,* 1, 41–57.

Daniel, S. and Geist, R. 1983. V-SCAN: an adaptive disk scheduling algorithm. In *International Workshop on Computer Systems Organization*. IEEE, 96–103.

Denehy, T. E., Arpaci-Dusseau, A. C., and Arpaci-Dusseau, R. H. 2002. Bridging the information gap in storage protocol stacks. In *Summer USENIX Technical Conference*. 177–190.

Denning, P. J. 1967. Effects of scheduling on file memory operations. In *AFIPS Spring Joint Computer Conference*. 9–21.

DeWitt, D. J., Ghandeharizadeh, S., Schneider, D. A., Bricker, A., Hui-IHsiao, and Rasmussen, R. 1990. The Gamma database machine project. *IEEE Transactions on Knowledge and Data Engineering 2,* 1, 44–62.

Douceur, J. R. and Bolosky, W. J. 1999. A large-scale study of file-system contents. In *ACM SIGMETRICS Conference on Measurement and Modeling of Computer Systems*. ACM Press, 59–70.

English, R. M. and Stepanov, A. A. 1992. Loge: a self-organizing disk controller. In *Winter USENIX Technical Conference*. Usenix, 237–251.

Fedder, G. K., Santhanam, S., Reed, M. L., Eagle, S. C., Guillou, D. F., Lu, M. S.-C., and Carley, L. R. 1996. Laminated high-aspect-ratio microstructures in a conventional CMOS process. In *IEEE Micro Electro Mechanical Systems Workshop*. 13–18.

Freedman, C. S., Burger, J., and DeWitt, D. J. 1996. SPIFFI-a scalable parallel file system for the Intel Paragon. *IEEE Transactions on Parallel and Distributed Systems 7,* 11, 1185–1200.

Fuller, S. H. 1972. An optimal drum scheduling algorithm. *IEEE Transactions on Computers 21,* 11, 1153–1165.

Gabber, E. and Shriver, E. 2000. Lets put NetApp and CacheFlow out of business. In *SIGOPS European Workshop*. 85–90.

Ganger, G. R. 1995. System-oriented evaluation of I/O subsystem performance. Ph.D. thesis, University of Michigan, Ann Arbor, MI.

Ganger, G. R. and Kaashoek, M. F. 1997. Embedded inodes and explicit grouping: exploiting disk bandwidth for small files. In *USENIX Annual Technical Conference*. 1–17.

Ganger, G. R., Worthington, B. L., Hou, R. Y., and Patt, Y. N. 1994. Disk arrays: high-performance, high-reliability storage systems. *IEEE Computer 27,* 3, 30–36.

Geist, R. and Daniel, S. 1987. A continuum of disk scheduling algorithms. *ACM Transactions on Computer Systems 5,* 1, 77–92.

Ghemawat, S. 1995. The modified object buffer: a storage management technique for object-oriented databases. Ph.D. thesis, Massachusetts Institute of Technology, Cambridge, MA.

Giampaolo, D. 1998. *Practical file system design with the Be file system*. Morgan Kaufmann.

Gibson, G. A., Nagle, D. F., Amiri, K., Butler, J., Chang, F. W., Gobioff, H., Hardin, C., Riedel, E., Rochberg, D., and Zelenka, J. 1998. A cost-effective, high-bandwidth storage architecture. In *Architectural Support for Programming Languages and Operating Systems*. 92–103.

Graefe, G. 1993. Query evaluation techniques for large databases. *ACM Computing Surveys 25,* 2, 73–170.

Griffin, J. L., Schindler, J., Schlosser, S. W., Bucy, J. C., and Ganger, G. R. 2002. Timing-accurate storage emulation. In *Conference on File and Storage Technologies*. USENIX Association, 75–88.

Griffin, J. L., Schlosser, S. W., Ganger, G. R., and Nagle, D. F. 2000a. Modeling and performance of MEMS-based storage devices. In *ACM SIGMETRICS Conference on Measurement and Modeling of Computer Systems*. 56–65.

Griffin, J. L., Schlosser, S. W., Ganger, G. R., and Nagle, D. F. 2000b. Operating system management of MEMS-based storage devices. In *Symposium on Operating Systems Design and Implementation*. USENIX Association, 227–242.

Hitz, D., Lau, J., and Malcolm, M. 1994. File system design for an NFS file server appliance. In *Winter USENIX Technical Conference*. USENIX Association, 235–246.

Hou, R. Y., Menon, J., and Patt, Y. N. 1993. Balancing I/O response time and disk rebuild time in a RAID5 disk array. In *Hawaii International Conference on Systems Sciences*.

Huang, L. and cker Chiueh, T. 1999. Implementation of a rotation latency sensitive disk scheduler. Tech. Rep. ECSL TR-81, SUNY Stony Brook.

IBM Corporation 1994. *DB2 V3 Performance Topics*. IBM Corporation.

IBM Corporation 2000. *IBM DB2 Universal Database Administration Guide: Implementation*. IBM Corporation.

Jacobson, D. M. and Wilkes, J. 1991. Disk scheduling algorithms based on rotational position. Tech. Rep. HPL–CSP–91–7, Hewlett-Packard Laboratories, Palo Alto, CA.

Kaashoek, M. F., Engler, D. R., Ganger, G. R., and Wallach, D. A. 1996. Server operating systems. In *ACM SIGOPS. European workshop: Systems support for worldwide applications*. ACM, 141–148.

Katcher, J. 1997. PostMark: a new file system benchmark. Tech. Rep. TR3022, Network Appliance.

Keeton, K. and Katz, R. H. 1993. The evaluations of video layout strategies on a high-bandwidth file server. In *4th International Workshop on Network and Operating System Support for Digital Audio and Video*. 228–229.

Kotz, D. 1994. Disk-directed I/O for MIMD multiprocessors. In *Symposium on Operating Systems Design and Implementation*. USENIX Association, 61–74.

Kotz, D., Toh, S. B., and Radhakrishnan, S. 1994. A detailed simulation model of the HP 97560 disk drive. Tech. Rep. PCS–TR94–220, Department of Computer Science, Dartmouth College.

Krieger, O. and Stumm, M. 1997. HFS: a performance-oriented flexible file system based on building-block compositions. *ACM Transactions on Computer Systems 15,* 3, 286–321.

Loney, K. and Koch, G. 2000. *Oracle 8i: The Complete Reference*. Osborne/McGraw-Hill.

Lumb, C. R., Schindler, J., and Ganger, G. R. 2002. Freeblock scheduling outside of disk firmware. In *Conference on File and Storage Technologies*. USENIX Association, 275–288.

Lumb, C. R., Schindler, J., Ganger, G. R., Nagle, D. F., and Riedel, E. 2000. Towards higher disk head utilization: extracting free bandwidth from busy disk drives. In *Symposium on Operating Systems Design and Implementation*. USENIX Association, 87–102.

Maluf, N. 2000. *An introduction to microelectromechanical systems engineering*. Artech House.

Manegold, S., Boncz, P. A., and Kersten, M. L. 2002. Generic database cost models for hierarchical memory systems. In *International Conference on Very Large Databases*. Morgan Kaufmann Publishers, Inc., 191–202.

Matthews, J. N., Roselli, D., Costello, A. M., Wang, R. Y., and Anderson, T. E. 1997. Improving the performance of log-structured file systems with adaptive methods. In *ACM Symposium on Operating System Principles*. ACM, 238–252.

Mayr, T. and Gray, J. 2000. Performance of the One-to-One Data Pump. http://research.microsoft.com/Gray/river/PerformanceReport.pdf.

McKusick, M. K., Joy, W. N., Leffler, S. J., and Fabry, R. S. 1984. A fast file system for UNIX. *ACM Transactions on Computer Systems 2,* 3, 181–197.

McVoy, L. W. and Kleiman, S. R. 1991. Extent-like performance from a UNIX file system. In *USENIX Annual Technical Conference*. USENIX, 33–43.

Mehta, M. and DeWitt, D. J. 1995. Managing intra-operator parallelism in parallel database systems. In *International Conference on Very Large Databases*. Morgan Kaufmann Publishers, Inc., 382–394.

Mehta, M. and DeWitt, D. J. 1997. Data placement in shared-nothing parallel database systems. *VLDB Journal 6,* 1, 53–72.

Menon, J. and Mattson, D. 1992. Comparison of sparing alternatives for disk arrays. In *ACM International Symposium on Computer Architecture*. 318–329.

Mohan, C., Haderle, D. J., Lindsay, B. G., Pirahesh, H., and Schwarz, P. M. 1992. ARIES: a transaction recovery method supporting fine-granularity locking and partial rollbacks using write-ahead logging. *ACM Transactions on Database Systems 17,* 1, 94–162.

Nagar, R. 1997. *Windows NT File System Internals: A Developer's Guide*. O'Reilly & Associates.

National Committee for Information Technology Standards 2002. *Working Draft SCSI Object-Based Storage Device Commands (OSD)*. National Committee for Information Technology Standards.

Network Appliance, Inc. 2002. *NetCache C2100*. Network Appliance, Inc. . http://www.netapp.com/products/netcache/netcache_family.html.

Ousterhout, J. K., Da Costa, H., Harrison, D., Kunze, J. A., Kupfer, M., and Thompson, J. G. 1985. A trace-driven analysis of the UNIX 4.2 BSD file system. In *ACM Symposium on Operating System Principles*. 15–24.

Patterson, D. A., Gibson, G., and Katz, R. H. 1988. A case for redundant arrays of inexpensive disks (RAID). In *ACM SIGMOD International Conference on Management of Data*. 109–116.

Patterson, R. H., Gibson, G. A., Ginting, E., Stodolsky, D., and Zelenka, J. 1995. Informed prefetching and caching. In *ACM Symposium on Operating System Principles*. 79–95.

Quantum Corporation 1999. *Quantum Atlas 10K 9.1/18.2/36.4 GB SCSI product manual*. Quantum Corporation.

Ramamurthy, R., DeWitt, D. J., and Su, Q. 2002. A case for fractured mirrors. In *International Conference on Very Large Databases*. Morgan Kaufmann Publishers, Inc., 430–441.

Rao, J. and Ross, K. A. 1999. Cache conscious indexing for decision-support in main memory. In *International Conference on Very Large Databases*. Morgan Kaufmann Publishers, Inc., 78–89.

Reddy, A. L. N. and Wyllie, J. 1993. Disk scheduling in a multimedia I/O system. In *International Multimedia Conference*. ACM Press, 225–234.

Reiser, H. T. 2001. ReiserFS v. 3 whitepaper. http://www.namesys.com/.

Riedel, E., Faloutsos, C., Ganger, G. R., and Nagle, D. F. 2000. Data mining on an oltp system (nearly) for free. In *ACM SIGMOD International Conference on Management of Data*. ACM, 13–21.

Rosenblum, M. and Ousterhout, J. K. 1992. The design and implementation of a log-structured file system. *ACM Transactions on Computer Systems 10,* 1, 26–52.

Ruemmler, C. and Wilkes, J. 1991. Disk Shuffling. Tech. Rep. HPL-91-156, Hewlett-Packard Company, Palo Alto, CA.

Ruemmler, C. and Wilkes, J. 1993. UNIX disk access patterns. In *Winter USENIX Technical Conference*. 405–420.

Santos, J. R. and Muntz, R. 1997. Design of the RIO (randomized I/O) storage server. Tech. Rep. 970032, UCLA Computer Science Department.

Santos, J. R., Muntz, R. R., and Ribeiro-Neto, B. 2000. Comparing random data allocation and data striping in multimedia servers. In *ACM SIGMETRICS Conference on Measurement and Modeling of Computer Systems*. ACM Press, 44–55.

Schindler, J., Ailamaki, A., and Ganger, G. R. 2003. Lachesis: robust database storage management based on device-specific performance characteristics. In *International Conference on Very Large Databases*. Morgan Kaufmann Publishing, Inc.

Schindler, J. and Ganger, G. R. 1999. Automated disk drive characterization. Tech. Rep. CMU–CS–99–176, Carnegie-Mellon University, Pittsburgh, PA.

Schindler, J., Griffin, J. L., Lumb, C. R., and Ganger, G. R. 2002. Track-aligned extents: matching access patterns to disk drive characteristics. In *Conference on File and Storage Technologies*. USENIX Association, 259–274.

Schlosser, S. W., Griffin, J. L., Nagle, D. F., and Ganger, G. R. 2000. Designing computer systems with MEMS-based storage. In *Architectural Support for Programming Languages and Operating Systems*. 1–12.

Schlosser, S. W., Schindler, J., Ailamaki, A., and Ganger, G. R. 2003. Exposing and exploiting internal parallelism in MEMS-based storage. Tech. Rep. CMU–CS–03–125, Carnegie-Mellon University, Pittsburgh, PA.

Schmidt, B., Northcutt, J., and Lam, M. 1995. A method and apparatus for measuring media synchronization. In *International Workshop on Network and Operating System Support for Digital Audio and Video*. 203–214.

Schmidt, F. 1995. *The SCSI Bus and IDE Interface*. Addison-Wesley.

Selinger, P. G., Astrahan, M. M., Chamberlin, D. D., Lorie, R. A., and Price, T. G. 1979. Access path selection in a relational database management system. In *ACM SIGMOD International Conference on Management of Data*. ACM Press, 23–34.

Seltzer, M., Bostic, K., McKusick, M. K., and Staelin, C. 1993. An implementation of a log-structured file system for UNIX. In *Winter USENIX Technical Conference*. 307–326.

Seltzer, M., Chen, P., and Ousterhout, J. 1990. Disk scheduling revisited. In *Winter USENIX Technical Conference*. 313–323.

Seltzer, M., Smith, K. A., Balakrishnan, H., Chang, J., McMains, S., and Padmanabhan, V. 1995. File system logging versus clustering: a performance comparison. In *USENIX Annual Technical Conference*. Usenix Association, 249–264.

Seltzer, M. I., Ganger, G. R., McKusick, M. K., Smith, K. A., Soules, C. A. N., and Stein, C. A. 2000. Journaling versus Soft Updates: Asynchronous Meta-data Protection in File Systems. In *USENIX Annual Technical Conference*. 71–84.

Shao, M., Schindler, J., Schlosser, S. W., Ailamaki, A., and Ganger, G. R. 2004. Clotho: decoupling memory page layout from storage organization. Tech. Rep. CMU–PDL–04–102, Carnegie-Mellon University, Pittsburgh, PA.

Shriver, E., Gabber, E., Huang, L., and Stein, C. A. 2001. Storage management for web proxies. In *USENIX Annual Technical Conference*. 203–216.

Shriver, E., Merchant, A., and Wilkes, J. 1998. An analytic behavior model for disk drives with readahead caches and request reordering. In *International Conference on Measurement and Modeling of Computer Systems*. ACM, 182–191.

Shriver, L., Smith, K., and Small, C. 1999. Why does file system prefetching work? In *USENIX*. 71–83.

Sienknecht, T. F., Friedrich, R. J., Martinka, J. J., and Friedenbach, P. M. 1994. The implications of distributed data in a commercial environment on the design of hierarchical storage management. *Performance Evaluation 20,* 1–3, 3–25.

Smith, K. A. and Seltzer, M. 1996. A comparison of FFS disk allocation policies. In *USENIX.96*. USENIX Assoc., 15–25.

Steere, D. C. 1997. Exploiting the non-determinism and asynchrony of set iterators to reduce aggreggate file I/O latency. In *ACM Symposium on Operating System Principles*. ACM, 252–263.

Sweeney, A. 1996. Scalability in the XFS file system. In *USENIX Annual Technical Conference*. 1–14.

Tacit Networks 2002. *Tacit cache appliance*. Tacit Networks. http://-www.tacitnetworks.com/.

Talagala, N., Dusseau, R. H., and Patterson, D. 2000. Microbenchmark-based extraction of local and global disk characteristics. Tech. Rep. CSD–99–1063, University of California at Berkeley.

Transactional Processing Performance Council 2002a. *TPC Benchmark C*. Transactional Processing Performance Council.

Transactional Processing Performance Council 2002b. *TPC Benchmark H*. Transactional Processing Performance Council.

Uysal, M., Merchant, A., and Alvarez, G. A. 2003. Using MEMS-based storage in disk arrays. In *Conference on File and Storage Technologies*. USENIX Association, 89–102.

VanMeter, R. 1997. Observing the effects of multi-zone disks. In *USENIX Annual Technical Conference*. 19–30.

VanMeter, R. 1998. SLEDs: storage latency estimation descriptors. In *IEEE Symposium on Mass Storage Systems*. USENIX.

Vengroff, D. E. 1994. A transparent parallel I/O environment. In *DAGS Symposium on Parallel Computation*. 117–134.

Vengroff, D. E. and Vitter, J. S. 1995. I/O-Efficient scientific computation using TPIE. Tech. Rep. CS-1995-18, Duke University.

VERITAS Software Company 2000. *VERITAS Volume Manager 3.1 Administrator's Guide*. VERITAS Software Company.

Vettiger, P., Despont, M., Drechsler, U., Dürig, U., Häberle, W., Lutwyche, M. I., Rothuizen, H. E., Stutz, R., Widmer, R., and Binnig, G. K. 2000. The "Millipede" – more than one thousand tips for future AFM data storage. *IBM Journal of Research and Development 44,* 3, 323–340.

Vin, H. M., Goyal, A., and Goyal, P. 1995. Algorithms for designing multimedia servers. *IEEE Computer Communications 18,* 3, 192–203.

Vitter, J. S. and Shriver, E. A. M. 1994. Algorithms for parallel memory I: two-level memories. *Algorithmica 12,* 2/3, 110–147.

Vogels, W. 1999. File system usage in Windows NT 4.0. In *ACM Symposium on Operating System Principles*. ACM, 93–109.

Wang, R. Y., Patterson, D. A., and Anderson, T. E. 1999. Virtual log based file systems for a programmable disk. In *Symposium on Operating Systems Design and Implementation*. ACM, 29–43.

Wilkes, J., Golding, R., Staelin, C., and Sullivan, T. 1996. The HP AutoRAID hierarchical storage system. *ACM Transactions on Computer Systems 14,* 1, 108–136.

Wise, K. D. 1998. Special issue on integrated sensors, microactuators, and microsystems (MEMS). *Proceedings of the IEEE 86,* 8, 1531–1787.

Wong, T. M. and Wilkes, J. 2002. My cache or yours? Making storage more exclusive. In *USENIX Annual Technical Conference*. 161–175.

Worthington, B. L., Ganger, G. R., and Patt, Y. N. 1994. Scheduling algorithms for modern disk drives. In *ACM SIGMETRICS Conference on Measurement and Modeling of Computer Systems*. ACM Press, 241–251.

Worthington, B. L., Ganger, G. R., Patt, Y. N., and Wilkes, J. 1995. On-line extraction of SCSI disk drive parameters. In *ACM SIGMETRICS Conference on Measurement and Modeling of Computer Systems*. 146–156.

Yu, X., Gum, B., Chen, Y., Wang, R. Y., Li, K., Krishnamurthy, A., and Anderson, T. E. 2000. Trading capacity for performance in a disk array. In *Symposium on Operating Systems Design and Implementation*. USENIX Association, 243–258.

A Modeling disk drive media access

An analytical model is useful for determining expected performance gains for current devices as well as those that do not yet exist. It can be used to determine how physical characteristics influence media access and how individual disk characteristics (i.e., head-switch time and zero-latency firmware feature) impact disk performance.

In the context of this dissertation, the analytical model derived in this section is used for predicting performance improvements with ensemble-based disk accesses that can be realized by applications when the ACCESS DELAY BOUNDARIES attribute is exposed to them. For a given a request size and its location, the model calculates the time for both ordinary accesses (i.e., not aligned on track boundaries) and ensemble-based accesses (i.e., aligned on track boundaries). The primary benefit of the model described in this section is its ability to make accurate predictions for any disk described by two parameters—the number of sectors per track, N, and the head switch time. This time is expressed as the number of sectors passed by during head switch, H, divided by the number of sectors per track.

A.1 Basic assumptions

Assume a disk with N sectors per track and a request of size S sectors, where $S \leq 2N$, with uniformly distributed requests across all sectors of a track. Then the probability of a track switch, P_{hs}, is

$$P_{hs}(S,N) = \begin{cases} 0 & \text{if } S = 1 \\ \sum_{i=2}^{S} \frac{1}{N} & \text{if } S \leq N \\ 1 & \text{otherwise} \end{cases} \tag{A.1}$$

The expected time T to access S sectors that can potentially span two tracks on a disk can be expressed as

$$T = (1 - P_{hs})T_1(N,S) + P_{hs}\left(T_1(N,S_1) + T_2(N,S,S_2)\right) \tag{A.2}$$

where $T_1(N, S_1)$ is the time it takes to access S_1 sectors on the first track and $T_2(N, S, S_2)$ is the time it takes to access S_2 sectors on the second track, given a request size of S sectors. For such requests, S_1 sectors are accessed on the first track, and S_2 sectors are accessed on the second track, where $S_2 = S - S_1$. For brevity, the times are expressed in number of revolutions for the remainder of the discussion.

A.2 Non-zero-latency disk

A non-zero latency disk has to wait until the first sector of S sectors arrives under the read/write head and only then starts accessing the data. As a consequence, when a track switch occurs, the head is always at the logical end of track 1. Thus, the head will always be positioned at the logical beginning of the track 2, which is the beginning of S_2 sectors.

A.2.1 No track switch

Let's express the time for reading S sectors from a track, T_1, assuming there is no track switch. The head can be positioned with probability $\frac{1}{N}$ above any sector of the track. Thus, we have to wait, with equal probability, between 0 and $(N-1)$ sectors before we can access the first sector of S. Once the first sector arrives under the head, it will take $\frac{S}{N}$ revolution to access the data. Therefore, the time T_1 to read S sectors is

$$T_1(N, S) = \frac{1}{N}\left(0 + \frac{1}{N} + \frac{2}{N} + \ldots + \frac{N-1}{N}\right) + \frac{S}{N} = \frac{1}{N^2}\sum_{i=0}^{N-1} i + \frac{S}{N} \qquad \text{(A.3)}$$

The first term is the expected rotational latency and is equal to $\frac{N-1}{2N}$.

A.2.2 Track switch

When a track switch occurs, which is with probability P_{hs}, then the disk head will be repositioned over track 2 in time to read the first sector of S_2. The time it takes to reposition the head on the new track is accounted for in the mapping of logical blocks to physical sectors and is called track skew. Let's call this skew $K$and assume that $K = H$ blocks. Thus the total time T_2 to access S_2 sectors on track 2 is

$$T_2(N, S_2) = \frac{H + S_2}{N} \qquad \text{(A.4)}$$

A.3 Zero-latency disk

A zero-latency disk can access the S sectors on the track and read them out of their logical order as soon as any of the requested sectors is under the read/write head. The data is then put into an intermediate buffer on the disk controller, reordered, and sent to the host in the correct order. As a consequence, a zero-latency disk will spend at most 1 revolution accessing S sectors on the track, where N is the number of sectors on the track and $1 \leq S \leq N$.

A.3.1 No track switch

Let's express the time T_1 for reading S sectors from a track, assuming there is no track switch, ignoring seek for the moment. There is $\frac{N-S}{N}$ probability that the head is not positioned above any of the S sectors we want to access and $\frac{1}{N}$ probability it is exactly above the first sector of S. Therefore, there is $\frac{1}{N-S+1}$ probability we are 0, 1, 2, or up to $N-S$ sectors away from the first sector in S. Since the time to access S sectors is $\frac{S}{N}$ once we arrive at the start of the sectors S, the time T_{1a} to read S sectors is

$$\begin{aligned} T_{1a} &= \frac{1}{N-S+1}\left(0+\frac{1}{N}+\frac{2}{N}+\ldots+\frac{N-S}{N}\right)+\frac{S}{N} \\ &= \frac{1}{N(N-S+1)}\sum_{i=0}^{N-S} i+\frac{S}{N} \end{aligned} \tag{A.5}$$

where the first term is the expected rotational latency.

There is a probability of $\frac{S-1}{N}$ that the head is anywhere within S sectors not including the first sector of S. Thus the total access time is one revolution and can be expressed as

$$T_{1b} = \frac{1}{S-1}(1+\ldots+1) = \frac{1}{S-1}\sum_{i=1}^{S-1} 1 = 1 \tag{A.6}$$

Combining the terms T_{1a} and T_{1b} and their respective probabilities, we can express the expected time for accessing S sectors without a track switch

$$\begin{aligned} T_1(N,S) &= \frac{N-S+1}{N}T_{1a}+\frac{S-1}{N}T_{1b} \\ &= \frac{N-S+1}{N}\left(\frac{1}{N(N-S+1)}\sum_{i=0}^{N-S} i+\frac{S}{N}\right)+\frac{S-1}{N} \\ &= \frac{(N-S+1)(N+S)}{2N^2}+\frac{S-1}{N} \end{aligned} \tag{A.7}$$

A.3.2 Track switch

Now, let's assume there is a track switch, which occurs with probability P_{hs}. Then there are S_1 sectors accessed at the first track and S_2 sectors accessed at the second track, where $S_2 = S - S_1$. The total time to access the S_1 sectors is $T_1(N, S_1)$. We have to express the time it takes to read the remaining S_2 sectors after the head has been moved to track 2.

There are two cases where the head can land upon a track switch. In the first case, when the last sector accessed by the head is the last sector of S_1, the head lands at the beginning of the S_2 sectors. This case occurs with probability $\frac{N-S_1+1}{N}$ because there are $N - S_1 + 1$ different positions where the head could have been when it started accessing S_1 sectors on track 1. Thus the time spent accessing track 2, T_{2a}, consists of waiting a fixed offset of O sectors, which takes $\frac{O}{N}$, and reading S_2 sectors, which takes $\frac{S_2}{N}$. Therefore,

$$T_{2a} = \frac{N - S_1 + 1}{N}\left(\frac{S_2}{N} + \frac{O}{N}\right) = \frac{(N - S_1 + 1)(S_2 + O)}{N^2} \tag{A.8}$$

In the second case, when the head last accessed any but the last sector of S_1, the head can land anywhere on track 2. This occurs with probability of $\frac{S_1-1}{N}$ and the time to read S_2 sectors is then T_{2b}.

Before expressing T_{2b}, let's examine the possible locations of the head as it lands on track 2. If $S_1 + S_2 \leq N$, then the head will always land outside of the S_2 sectors. If $S_1 + S_2 = 2N$, then the head will always land inside the S_2 sectors, since both S_1 and S_2 are of size N. Finally, for the case of $N < S_1 + S_2 < 2N$, there is an overlap between S_1 and S_2. The size of the overlap is $S_1 + S_2 - N$ sectors, thus the probability of landing inside the overlap is $\frac{S_1+S_2-N}{S_1} - 1$ since there are $S_1 - 1$ possibilities of leaving track 1 and landing on track 2. The probability of landing outside this overlap, and therefore outside of S_2, is just $1 - \frac{S_1+S_2-N}{S_1-1}$, which simplifies to $\frac{N-S_2}{S_1-1}$. See figure A.1 for more details. If there is a track skew of K sectors, K is added to S_2. Now, we can express the probability P_l of landing outside of S_2 as

$$P_l = \begin{cases} 1 & \text{if } S_1 + S_2 + K \leq N \\ \frac{N-S_2}{S_1-1} & \text{if } S_1 + S_2 + K > N \\ 0 & \text{if } S_1 + S_2 + K = 2N \end{cases} \tag{A.9}$$

If the head lands on top of any part of S_2, then the total time T_{2c} to read the S_2 sectors is $\frac{S_2}{N}$ with a probability of $\frac{1}{S_2}$. Otherwise, it takes an entire revolution. Thus,

$$T_{2c} = \frac{1}{S_2}\left(\frac{S_2}{N} + 1 + \ldots + 1\right) = \frac{1}{N} + \sum_{i=1}^{S_2-1} \frac{1}{S_2} = \frac{1}{N} + \frac{S_2 - 1}{S_2}$$

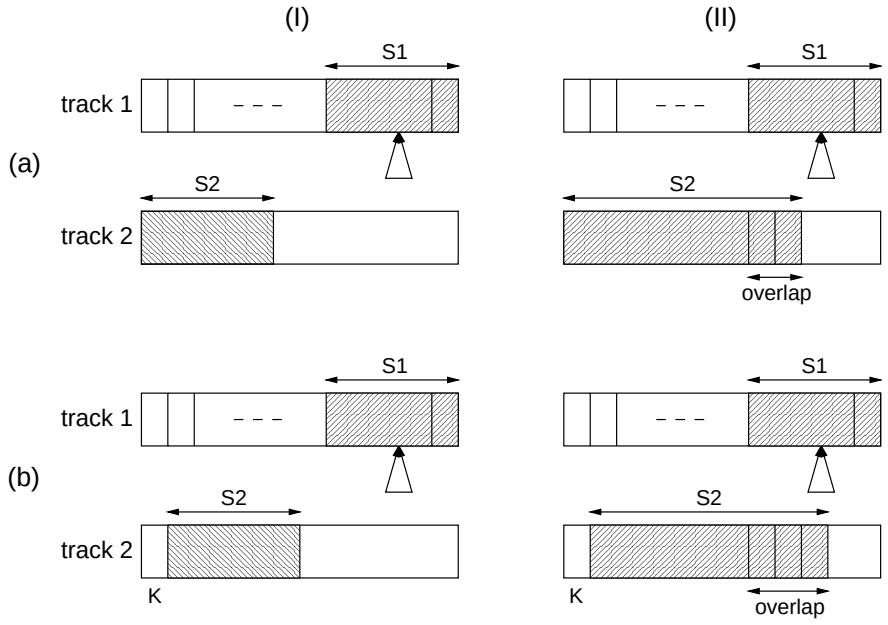

Fig. A.1: **Accessing data on disk track.** This picture depicts the situation when the disk head departs from anywhere within the S_1 sectors but the last sector. In (a) it is assumed that head switch is instantenous and that there is no track skew. In (b), there is a track skew of $K = 1$, depicted by the gap at the begining of track 2. The head switch is still instantenous. The first column (I) depicts the situation where there is no overlap between S_1 and S_2 and thus $P_l = 1$. The second column (II) depicts the situation with an overlap between S_1 and S_2 and thus $P_l = 1 - \frac{2}{S_1 - 1}$ and $P_l = 1 - \frac{3}{S_1 - 1}$ for case (a) and (b) respectively.

Given that the head departed from anywhere within the S_1 sectors but the last sector, the time T_{2b} spent accessing S_2 sectors can be expressed as

$$T_{2b} = P_l \left(\frac{S_2}{N} + \frac{W}{N} \right) + (1 - P_l) T_{2c}$$

where W is the number of sectors spent waiting for the beginning of S_2 and can be expressed as

$$\begin{aligned} W &= \frac{1}{N - S_2} \left(1 + 2 + \ldots + (N - S_2)\right) \\ &= \frac{1}{N - S_2} \sum_{i=1}^{(N - S_2)} i = \frac{1}{N - S_2} \frac{(N - S_2)(N - S_2 + 1)}{2} \\ &= \frac{(N - S_2 + 1)}{2} \end{aligned}$$

Combining the terms T_{2a} and T_{2b} and their respective probabilities, we can

express the expected time T_2 to access the S_2 sectors on track 2

$$\begin{aligned} T_2(N,S,S_2) &= \frac{H}{N} + \frac{N-S_1+1}{N}T_{2a} + \frac{S_1-1}{N}T_{2b} \\ &= \frac{H}{N} + \frac{(N-S_1+1)^2(S_2+O)}{N^3} + \\ &\quad + \frac{S_1-1}{N}\left(P_l\frac{N+S_2+1}{2N} + (1-P_l)\left(\frac{1}{N}+\frac{S_2-1}{S_2}\right)\right) \end{aligned}$$

where $\frac{H}{N}$ is the time for head switch. Substituting S_1 in the above equation for $S - S_2$ we can express T_2 as

$$\begin{aligned} T_2(N,S,S_2) = \frac{H}{N} + \frac{(N-S+S_2+1)^2(S_2+O)}{N^3} + \\ + \frac{S-S_2-1}{N}\left(P_l\frac{N+S_2+1}{2N} + (1-P_l)\left(\frac{1}{N}+\frac{S_2-1}{S_2}\right)\right) \end{aligned} \quad \text{(A.10)}$$

If we assume that a head switch takes exactly K sectors, where K is the track skew, then $H = K$, $O = 0$, and T_{2c} is always 1 revolution since the head can never land precisely at the first sector of S_2, given that it departed from the $S_1 - 1$ possible sectors on track 1. The equation A.10 then simplifies to

$$\begin{aligned} T_2(N,S,S_2) &= \frac{K}{N} + \frac{(N-S+S_2+1)^2 S_2}{N^3} + \\ &\quad + \frac{S-S_2-1}{N}\left(1-P_l+P_l\frac{N+S_2+1}{2N}\right) \end{aligned} \quad \text{(A.11)}$$

A.4 Expected Access Time

Having defined all the terms in equation A.2 for both non-zero and zero latency disks, we can express the equation as

$$T = (1-P_{hs})T_1(N,S) + P_{hs}\sum_{i=1}^{S-1}\frac{1}{S-1}\left(T_1(N,i) + T_2(N,S,S-i)\right) \quad \text{(A.12)}$$

which gives the expected access time for S sectors that can span two tracks.

B Storage interface functions

This C header file defines a storage interface that exposes performance attributes. These functions and structures were used in the prototype implementations described in this dissertation.

```
#ifndef STORIF_H
#define STORIF_H

// size of the smallest logical block (in bytes)
#define SIF_BLOCK_SIZE          512

typedef struct lv_options {
    uint4_t parallelism;         // level of parallelism
    uint4_t depth;               // efficient blocks
    uint4_t capacity;            // # of SIF_BLOCK_SIZE blocks
    uint4_t volume_block_size;   // in SIF_BLOCK_SIZE blocks
} lv_opts_t;

#define SIF_IOV_MAXLEN     1024

typedef struct sif_iovec {
    uint4_t num_elements;
    struct iovec v[SIF_IOV_MAXLEN];
} sif_iov_t;


rc_t sif_inquiry(lv_t *lvh, lv_opts_t *opts);

rc_t sif_ensemble(lv_t *lvh, uint4_t lbn,
                      uint4_t *low, uint4_t *high);
```

```
rc_t sif_parallel_ensemble(lv_t *lvh, uint4_t lbn,
                      uint4_t *low, uint4_t *high);

rc_t sif_equivalent(lv_t *lvh, uint4_t lbn, uint4_t lbns[],
                      uint4_t *cnt);

rc_t sif_read(lv_t *lvh, uint4_t lbn, uint4_t cnt, sif_iov_t *data);

rc_t sif_write(lv_t *lvh, uint4_t lbn, uint4_t cnt, sif_iov_t *data);

rc_t sif_batch_read(lv_t *lvh, uint4_t *lbn[], uint4_t *bcnt[],
      sif_iov_t *bufs[], uint4_t num);

rc_t sif_batch_write(lv_t *lvh,uint4_t *lbn[], uint4_t *bcnt[],
      sif_iov_t *bufs[], uint4_t num);

#endif /* STORIF_H */
```